THESIS

BRAIDED RIVER RESPONSE TO EIGHT DECADES OF HUMAN DISTURBANCE, DENALI NATIONAL PARK AND PRESERVE, AK

Submitted by

Mariah Richards

Department of Geosciences

In partial fulfillment of the requirements

For the Degree of Master of Science

Colorado State University

Fort Collins, Colorado

Summer 2016

Master's Committee:

Advisor: Sara Rathburn

Derek Booth
Peter Nelson
Ellen Wohl

ABSTRACT

BRAIDED RIVER RESPONSE TO EIGHT DECADES OF HUMAN DISTURBANCE, DENALI NATIONAL PARK AND PRESERVE, AK

The spatial complexity and stochastic nature of braided rivers complicate our ability to quantify natural rates of sediment transport and limit our understanding of braided river response to human disturbance. The Toklat River in Denali National Park and Preserve, a braided tributary of the Kantishna River draining the north-facing slopes of the Alaska Range, exemplifies these challenges. Eight decades of localized channel confinement due to installation of a causeway in the 1930's and over three decades of gravel extraction since the 1980's have occurred on the Toklat River adjacent to the Denali Park Road. A unique, multi-scalar and temporally diverse dataset records the responses of the river over a 10-km reach. I evaluated trends in short-term sediment storage through LiDAR differencing and analyzed long-term planform change using braiding index, braiding beltwidth and topographic ruggedness derived from aerial photographs. Two reference reaches along comparable adjacent braided rivers, with varying levels of confinement and no gravel extraction, illuminate the relative influence of these human disturbances on channel and planform change. Comparisons of 2009 and 2011 LiDAR-derived DEMs showed a statistically significant volumetric loss of -30,300 ± 27,600 m^3 over 4 km of active braidplain within the study reach. Braidplain sediment loss adjacent to the channel-confining Denali Park Road bridge crossing was comparable to that removed biennially through gravel extraction downstream (17,100 m^3). Upstream of both the gravel extraction site and the bridge crossing, the braiding beltwidth decreased by 400 m and the braiding index lowered from eight to one between 1988 and 2011.

The reference reaches did not display such noticeable morphologic adjustments, implying upstream migration of gravel extraction and confinement impacts, which can significantly alter flow character, leading to increased localized stream power, degradation and infrastructure damage. These results are relevant to assessing the variety and spatial extent of human disturbance on braided river systems in general.

ACKNOWLEDGMENTS

Funding was provided by Denali National Park and Preserve, Federal Highways Adminsitration, GSA QG&G, and Warner College of Natural Resources. Thank you to my advisor, Sara Rathburn, committee members, Derek Booth, Ellen Wohl and Peter Nelson, and National Park Service supervisor Denny Capps. Grateful acknowledgement to Dave Schirokauer, Paul Franke, Brad Ebel, Stephanie Moret, Pamela Sousannes, Andrew Collins, Shannon Coykendall, Britta Schroeder, Joseph Mangano, Daniel Brogan, Peter Ashmore, Janet Curran, Ken Karle, David Dust, Fisher Ankney, and the entire Fluvial Geomorphology Group. Thank you to my Uncle Chris and Aunt Lise for all the wisdom and good meals and red wine you've shared. Thanks to my parents, sister and Jonathan for your humor, encouragement and patience.

TABLE OF CONTENTS

LIST OF FIGURES

1. INTRODUCTION

1.1 Braided River Processes

Multiple, shallow channels that deviate and recombine to adjust to high flows and associated sediment loads create the braided river planform. These channels, known as braids, convey portions of total flow that vary in response to changing inputs of water and sediment. Braiding is a result of a constant play between erosion and deposition at the bed and banks dictated by stream power and shear stress. The stalling of bedload pulses initiate bar formation, the subsequent bifurcation and confluence of flow above and below the bar. Small-scale roughness due to variations in grain size create rapidly varying sediment transport dynamics along the wetted perimeter (Ashmore, 1991). The small scale mechanisms by which large-scale braiding occurs are through the creation and subsequent dissection of sediment deposits in the forms of central and transverse bars (Wheaton et al., 2013; Ashmore, 1991). Topographic variations combined with energy variability associated with adjustments to boundary conditions, particularly the rate of water and sediment input, lead to complex patterns of flow and sediment flux that produce the braided planform across scales. These "self-similar" processes can occur on small scales (e.g., centimeters to meters) and influence those that materialize on larger scales (e.g., meters to kilometers) and vice versa (Ashmore and Rennie, 2013; Lane et al., 2010; Hicks et al., 2002; Sapozhnikov and Foufoula-Georgiou, 1996). These processes occur across a range of spatial and geographical scales from the 20-km-wide floodplains of the Brahmaputra River of Nepal to a 1-m-wide flume (Takagi et al., 2007).

The conditions most commonly associated with braiding are 1) high sediment loads (specifically bedload) (Germanoski and Schumm, 1993); 2) erodible, non-cohesive banks(Hicks

et al., 2008; Gran and Paola, 2001); and 3) high stream power, a function of discharge and slope (Ashmore and Rennie, 2013; Leopold and Wolman, 1957). Eaton et al. (2010) document that an increase in average grain size decreases the likelihood of a braided planform in favor of a meandering one. Gran and Paola (2001) suggest that the ratio of discharge to sediment supply, or transport capacity, is the ultimate control on river planform, channel geometry, and gradient in alluvial sedimentary basins. Despite the extensive research on braided rivers, quantification of many of their processes and drivers remains a challenge.

1.2 Braided River Process Quantification

1.2.1 Difficulties and Limitations

Traditional methods fall short in capturing the appropriate temporal and spatial scales of braided river process due to the difficulties associated with measuring braided river boundary conditions such as water and sediment inputs. Quantification of braided river discharge and flow regime is challenging because of planform and channel geometry variability. Gage data from braided rivers often underestimate discharge as flow shifts from the channel containing the gage to an adjacent one (Curran and McTeague, 2011). Furthermore, the unstable nature of braided river channel geometry in response to rapidly changing boundary conditions complicates the application of hydraulic geometry relationships (Ashmore and Sauks, 2006; Hicks et al., 2002). The number of channels across a given floodplain can make hydraulic geometry relations difficult to apply on a reach scale, although the individual anabranches have been shown to correlate well with both at-a-station and downstream hydraulic geometry equations (Ashmore and Rennie, 2013).

Quantification of sediment dynamics of braided rivers is difficult due to heterogeneity of topography and associated flow dynamics, as well as limitations to the spatial and temporal scale

of sampling (Ashmore, 2013). Topographic variations create areas of increased shear stress adjacent to areas experiencing shear stresses well below the threshold for incipient motion (Nicholas, 2000; Nicholas et al., 1995). This continues at a larger scale where some channels are actively moving sediment while others are inactive (Ashmore et al., 2011). A relationship between channel geometry and bedload has been investigated by Mosley (1982), Ashmore (1991), and Nicholas (2000), but remains a metric that cannot be applied across systems. Further difficulties arise when the sampling methods used are not appropriately matched to the scale of driving processes. Inconsistency of scale can result in an underestimation of morphologic or volumetric change if bedload sampling is limited spatially or temporally (Brasington et al., 2000). Unfortunately, sampling that attempts to capture all of these temporal and spatial variations of sediment transport may not be feasible (Fuller et al., 2003). In summary, braided rivers are unique, dynamic and difficult to study in the field. To account for variability inherent to these systems, volumetric or morphological metrics have been developed that incorporate a larger spatial and temporal scale and do not rely on field-based methods common to other river planforms.

1.2.2 Remote Sensing Techniques

Technologies capable of characterizing a broader range of processes-- from watershed scales to bar deposition and erosion-- and visually and volumetrically assessing morphologic and planform features to infer change over multiple decades have increased our understanding of braided rivers. Aerial and terrestrial LiDAR have expanded the accessibility of high-resolution datasets across large ($>10^3$ m) spatial scales (Wheaton et al., 2010; Brasington et al., 2000). Cost-effective aerial photogrammetry can provide high-resolution topographic data across medium (10^2 m) scales, increasing the widespread ability to create these datasets (Westoby et al., 2012). Aerially-derived techniques, not only LiDAR but also aerial photogrammetry, can be applied

remotely, opening up areas previously inaccessible to data acquisition (Javernick et al., 2014; Croke et al., 2013; Westoby et al., 2012). Analytical tools for these datasets have also evolved alongside these acquisitional methods. Recent development of Geomorphic Change Detection Software (Wheaton et al., 2008) has allowed more accurately calculated error to be incorporated into volumetric change detection analyses between DEMs derived by LiDAR, photogrammetry, or GPS. This can provide more robust estimates of volume change than those previously underestimated using uniform error calculations (Wheaton et al., 2010).

1.2.3 Morphologic Metrics

Although the availability of these technologically advanced methods has increased, they remain cost-prohibitive for broad spatial application or remote localities. Thus, the relationships between geomorphologic processes and forms, and the boundary conditions that drive them, have continued to be investigated through traditional measurement methods, such as aerial imagery or topographic surveying. Furthermore, these planform and channel characteristics can be used as time series data to understand rate and magnitude of change within a river system (Egozi and Ashmore, 2009; Gran and Paola, 2001; Ashmore, 1991; Mosley, 1982). Planform and channel metrics associated with the braided planform are braiding beltwidth, active width, width-to-depth ratios, and braiding index. Braiding beltwidth is defined as the total width of floodplain subject to annual morphologic change, such as overbank flooding or channel occupation, whereas active width is defined as the combined width of all channels actively transporting material (Ashmore et al., 2011; Bertoldi et al., 2009). Width-to-depth ratio (W:d) is defined as the bankfull channel width divided by the maximum channel depth or thalweg. Braiding index (BI) can be measured as the number of channels intersected in a given cross-section (Egozi and Ashmore, 2009; Howard et al., 1970), the ratio of the total length of channel divided by the length of the reach (Mosley, 1982;

Hong and Davies, 1979), or the ratio of bar length within a reach divided by total reach length (Brice, 1964; 1960). BI is a metric developed to quantify changes in river planform that may reflect alterations to boundary conditions or local impacts. It is universally accepted that braiding index is a direct consequence of discharge and stream power (Ashmore and Rennie, 2013; Ashmore et al., 2011; Bertoldi et al., 2009; Surian, 1999; Maizels, 1979; Howard et al., 1970), but it is still debated how this index correlates to sediment transport and energy dissipation (Ashmore, 2013; Nicholas, 2000; Germanoski and Schumm, 1993).

Beltwidth also adjusts itself to changing boundary conditions but is less dependent on discharge than braiding index, and likely more dependent on sediment inputs (Ashmore and Rennie, 2013; Bertoldi et al., 2009). If the flow is sediment-laden, channel beds are more likely to aggrade and adjacent, low-lying surfaces will become occupied as the channel shifts, increasing the braidplain laterally (Hicks et al., 2008; Kondolf et al., 2002; Germanoski and Schumm, 1993). If the flow is sediment-deprived, it is likely to recruit material from channel bed and banks, leading to incision (Kondolf, 1997). Sediment-deprived flow is also likely to result in increased ruggedness, which reflects the variance in elevation values of the morphologically active braidplain (Scown et al., 2016), due to degradation of channel beds (Germanoski and Schumm, 1993). This would result in a decrease in braiding beltwidth over time if the channel continued to recruit material vertically, suggesting a dependence on sediment input.

Width-to-depth ratio (W:d) is a metric of channel geometry used to interpret channel response to boundary conditions and distinguish thresholds between multi-thread and single thread channels (Dust and Wohl, 2012; Eaton et al., 2010). Increased W:d is associated with decreased sediment transport (Dust and Wohl, 2012). Increased braiding index and beltwidth are generally linked to increased channel W:d; but, this is not a fixed descriptor due to the rapid adjustments

characterizing braided networks (Surian, 1999). Although an increase in W:d is associated with decreased sediment transport, an increase in topographic variation and thus localized "scour pools" with high shear stress could produce enhanced transport (Nicholas, 2000). Additionally, the form of deposition may play a role in sediment transport rates. A bar deposited within a wide channel could decrease W:d substantially, and thus increase shear stress and transport rates on either side of the bar (Dust, 2014). In addition to the relationship to sediment transport rates, W:d also relates to discharge and is incorporated within hydraulic geometry functions used to define a distinguishing threshold for the occurrence of braiding (Eaton et al., 2010). Eaton et al. (2010) suggest the transition from meandering to braiding occurs around W:d of 50. The described relationships between W:d and boundary conditions indicate the value of this metric to interpret change in inputs over time.

Although progress has been made investigating the interactions between morphologic characteristics and process drivers that determine the form of braided rivers, these relationships are complicated by the uniqueness of each river. Quantifying sediment transport and other morphologic processes remains challenging due to the rapidly fluctuating and spatially diverse nature of braided rivers. Investigating the response of a braided river to human alterations reveals further challenges.

1.3 Humans and Braided Rivers

Humans throughout history have been intimately tied to rivers as sources of food, water and hygiene. The development of agrarian cultures tightened this bond and increased our vulnerability to the inherent morphologic and hydrologic processes that define a river system. The conveyor belt-like system of both water and sediment has led to rivers being exploited for their natural resources. From harnessing the energy from rivers for watermills in Ancient Rome (40 BC)

to the construction of over 800,000 dams worldwide, humans continue to exploit rivers (Jacob-Rousseau, 2015).

In addition to human water use, the sand and gravel transported by water are also a valuable resource. River sediments generate ideal aggregate material used in the construction of roads, pipelines, and septic systems. Rivers themselves accomplish part of the processing by breaking down the less resistant substrates and transporting them downstream, leaving behind robust material ideal for construction. Another incentive for river mining is the added convenience of finding a gravel source near the demand and thus minimizing transport costs, which account for the majority of gravel mining overhead (Kondolf, 1997). Exploitation of river sediment is not without consequence, however. Collins and Dunne (1987) broadly summarize the consequences of mining alluvium by altering bed elevation and morphology, and modifying banks and channel patterns. Gravel extraction of alluvium has been documented to affect aquatic and riparian habitat through physical alteration of channel geometry, such as decreased channel width, alterations to slope or loss of heterogeneous bed topography (Kondolf et al., 2002; Kondolf, 1997). The alterations due to gravel mining can be expressed on a larger scale as a simplification to braidplain planform, incision and undermining of infrastructure through headcut initiation (Hicks et al., 2008; Piégay et al., 2006; Meador and Layher, 1998; Collins and Dunne, 1989).

Additional drivers of braided river alteration can take the form of confinement, dams, reservoirs, or land-use change. Encroaching vegetation, land use change, confinement and incision all contribute to braidplain simplification and can damage ecosystems that rely on lateral connectivity (Allan, 2016; Boix-Fayos, 2007; Rinaldi et al., 2005; Walling, 2004; Coulthard, 2001; Arding, 1998; Meador and Layher, 1998; Graf, 1981). Human-influenced valley confinement has been suggested as the primary factor influencing a simplification of river planform in the Platte

River and thus the degradation of associated habitats (Fotherby, 2009). Confinement, via road crossings or encroaching infrastructure such as revetments, is correlated to the diminished numbers of braided planforms across Europe (Ashmore, 2013). Confinement works to increase localized stream power and thus sediment transport capacity, creating an imbalance between water and sediment inputs. Increases to sediment transport capacity that exceed sediment supply may cause severe incision of the bed and to a lesser degree erosion of the banks, deepening the channel and incising into the floodplain, resulting in a simplification of the overall braid planform and disconnection between the river and its floodplain (Kondolf et al., 2002). Dams and reservoirs result in a similar imbalance in water and sediment due to the sediment depletion of flow downstream of the obstruction and the potential for incision (Kondolf, 1997). This imbalance as well as the loss of high magnitude flows can result in the abandonment of adjacent floodplain. Encroaching vegetation, a consequence of a decrease in high magnitude flows, works to increase bank resistance to a point where removing vegetation through high flows is increasingly difficult (Gran and Paola, 2001). Land-use changes in a watershed such as de- or re-forestation have been shown to initiate or terminate braiding processes (Kondolf et al., 2002).

Similar to the driving processes of braided rivers, braided river responses to alterations have been shown to transcend scale and geographic boundaries as well (Hicks et al., 2002; Sapozhnikov and Foufoula-Georgiou, 1996). The relationships between human impacts and river response can be transferrable across geographic ranges and spatial scales (Walling, 2006; Wohl, 2006; Surian and Rinaldi, 2003; Kondolf, 1997). Categorization of human impacts to mountain streams (Wohl, 2006) resulted in specific recommendations to minimize disturbance to the ecologic and geomorphic function of these systems that can be applied across biomes.

Investigation of common disturbances to boundary conditions of braided rivers and the predicted channel and planform response can contribute to a braided river framework applicable globally.

1.4 Study Goals

Past studies have correlated gravel extraction and confinement with channel bank undercutting, incision, and subsequent undermining of infrastructure (Kondolf, 1997; Collins and Dunne, 1989). A unique opportunity exists in Denali National Park and Preserve to investigate the effects of both gravel extraction and channel confinement on a braided river with minimally-glaciated headwaters in the Park (Podolak, 2013). As such, a primary management concern of Denali National Park and Preserve is to protect natural resources and Park infrastructure, while simultaneously extracting gravel from a reach of the Toklat River to maintain the Park road. This reach of the Toklat River is also confined by the Park road crossing, consisting of two bridges spanned by a causeway, as well as adjacent infrastructure. As a result of these multiple influences, the first study goal is to quantify the relative and absolute geomorphic effects of gravel mining and confinement on the River to assist the National Park Service with land management decisions concerning natural resources and infrastructure. Discerning the relative impact of these human disturbances will provide important guidance on how to focus resources to most sustainably support the natural processes of the Toklat River. A second goal is to determine appropriate and cost-efficient methodologies for quantifying changes to and monitoring of altered braided river systems. This goal is based on recognition of limitations associated with acquisition of high resolution data that many land managers face. Evaluation of the relationship between known areas of degradation on the Toklat River and changes to the river planform and braidplain characteristics could produce morphologic metrics capable of quantifying change associated with human disturbance. This research will investigate the relative effects of the gravel extraction and the

bridge confinement and develop metrics of morphologic change through three research hypotheses:

Hypothesis 1: Human activity has led to degradation of the braidplain adjacent to the road-crossing and within the gravel extraction zone.

Hypothesis 2: This degradation correlates to metrics of braided river morphologic change, indicated by the literature to be an increase in ruggedness and a decrease to braiding index and braiding beltwidth.

Hypothesis 3: The causeway is contributing the majority of degradation, indicated by comparisons of temporal variation between planform change of this system and two reference reaches.

2. STUDY AREA

2.1 Denali National Park and Preserve

The area now known as Denali National Park and Preserve was inhabited by the Dichinanek' Hwt'ana ("Upper Kuskokwim Athabaskan") for centuries before it was visited by prospectors, military expedition parties and eventually a promoter of conservation through preservation, Charles Sheldon, in 1906 (Bryant, 2011). This area was first established as a national park in 1915, with subsequent additions to the preserve boundary made in 1976. A long-standing Park goal is to preserve wilderness and the life dependent on it by upholding rigorously defined resource management principles through scientifically based study and implementation. A current challenge for Park management is to determine a sustainable source of gravel to maintain the 145-km Park road and address concerns about the health of a river with headwaters in the Park.

The Toklat River, a 135-km-long braided tributary of the Kantishna River, drains the north-facing slopes of the Alaska Range and ultimately feeds into the Yukon River which terminates in the Bering Sea (Figure 1). The location of concern and the study area of this research lies approximately 20 km downstream from the partially-glaciated headwaters of the Toklat River. The study reach is approximately 4 km long and 1 km wide in an area of adjacent human impacts (Figure 2). Reference reaches used in this research lie east of the Toklat River, in the basins of the East Fork of the Toklat and the Teklanika River (Figure 1), selected for their similar drainage area, slope and planform, and differing levels of confinement associated with the Park Road crossing.

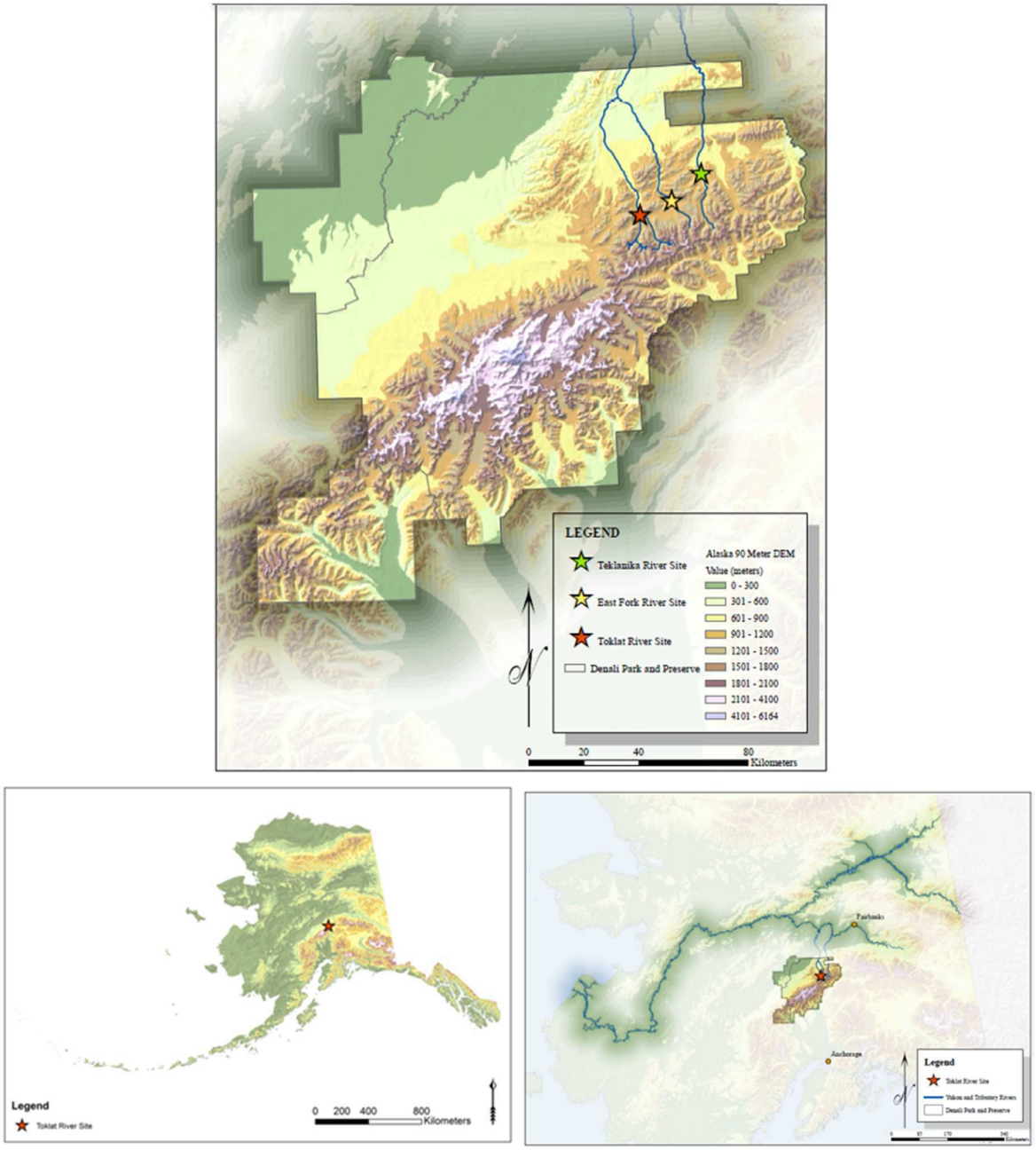

Figure 1: Location maps showing (a) the three field locations, the Toklat River (red star), East Fork (yellow star) of the Toklat River, and the Teklanika River (green star) within Denali National Park and Preserve, (b) the field site (red star) within the Alaska Range (high eleveation band arcing southwest to northeast), and (c) the Yukon River and its tributaries, including the Toklat River and its reference reaches.

2.2 Bedrock Lithology of the Toklat Basin

The Toklat River headwaters and current extent of glaciers in the basin reside in the Cambrian-Jurassic Mystic and Dillinger stratigraphic sequences (DENA Inventory Report, 2010).

This sequence includes turbidites, pelagite, flysch, chert, shale, limestone, sandstone and conglomerate, representing a range of marine coastal environments accreted onto the North American craton. Upstream of the study site the varied rock becomes more consistently Triassic-aged flysch. Exposures of subaerial and submarine basalt flows known as the Nikolai Formation outcrop throughout the West and East Branches, and are metamorphosed to a lower greenschist facies (DENA Inventory Report, 2010). A small portion of the East Branch of the Toklat River cuts through felsic volcanic rocks of the Cantwell Formation that make up the majority of the East Fork basin. Downstream from the road crossing across the Toklat River, the fossil-bearing sedimentary rocks of the Cantwell Formation outcrop. Very similar lithologies are found within the reference reach basins.

2.3 Climatology

Denali National Park and Preserve lies to the north and south of the farthest north bend in the Alaska Range (Figure 1). The southern facing slopes of the Alaska Range within the Park accumulate substantial amounts of rain and snowfall, while the northern facing slopes are much drier. The field site lies to the north of the range, such that a rain shadow effect causes lower precipitation rates and significantly cooler temperatures than the southern facing slopes. Variations in temperature, snow pack and precipitation significantly impact the flow regime of the Toklat River and thus have implications for sediment transport and deposition. Long-term deviations from average temperatures and precipitation totals have led to glacial recession throughout the Park and the Alaska Range. These changes affect sediment input to glacially-fed rivers and can alter channel characteristics over time. Whether glacial retreat results in aggradation or degradation in the associated river continues to be studied, and most likely varies by system (Peizhen et al., 2001; Maizels, 1979). It has also been predicted that magnitude and frequency of precipitation events

will increase substantially in this basin in particular, and subarctic basins in general (Crossman et al., 2013).

Recent deviations from average annual temperatures have been documented on the Toklat River and statewide (Sousanes and Hill, 2015). In 2013, the average annual temperature for the Toklat River Valley was -2.27°C with average summer precipitation of 0.25 m (Sousanes and Hill, 2013). The average temperature for 2013 was 0.8°C warmer than annual data averaged between 2003 and 2013. The average winter temperature in 2014 for this region was -12.0°C (approximately 2.5°C warmer than the 1981-2010 average, and 3.4°C warmer than the 1926-2014 average). In 2014, 0.28 m of snow was measured on the ground by February, which was 0.20 m less than the average calculated from data collected from 1926-2014 (Sousanes and Hill, 2015). Temperature and precipitation data are derived from the Toklat River weather station from 2005 until present. Prior to this, all climate data are derived from the Park headquarters weather station and are thus generalized across large distances.

2.4 Human Impacts

2.4.1 Causeway and Revetments

The Toklat River has experienced eight decades of human impact by confinement from a causeway and erosion mitigation structures (Figures 2, 3 and 4). The first road crossing of the Toklat River was constructed in 1931 (Figure 4a) and consisted of two bridges and a causeway that spanned 45% of the total valley width, connecting the two bridges. Erosion mitigation structures were built in 1931 during construction of the first bridge and causeway installation and have been expanded since (Figure 4b). Subsequent iterations of causeways spanned 62% (constructed in 1954) and 60% (constructed in 1986) of the total valley width (CardnoENTRIX,

2013). During the majority of the last eight decades, flow in the Toklat River was split between the two bridges on either side of the causeway: The East Branch flowed through the East Bridge and the West Branch flowed through the West Bridge. Currently, however, all flow is concentrated beneath the East Bridge (Figure 2) and thus flow occupies only 20% of the previously active braidplain at the road crossing.

When the Park boundary was first delineated, no Park infrastructure encroached upon the Toklat River floodplain (Figure 5a). Between 1955 and 1957 Toklat Road Camp, consisting of summer housing for Park employees, equipment storage, and a road connecting Road Camp to the Park road, was built in its current location on previously active floodplain (Figure 5b). In 1988 a Visitor Rest Area was built on an area that was designated as active floodplain as recently as 1953 (CardnoENTRIX, 2013). Currently, 65% of the river flowing through the Wilderness Exclusion area, designated for development within the Park, is lined on one side by erosion mitigation structures, such as barbs, revetments and gabions.

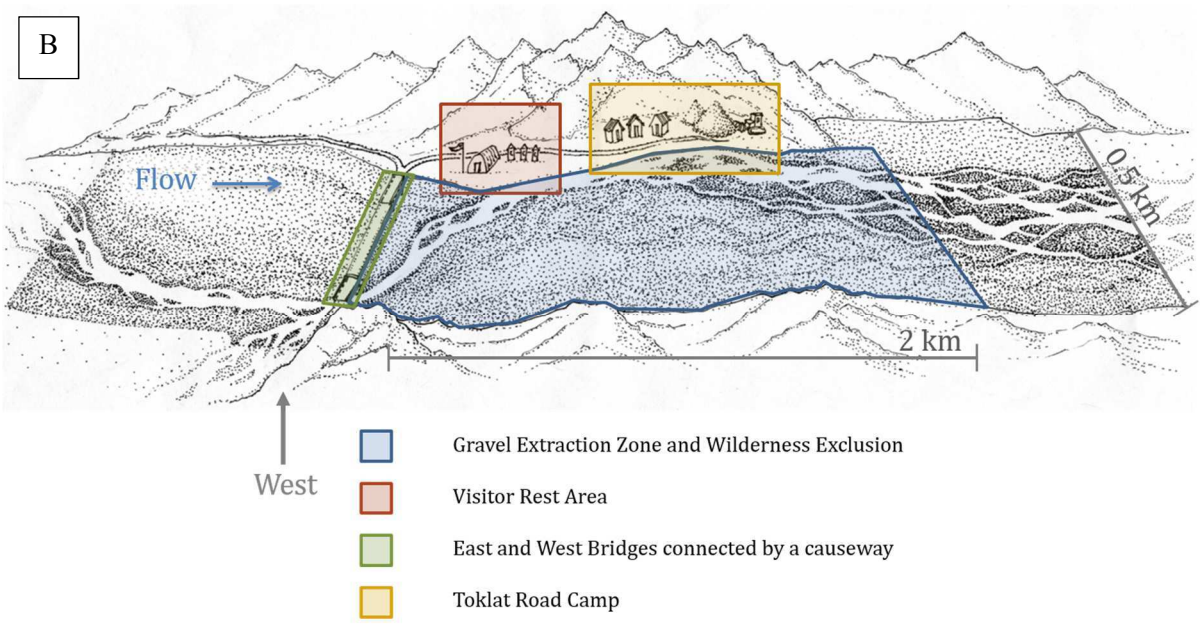

Figure 2: Site maps of the study reach showing locations of human impacts on an aerial image taken September of 2007 looking downstream (A) and a site map looking west across the floodplain towards Toklat Road Camp (B). Both figures depict gravel extraction boundary (blue), Visitor Rest Area and Toklat Road Camp infrastructure (red and yellow, respectively) and confinement (green). Flow and north direction are top to bottom in upper figure and left to right in the lower figure.

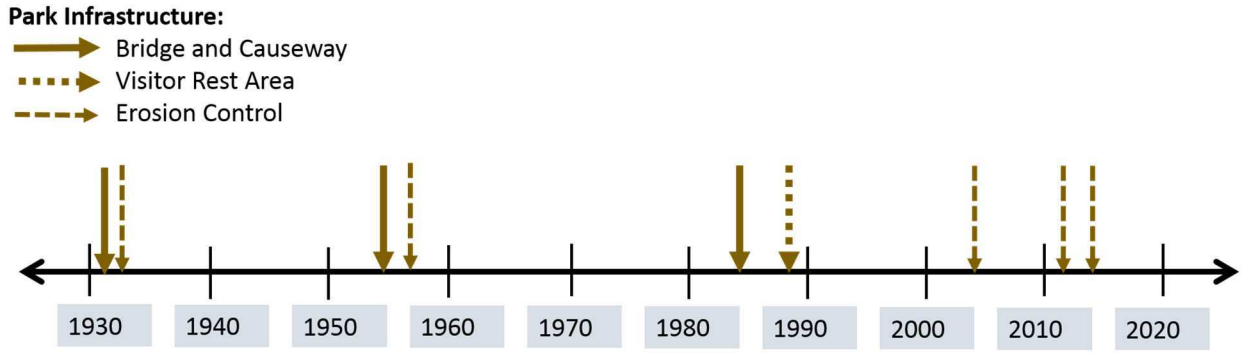

Figure 3: Timeline showing construction dates of infrastructure, such as bridges and revetments, along the Toklat River.

Figure 4: Image on left shows the first iteration of the East Bridge and a small section of the causeway across the Toklat River built in 1931 (NPS 1950). View is to the west and flow is left to right. Image on right shows erosion mitigation structures or revetments installed along the East Branch of the Toklat River (NPS 1982). View is to the east and flow is towards viewer. Grizzly bear for scale.

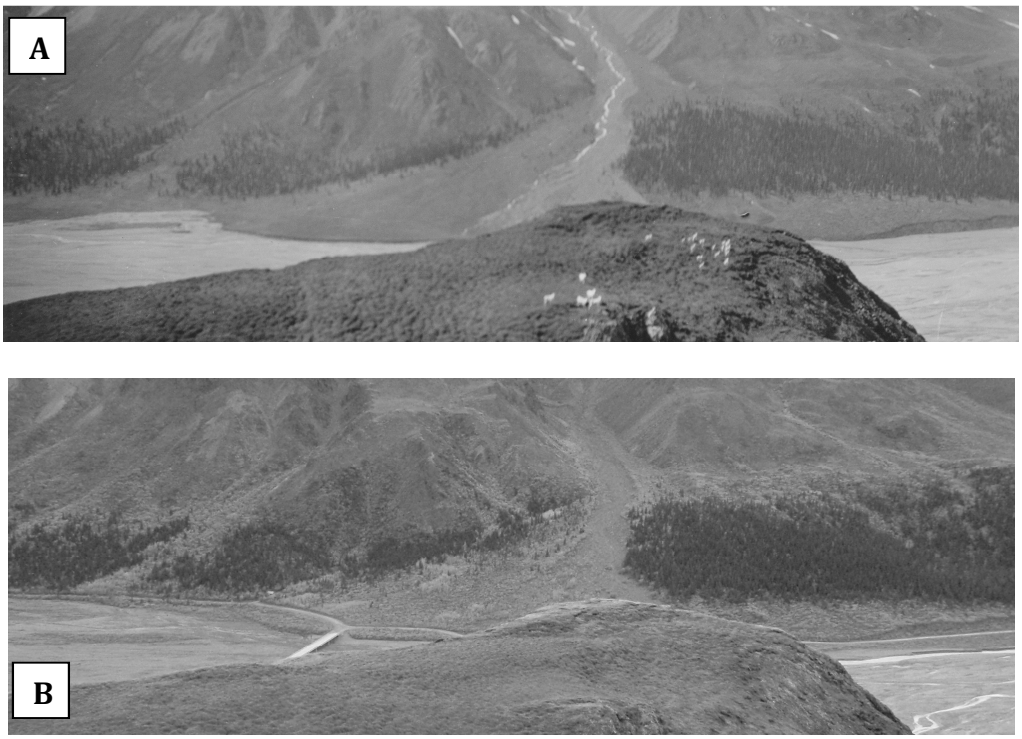

Figure 5: Image A is a historical photo circa late 1920's from above the eastern side of the Toklat River overlooking the future road crossing. This photo was reoccupied in 2009 shown in Image B. Note location of road in Image B overlapping the area that was previously active floodplain in Image A.

2.4.2 Gravel Extraction

On a biennial basis, Denali National Park and Preserve extracts gravel from the 600-m-wide active floodplain of the braided Toklat River within the wilderness exclusion area to maintain the Park road (Figure 2). To obtain authorization for the extractions, an Environmental Assessment was completed in 1992, based on numerical modeling and field studies conducted by the National Park Service (NPS) on the Toklat River to test the post-extraction reclamation potential of rivers within the Park (Karle, 1990; NPS, 1992). Here, "reclamation" is defined as the reoccupation of the excavated area by the river and the reestablishment of natural channel geometries. Gravel extraction on the Toklat River occurs using a bulldozer that scrapes the surface of the floodplain or braidplain and an excavator that lifts the material into a rock truck that transports the material to the adjacent Toklat Road Camp, an area of seasonal housing, Park facilities and equipment storage (Figure 6). Potential excavation geometries explored in the 1990 report included two straight channels (one parallel and one perpendicular to the axis of flow), a circular channel, and an arcing channel intended to mirror a natural bend in the river. These studies culminated in the development of a 'mirror-channel technique'—mirroring natural, active channel dimensions on dry ground to create a symmetrical lens shape, essentially splitting the flow in half—due to its cost-effectiveness and anticipated rapid reclamation (NPS, 1992).

The mirror–channel technique continued through 2010; it was altered in 2012 to incorporate more of the inactive floodplain to allow more efficient extraction. This resulted in the 'double-helix' technique that allowed a braided channel form to be excavated into higher and less-frequently inundated floodplain. In 2014 additional methods were tested to incorporate more of the abandoned floodplain to the east. These took the form of bar and bank lowering, in which the area adjacent to the active channel is reduced to a lower level to allow occupation of flow; and

floodplain lowering, which reduces the overall height of the recently abandoned floodplain to the east that prevents flow from occupying the entire width of the floodplain. These geometries were reclaimed by flow of the Toklat later that season, suggesting a combination of successful geometry and placement.

The volumes of sediment extracted were unmeasured until 2001. Following this, a brief two-year period of 5,700 m^3 was followed by the current biennial volume allotment of 17,100 m^3 (Figure 7). Locations of the extraction sites have been recorded since 2008 (Figure 8).

Figure 6: An excavtor dumps recently excavated sediment into a rock truck that will transport the material to the adjacent Road Camp along the Toklat River. View is south and upstream.

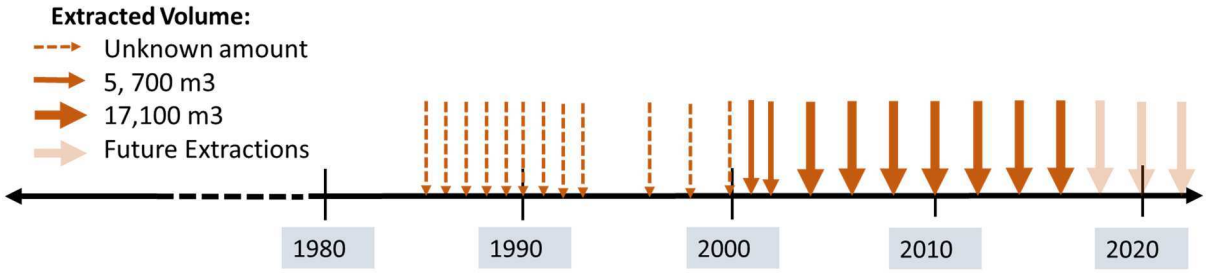

Figure 7: Timeline showing volume allotments for gravel extraction over time along the Toklat River.

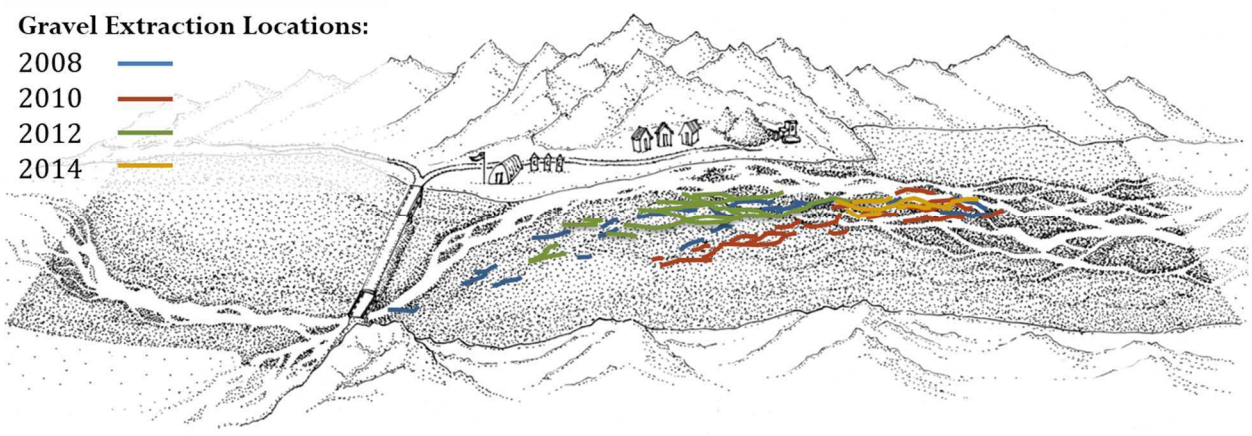

Figure 8: Site map showing locations of biennial gravel extractions since 2008. Each year indicated represents a total gravel volume of 17,100 m^3 extracted from the associated locations.

2.5 Bedload Estimations

Total extraction volumes from historical gravel mining were allotted as a percentage of the estimated total bedload. Total bedload within this reach was estimated by Emmett (1996) from samples collected in 1988 and 1989, when 12 separate measurements of bed-material transport were collected over a period of two years. Emmett (1996) estimated bankfull discharge (used as a surrogate for a 1.5-year recurrence interval flow) as 38 m^3/s using width, depth and velocity measurements over a two-year period. In contrast, Podolak (2013) estimated the 2-year recurrence interval peak discharge at 81 m^3/s, using regional regressions developed by Curran et al. (2011), resulting from an estimated 1.2 m mean annual precipitation. The recommendations of an annual gravel extraction rate of 4% of total bedload (Karle, 1990), and a current biennial extraction rate of 10% (17,100 m^3) of the estimated total bedload, were based on Emmett's (1996) calculations. These extractions are completed within a designated area (Figure 3) within the wilderness exclusion area.

Data from Emmett (1996) show that less than an order of magnitude of change in discharge corresponds to more than two orders of magnitude of change in bedload (Figure 9). This large

variability and the unpredictable nature of discharge and sediment loads on the Toklat River suggest extraction volumes based solely on spatially and temporally limited measurements of bedload may be questionable (CardnoENTRIX, 2012; J. Curran, Personal Communication, 2015). The 1988-1989 bedload measurements occurred over a narrow range of discharges and only quantified flux, thus not distinguishing between the amounts of material deposited within the area of extraction and that transported through the study area. Distinguishing between sediment input and output requires a more comprehensive investigation, using a variety of data spanning a range of spatial and temporal scales, which is necessary to evaluate the potential effects of ongoing gravel extraction on reach-scale sediment volume and channel morphologic change.

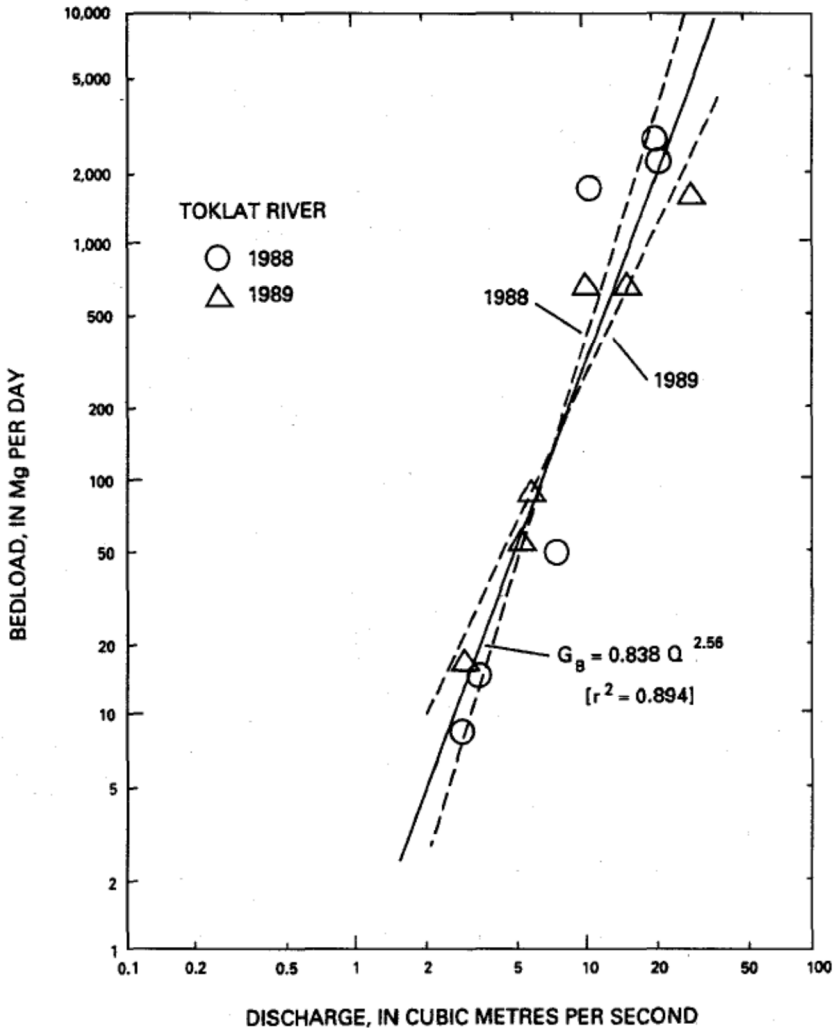

Figure 9: Figure from Emmett et al. (1996) showing relationship between bedload transport rate and discharge along the Toklat River using data collected in 1988 and 1989. Note large variability in bedload associated with relatively small changes in discharge.

2.6 Reference Reaches

Two reference reaches, the East Fork of the Toklat and the Teklanika Rivers (Figure 10), were selected to represent minimally altered braided river systems experiencing significant (although naturally occurring) channel confinement and minimal confinement, respectively. The reference reaches were selected not only for their proximity and comparable drainage area size, but also for key differences between their management compared to that on the Toklat River. The Toklat River represents impacts associated with gravel extraction and confinement. The East Fork

represents a naturally confined system, and the Teklanika represents a minimally confined system, neither of which experience gravel extraction.

Potential future development of the two reference reaches is also intimately tied to the Toklat River and its future as a natural and social resource. The East Fork has been approved for gravel extraction volumes up to 4,100 m^3 in the area of its natural confinement and road crossing. The Teklanika is a candidate for infrastructure development in order to decrease the numbers of visitors traveling farther west along the Park road, and to potentially eliminate the need for existing tourism infrastructure at the Toklat River.

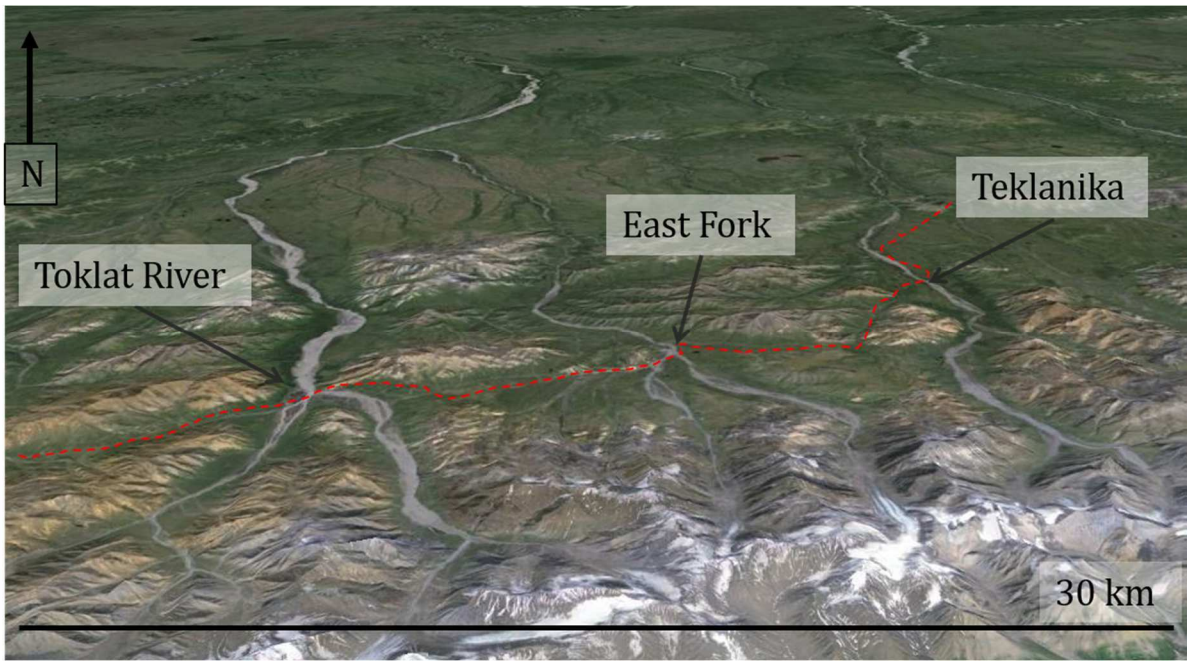

Figure 10: Google Earth imagery showing locations of the reference reaches and the Toklat River along the Park road. Black arrows indicate intersection between the river and the Park road. Perspective is looking down the north slope of the Alaska Range and flow is from south to north.

Field site locations on all three rivers are at the intersection of the Park road with the river valleys. The Park road crosses the Teklanika (TEK) at mile 27 and the East Fork of the Toklat River (EF) at mile 43. The intersection of the Park road and the Teklanika River lies farther downstream from its headwaters than the other two systems, resulting in a lower average slope

through the reference study site. Here the contributing watershed consists of five adjacent basins, giving it a comparable watershed size to the TEK but a steeper slope than either the TEK and Toklat River. The areas of interest in the reference reaches are approximately 0.25 km wide and 1.5 km long, spanning 0.75 km both upstream and downstream of the bridge.

The East Fork (EF) of the Toklat and the Teklanika (TEK) Rivers lie in adjacent watersheds and the East Fork's western edge lies adjacent to the main fork of the Toklat River. The headwaters of all three basins are carved into the Cambrian-Jurassic Mystic and Collinger stratigraphic sequences. The primary geologic difference between these basins is the presence of the volcanic rocks from the Cantwell Formation in the East Fork and Teklanika basins, which is relatively absent in the Toklat basin. The large presence of volcanic rock of the Cantwell Formation on the reference reaches suggests rapid weathering rates and may contribute to its smaller grain size. All three basins experience comparable climate due to their close proximity, although weather patterns on an hourly or daily basis may vary. Site specific precipitation and temperature data in the TEK and EF basins are not available, so the Park Headquarters weather station was used as a proxy.

3. METHODS

The Toklat River has a long history of data collection due to the Park's interest in the river response to human disturbance. This provided the foundation for a spatially and temporally diverse dataset that was built upon in the 2015 field season. The varied nature of this dataset, including the distribution throughout the field site (Extent) and over time (Year Acquired), is summarized in Table 1.

Table 1: Spatial and temporal extents of data sets used and their associated analysis method.

Analysis	**Data**	Year Acquired	Extent
Volumetric	**LiDAR**	2009	Full
Volumetric	**LiDAR**	2011	Full
Volumetric	**Aerial Photogrammetry**	2015	Partial
Morphologic	**Aerial Photos**	1953	Partial
Morphologic	**Aerial Photos**	1964	Partial
Morphologic	**Aerial Photos**	1988	Partial
Morphologic	**Aerial Photos**	1996	Partial
Morphologic	**Aerial Photos**	2004	Partial
Morphologic	**Aerial Photos**	2009	Partial
Morphologic	**Aerial Photos**	2011	Partial
Morphologic	**Oblique Photos**	1963	Partial
Morphologic	**Oblique Photos**	1956	Partial
Morphologic	**Oblique Photos**	1955	Partial
Morphologic	**Oblique Photos**	1964	Partial
Morphologic	**Channel W:d (Field)**	2015	Point
Morphologic	**Grain Size (Field)**	2015	Point
Morphologic	**Braidplain Slope (Google Earth)**	2013	Full
Morphologic	**Channel Slope (Field)**	2015	Full

3.1 Volumetric Change Detection

Three surfaces were used for volumetric change detection analysis. Airborne Light Detection and Ranging (LiDAR) was acquired of the Toklat River field site in 2009 by Aero-metric, Inc., and in 2011 by REY Engineers, Inc. Aerial photogrammetry techniques specific to Matt Nolan of the University of Alaska Fairbanks were employed in June, 2015 over a limited portion of the area previously covered by LiDAR in 2009 and 2011 (Figure 11). Photogrammetric analyses included the active braidplain of 2015, 0.5 km upstream and downstream of the East Bridge, and the Bridge Subreach.

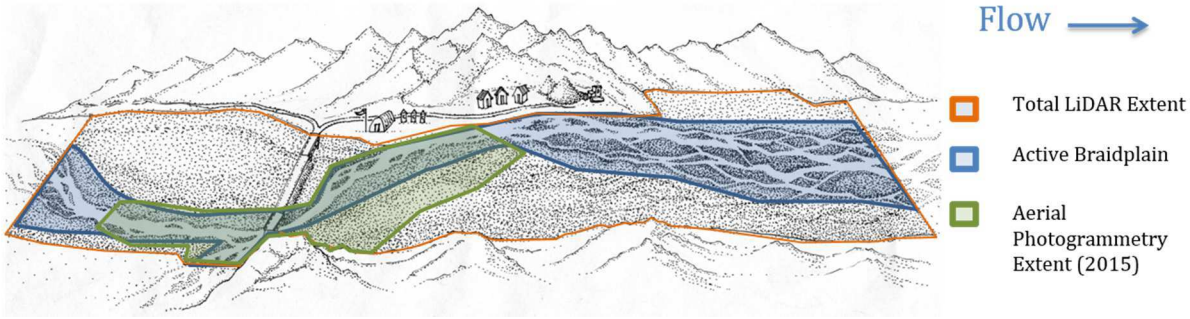

Figure 11: Illustration showing the extents of LiDAR and aerial photogrammetry surfaces used for volumetric change detection analyses along the Toklat River. Note location of bridges, causeway, Visitor Rest Area and Road Camp as identified in Figure 3.

Spatially focused analyses were conducted within the overall LiDAR extent using the LiDAR data acquired in 2009 and 2011, and a portion of the data acquired by aerial photogrammetry in 2015 (Figures 12 and 13). Two functional zones were delineated; Subreaches and Influential Impact Zones, based on management concerns, field surveys, braidplain slope measurements, planform and the results from the full-extent 2009-2011 volumetric change detection. Subreaches were established equal distance downstream from and upstream of the causeway in areas of varying braidplain slopes and extended to the farthest upstream extent of the LiDAR coverage (Figure 12). These Subreaches are valley-spanning rectangles located upstream

of the East Bridge on the East and West Branches of the Toklat (Upstream), adjacent to the East Bridge downstream (Bridge), and adjacent to the Toklat Road Camp (Downstream). Due to a lack of data, the area capturing the East Branch of the Toklat was not included in analyses. Supplementary analyses of the proportion of total locations of gravel removal within each Subreach were calculated as the length within the boundaries of each Subreach divided by the total length of extractions from that year. "Influential Impact Zones" were subjectively defined as areas assumed to be functionally equivalent throughout their lateral and downstream extents, based on field observations and management implications. These delineate boundaries around the confinement associated with the causeway, upstream and downstream revetments, and the 2010 gravel extraction area (Figure 13).

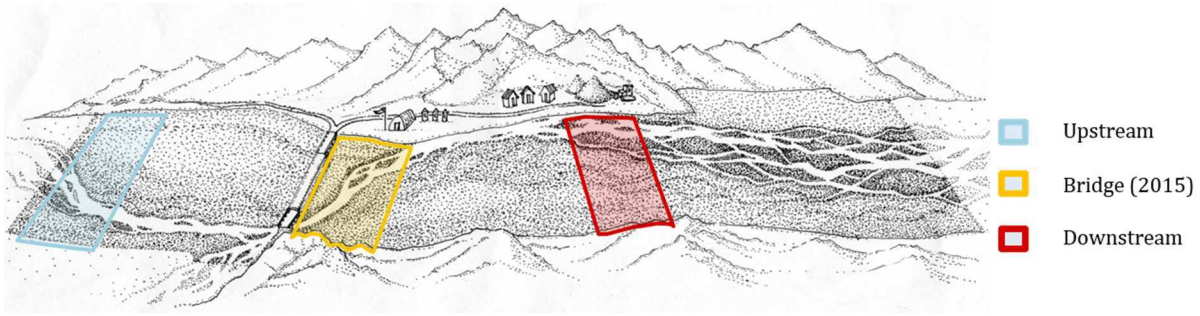

Figure 12: Illustration showing the extents of the Subreaches used for volumetric change detection analyses along the Toklat River. All analyses within the Subreaches used 2009 and 2011 LiDAR surfaces. Analyses of the Bridge Subreach also incorporated the 2015 photogrammetric surface. Note location of East and West Bridges, causeway, Visitor Rest Area and Road Camp.

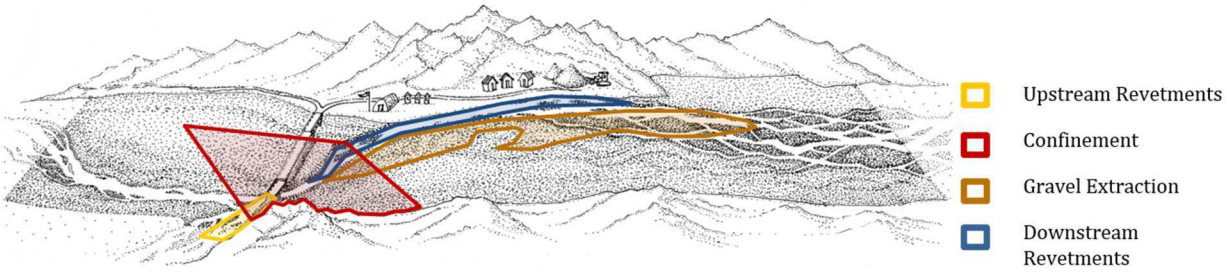

Figure 13: Illustration showing the extents of the Influential Impact Zones used for volumetric change detection analyses along the Toklat River. Note location of East and West Bridges, causeway, Visitor Rest Area and Road Camp.

The 2009 and 2011 LiDAR data were orthogonal (same grid resolution) but not concurrent (grids were not aligned). Data concurrency was obtained using the Clip tool raster processing options in ArcMap (ESRI, 2016). The 2015 photogrammetry data were processed and DEMs were constructed by the GIS Specialist of Denali National Park and Preserve. The 2015 data were neither orthogonal nor concurrent and additionally required projection into the coordinate system associated with the 2009 and 2011 datasets. Further processing entailed projection, unit conversion and grid alignment for accurate comparisons to the 2009 and 2011 surfaces. Orthogonality was altered within the raster processing options while applying the Project tool in ArcMap (ESRI, 2016). Units were adjusted using Raster Calculator (ESRI, 2016). The Resample tool in ArcMap was used to alter grid size using bilinear interpolation and the Clip tool raster processing options corrected concurrency issues (ESRI, 2016). Vertical adjustment of the 2015 data was necessary using the Extract Multi-values to Points tool (ESRI, 2016). The elevations of 125 assumed stable points of land from 2009 and 2011 were used to acquire a minimum root mean square error (RMSE) between 2015 values and an average of 2009 and 2011. The value that minimized the RMSE (14.95 m) was used as the vertical adjustment factor for the 2015 aerial photogrammetry data. Additionally, point data were extracted from the 2015 raster to create comparable analyses with the 2009 and 2011 datasets using available software.

To estimate uncertainty in surface representation and thus volumetric change detection, Geomorphic Change Detection (GCD) software was used (Wheaton et al., 2013b, 2010; Brasington et al., 2003). GCD quantifies and integrates the spatial variability of uncertainty into the analysis of Digital Elevation Models (DEMs) of Difference (DoD) to provide a more robust estimate of volumetric change. This is completed by combining the two standard deviations of error (SDE) associated with each surface using the following equation (Brasington et al., 2003):

$$U_{crit} = t\left(\sqrt{SDE_{new}^{2} + SDE_{old}^{2}}\right)$$

where U_{crit} is the critical threshold error; t is the student's t-value based on an 80% confidence level; SDE is derived from a Fuzzy Inference System (FIS) and the subscripts *new* and *old* indicate the relative date of the input DEMs. FIS is a repeatable mapping process that moves from defined inputs, to less-clearly defined rules that apply weight to the inputs, and calibrates a defined output (Jang, 1993). In GCD, an FIS creates a framework for the measured or derived inputs, which weights them according to specifications in order to arrive at an output that is appropriate for the survey and spatial variability (Wheaton et al., 2010). This entails creating membership functions within each input that organize incoming data into "fuzzy" ranges. Rules are defined that calculate an uncertainty output based on the membership of the data. For example, if model inputs are surface slope and point density, and the data fall into or are members of high slope and low point density ranges, output uncertainty will be high. Inputs of surface slope, point density, and interpolated error were used to create a FIS for the LiDAR data from 2009 and 2011. All LiDAR change detection analyses in this study used an 80% confidence interval for error prediction, selected based on data and software limitations, as well as management needs (Bradford et al., 2005; Mapstone, 1995). Uncertainty in the photogrammetry data was approached similarly to that of the LiDAR data using point data extracted from raster pixels.

3.2 Morphologic Change Detection

Aerial photographs spanning 1953 to 2011 were analyzed to determine the morphologic response of the Toklat, East Fork of the Toklat (EF) and Teklanika Rivers (TEK) to varying degrees of confinement associated with the Park road crossing. The Toklat River represents a system affected by gravel extraction, revetments and unnatural confinement; the EF experiences

natural confinement; and the TEK undergoes minimal confinement. Imagery used in this analysis consisted of aerial photographs acquired from all three systems during the years 1953, 1964, 1988, and 1996, and commercial IKONOS imagery from 2004 (Table 1). Additional imagery associated with LiDAR acquisition was available for the Toklat River for 2009 and 2011. Airphotos were georeferenced using four or more stationary locations as control points, such as the bridge corners and clear rock outcrops.

3.2.1 Braiding Index

Braiding index (BI) was measured from the above-mentioned aerial imagery using the methods developed by Brice (1960) and supported by Ashmore (2011). BI, defined as the number of channels intersected by a given cross-section, was calculated using cross-sections created in ArcMap perpendicular to the dominant flow direction, within Subreaches. Three separate Subreaches were created along the Toklat River to represent a similar level of impact and braidplain slope, and thus homogenous data populations (Figure 14). Each Subreach consisted of 30 cross-sections spaced nine meters (~30 feet) apart. One Subreach was placed upstream of the causeway and bridges, spanning the West Branch (Upstream) to represent upstream influence of the causeway. Thirty cross-sections were placed immediately downstream from the East Bridge to represent the maximum influence of confinement (Bridge). Lastly, 30 cross-sections were placed adjacent to Road Camp to capture influence due to the gravel extraction and minimal influence from confinement (Downstream). BI data were analyzed over time and across locations using R statistical software.

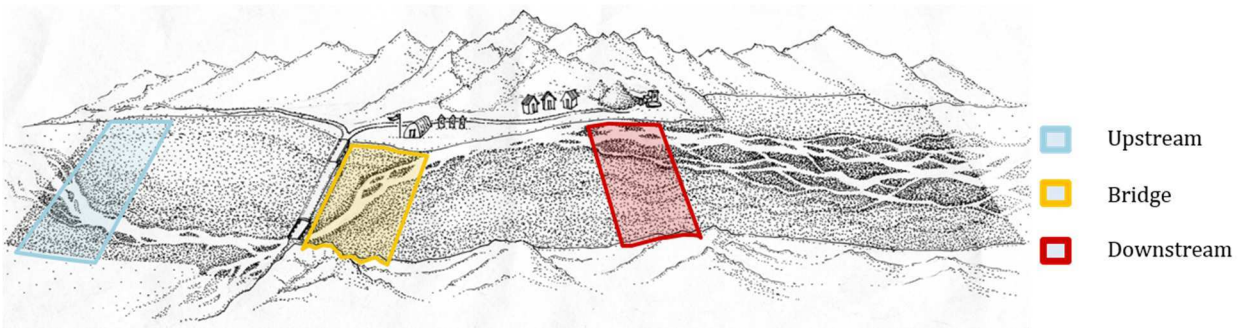

Figure 14: Illustration showing extent of Subreaches used for morphologic change detection analyses. Calculations of braiding Index and beltwidth used 30 adjacent cross-sections within the Subreaches depicted above, while ruggedness was extracted from the entire area within the Subreaches.

3.2.2 Braiding Beltwidth

Braiding beltwidth, defined by Bertoldi (2009) as the width of the whole area subjected to morphological processes, was chosen as a metric shown to have minimal dependence on discharge (Ashmore et al., 2011; Bertoldi et al., 2009; Takagi et al., 2007). Braiding beltwidth was defined throughout this analysis as the width of the valley subjected to recent morphological processes and thus activated within the year. Recent flow activity often results in higher amounts of glacial silt deposits that retain moisture and cause a darker gray color visible in aerial imagery, and thus is used as a defining characteristic of active braidplain. Thus, the designation of active braidplain does not require active flow, but visibly and recently activated and wetted surfaces as signified by silt deposits. Field observations indicate silt deposits are transported through aeolian processes within approximately a year of deposition if left exposed and dried; thus, existing silt deposits signify surface activation within a year (Figure 15). The inactive braidplain consists of minimally vegetated terraces and terraces distinguishable by iron oxidized weathering of alluvium due to a lack of frequent inundation (Figure 16).

Aerial photographs were used to assess the evolution of the braiding beltwidth over the time period of interest using the 30 adjacent cross-sections within the Subreaches (Figure 14).

Braiding beltwidth was measured as the cumulative distance along the cross-section that contained active flow or appeared dark brown or gray, associated with silt deposition and moisture retention. This metric was measured for all available years of aerial photography (Table 1).

Figure 15: Photograph depicts braidplain beltwidth as indicated by line. Note active channels and lack of vegetation (left) adjacent to abandoned, vegetated floodplain (right).

Figure 16: Photograph showing non-active braidplain consisting of minimally vegetated terraces and terraces distinguishable by iron oxidized weathering rinds due to a lack of frequent inundation. View is west across the Toklat River and towards Road Camp. Note color difference between active braidplain in distance and non-active surface in foreground.

3.2.3 Ruggedness

Ruggedness is defined here as the variance in elevation values from point data, similar to the standard deviation of elevation values as defined by Scown et al. (2015). For this analysis, vegetated terraces were excluded in order to focus on topographic variation within the active braidplain (Figure 17). Ruggedness was calculated by extracting point data from the 2009 and 2011 LiDAR sets of the Toklat River in the Subreaches used for volumetric and morphologic change detection analyses. Only the point data from the defined active braidplain were extracted for ruggedness analysis. The variances of these data were compared using an F-test in R statistical software that produces a 95% CI interval for the ratio of variances as well as a p-value to indicate significance. Data were analyzed by Subreach for a statistically significant difference in variance between elevation data extracted from LiDAR surfaces from 2009 and 2011.

Figure 17: Photograph showing ruggedness within braidplain indicated by dotted line showing relief between recently active surface and currently active channel. Recent activation is indicated by silt deposition shown right of center.

3.2.4 Slope

Google Earth's vertical datum WGS 84 EGM96 Geoid was used to extract average slope of the areas established for BI and beltwidth analyses and a reach-spanning slope for each year. The same datum was used to analyze slope in the two reference reaches within the Subreaches and along the full study reach. The Google Earth imagery was not of sufficient quality to use for other morphologic change detection analyses but sufficed for general trends in slope in the regions of interest. Additionally, the thalwegs of cross-sections measured in May 2015 along the Toklat River and its reference reaches were used to estimate a reach-averaged channel slope.

3.2.5 Width-to-Depth Ratios

Variation in channel width-to-depth ratios (W:d) between the study reach and its reference reaches was captured through a topographic survey of representative cross-sections using a real-time kinematic (RTK) GPS. Cross-sections were oriented perpendicular to the main thread of flow,

with adjustments made to account for changing flow direction of individual braids. Topographic points were acquired at the break in floodplain above the channel, at the water surface, and at low points of the channel bed. Wider channels were represented with more than one minimal bed elevation to describe the multi-thread geometry, while narrower channels consisted of only one thalweg measurement. Occasionally wider channels were transected where multiple braids had joined, creating a wide water surface with an undulating bed surface, typically consisting of two to three thalwegs separated by higher points of aggraded sediment.

W:d values, using maximum depth of thalweg, were determined from channel cross-sections using ArcMap. Width was measured as the distance between water surface points and depth as the lowest measured elevation point along the bed surface. Boxplots of W:d upstream and downstream of the source of confinement along each of the reference reaches were generated in R. Additionally, the Toklat River data were plotted on a finer scale showing cross-sections acquired at the upstream West and East Branches, the confluence between the two, downstream of the East Bridge, and downstream of Road Camp (Figure 18).

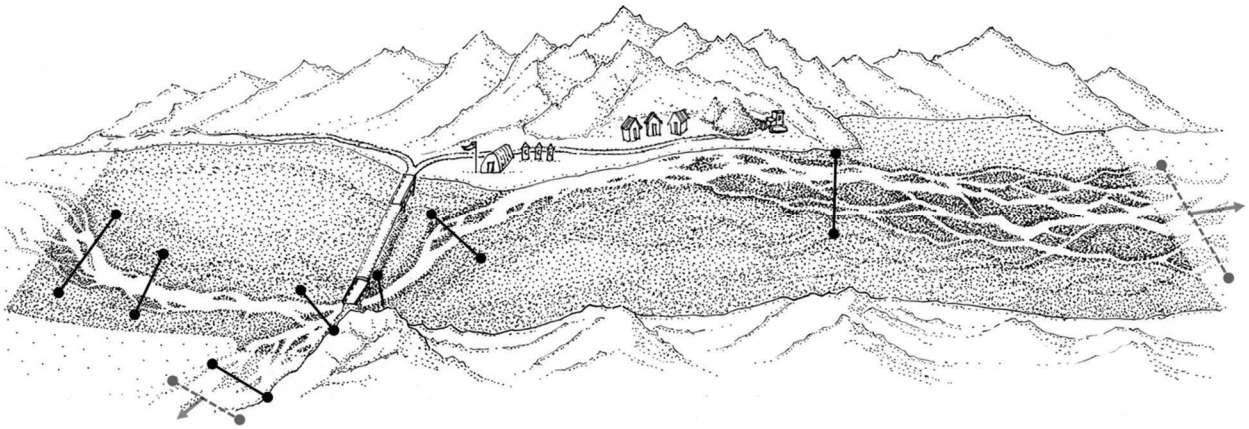

Figure 18: Site map showing the locations of W:d measurements acquired with RTK GPS in 2015. Cross-sections in situ are indicated by black lines, and cross-sections upstream on the East Branch and downstream of the study reach are indicated with a dotted line and arrow.

3.2.6 Grain Size

Grain size analyses were conducted in the study site and its reference reaches using a modified Wolman technique consisting of 100 intermediate grain size diameter measurements at each site (Wolman, 1954). The Toklat survey incorporated more sampling sites to capture small-scale changes in D_{50} and D_{84} associated with varying levels of human disturbance. Eleven grain size sampling sites on the Toklat spanned upstream of the East Bridge on both the West and East Branches, and 500 m downstream from the gravel extraction zone boundary.

3.2.7 Stage Measurements

A TruTrak capacitance rod with data logger was installed on the Toklat beneath the East Bridge in May, 2015. The stage recorder was located in an area of low-energy flow at the time of installation, although local staff observation suggested that area had received the majority of both the East and West Branches' flow two days prior to installation. High discharges later in the season undermined the fence post to which the stage recorder was mounted and the instrument was lost. Hence, Toklat River stage data are unavailable.

3.2.8 Repeat Oblique Photographs

Repeat ground-based photography was used to assess qualitative changes on the Toklat and its reference reaches (Table 1). Historical imagery was acquired from the Park's historical archives, past research efforts and the NPS regional office in Anchorage. Reoccupation of sites was completed in areas that were accessible in summer of 2015.

3.2.9 Federal Highways Bridge Elevation Data

Elevation data beneath the Toklat, East Fork and Teklanika bridges were acquired from the Federal Highway Administration. Measurements were taken from each bridge down to water level

or floodplain surface. Repeat measurements were conducted annually to biennially initiating in 1996. Observation of the field methods employed for bridge measurements suggest that these data were not accurately or consistently surveyed at a resolution useful to this analysis, and thus, are not discussed further.

3.2.10 Weather Station Data

Weather station data for the Toklat River provided weekly records of precipitation that correlate with aerial photographs and LiDAR sets acquired after 2005. Weather station data from the Park Headquarters were used for all older aerial and oblique photographs to correlate precipitation to river flow. Precipitation here is used as a proxy for discharge to minimize inaccurate comparisons of morphologic metrics that are representative of flow magnitudes and not the result of human disturbance. Only aerial photographs from years that have precipitation records of < 5 cm over the last 48 hours were deemed appropriate for comparison to ensure comparable flow conditions.

4. RESULTS

The results of the analyses of volumetric change (using LiDAR and aerial photogrammetry derived surfaces) and morphologic change (using braiding index, beltwidth and ruggedness metrics) are summarized in Table 2 and Figure 19.

Table 2: Results of volumetric and morphologic change detection associated with Subreaches.

			Change over time period indicated		
Data Source	Data	Time Interval	Upstream Subreach	Bridge Subreach	Downstream Subreach
LiDAR	Volume Change	2009 - 2011	-3500 ±1900 m^3	-8400 ± 2600 m^3	6200 ± 2740 m^3
Aerial Photogrammetry	Volume Change	2011 - 2015		-6100 ± 3500 m^3	
Aerial Photogrammetry	Volume Change	2009 - 2015		-14800 ± 3800 m^3	
Aerial Imagery	Braiding Index	1953 - 2011	-6	-7	-4
Aerial Imagery	Beltwidth	1953 - 2011	-575 m	-50 m	80 m
LiDAR	Ruggedness (ratio of variances)	2009 - 2011	0.97	0.82	1.07
Survey	W : d	2015	21	27	36
Survey	Grain Size (D84)	2015	47 mm	45 mm	32 mm
Google Earth	Slope	2013	0.018	0.013	0.015

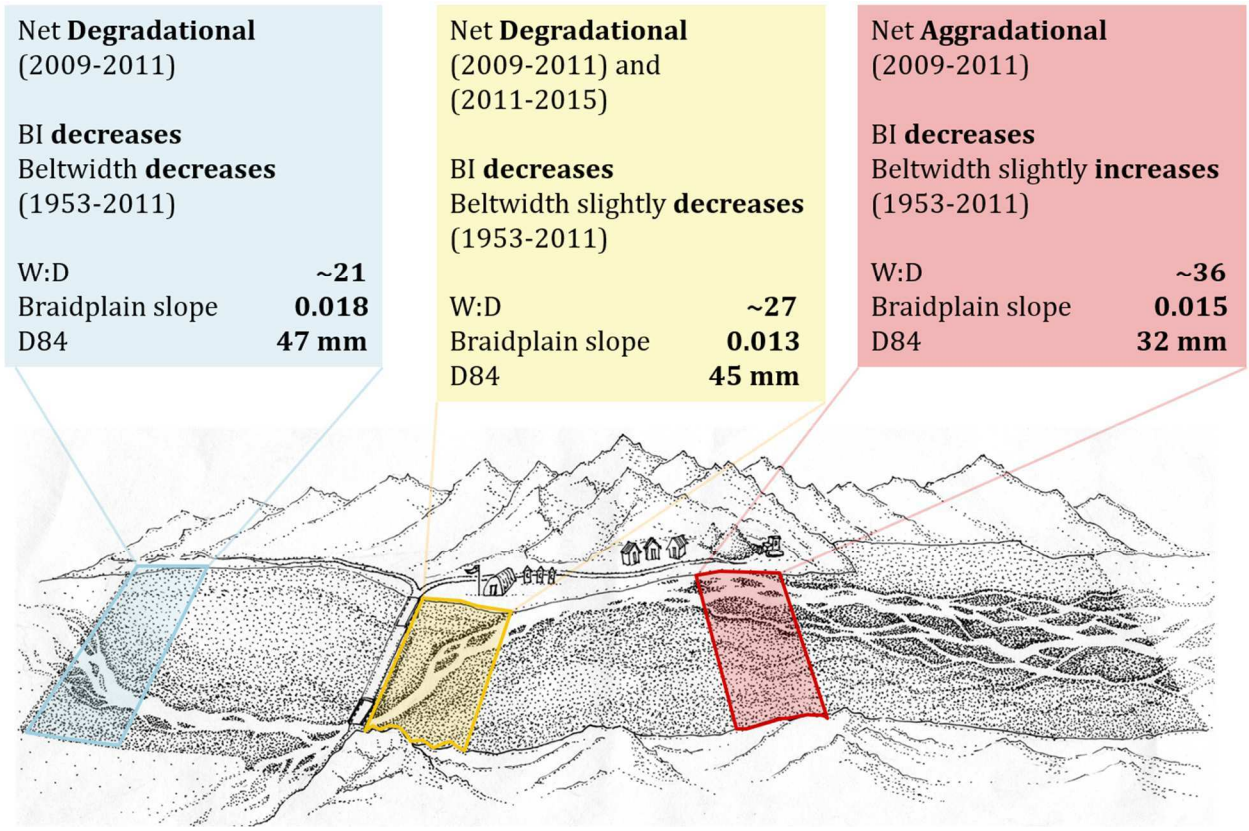

Figure 19: Summary of results associated with Subreaches produced from volumetric and morphologic change detection analyses as well as system characterization data.

4.1 Volumetric Change Detection

Between 2009 and 2011, approximately 17,100 m^3 of gravel were extracted from the braidplain of the Toklat River. Analysis of the 4 km of active braidplain defining the study reach (Figure 11), encompassing all three subreaches and all four influential impact zones, showed significant net degradation within the braidplain between 2009 and 2011, -30,300 ± 27,600 m^3, at the 80% confidence interval between 2009 and 2011 (Figure 20 and 21). Braidplain aggradation or degradation, shown in Figure 20, are used to describe the general location of volume change. Channels that were abandoned between 2009 and 2011 are defined as part of the braidplain and thus degradation associated with individual channels is incorporated into the total braidplain

degradation. Channel abandonment of the 2009 main channel immediately downstream of the East Bridge is indicated in Figure 20. Degradation indicated within this channel may appear enhanced due to the difference between water surface (detected in 2009) and channel bed (detected in 2011).

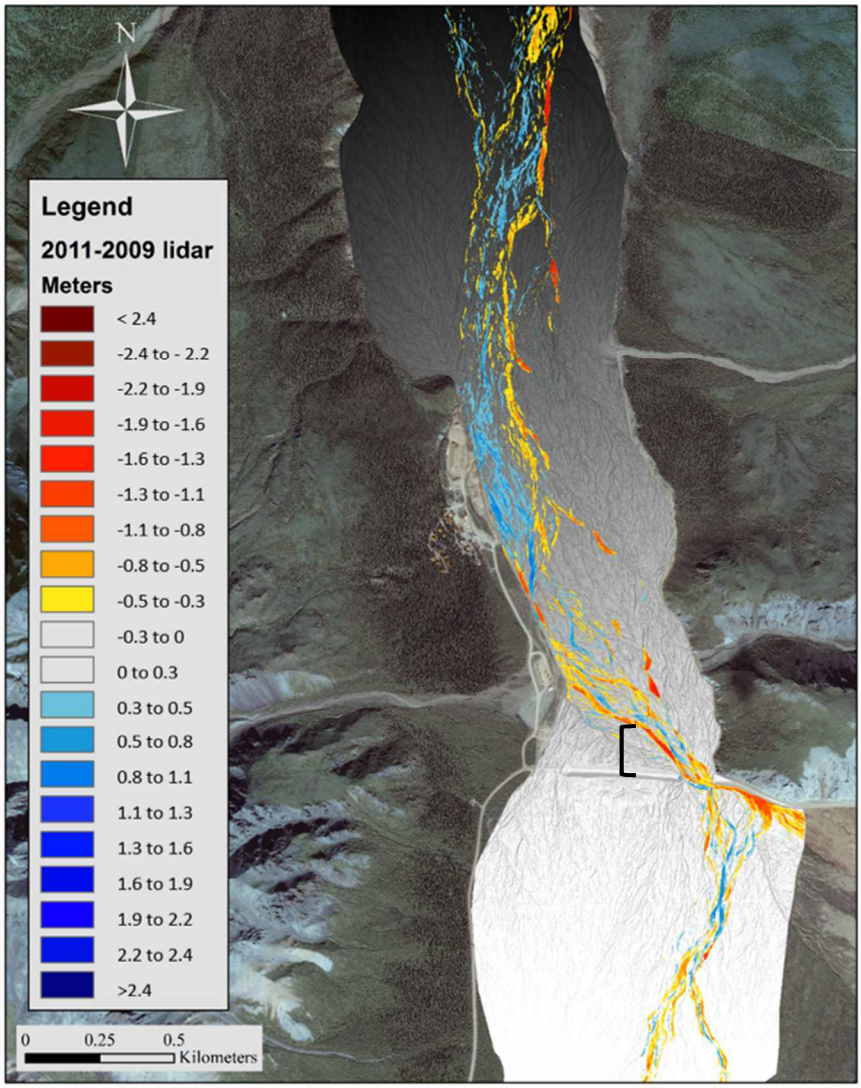

Figure 20: Results of GCD volumetric change detection at 80% confidence for the study reach of the Toklat River. Black bracket indicates the abandonment of the 2009 main channel (red).

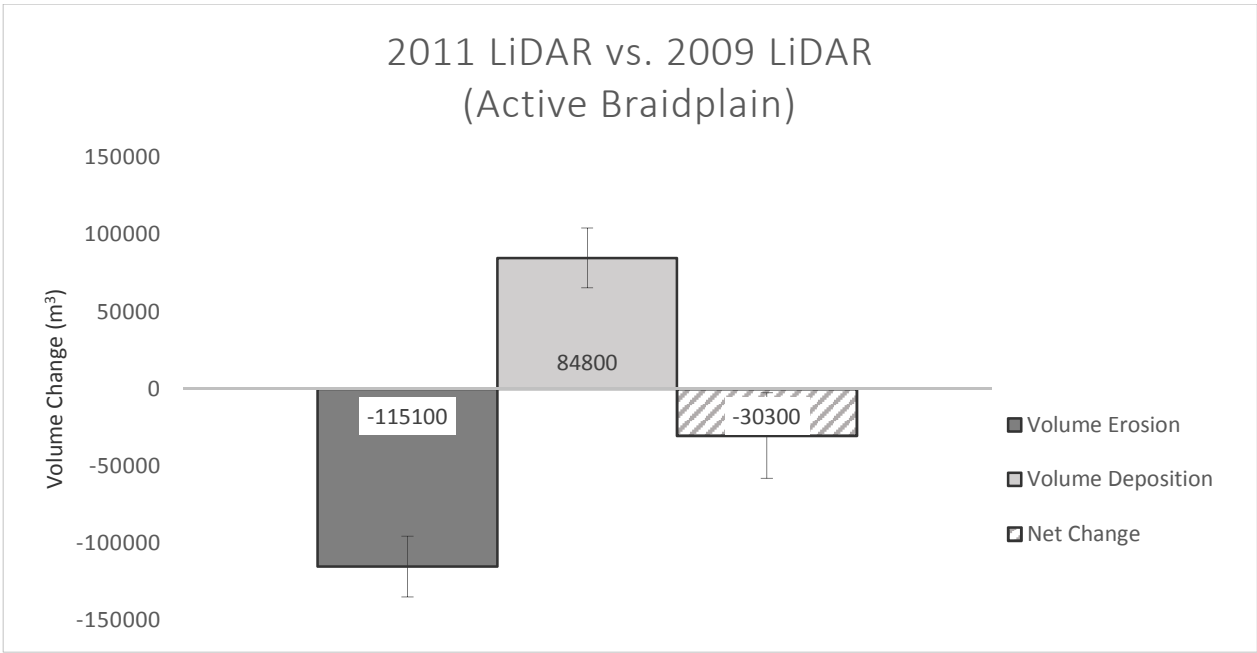

Figure 21: Barplot showing erosion, deposition and net change of the active braidplain of the Toklat River between 2009 and 2011. 80% confidence intervals are represented by the error bars.

Aerial photogrammetry data from 2015 (extent shown in Figure 11), compared to 2009 and 2011, showed significant degradation on the Toklat River at the 80% confidence level (Figure 22). A sediment volume loss of -65,800 ± 18,700 m^3 is evident between 2009 and 2015 (Figure 22), which spans three gravel extractions in 2010, 2012, and 2015, that removed a total of 51,300 m^3. The majority (77%) of gravel removed in 2010, 2012 and 2014 was sourced from downstream of the area captured by aerial photogrammetry, indicating that the 2015 volumes are minimal estimates of total volume change within the study reach over this six-year period (Appendix Table 5). A statistically significant volume of -41,000 ± 17,700 m^3 was measured between 2015 and 2011 (Figure 22), a time period that spans two extractions in 2012 and 2014 that removed a total of 34,200 m^3 of gravel. The majority of gravel extraction (80%) occurred downstream of this area, however, again suggesting that this is likely a minimum volume loss estimate for the study reach.

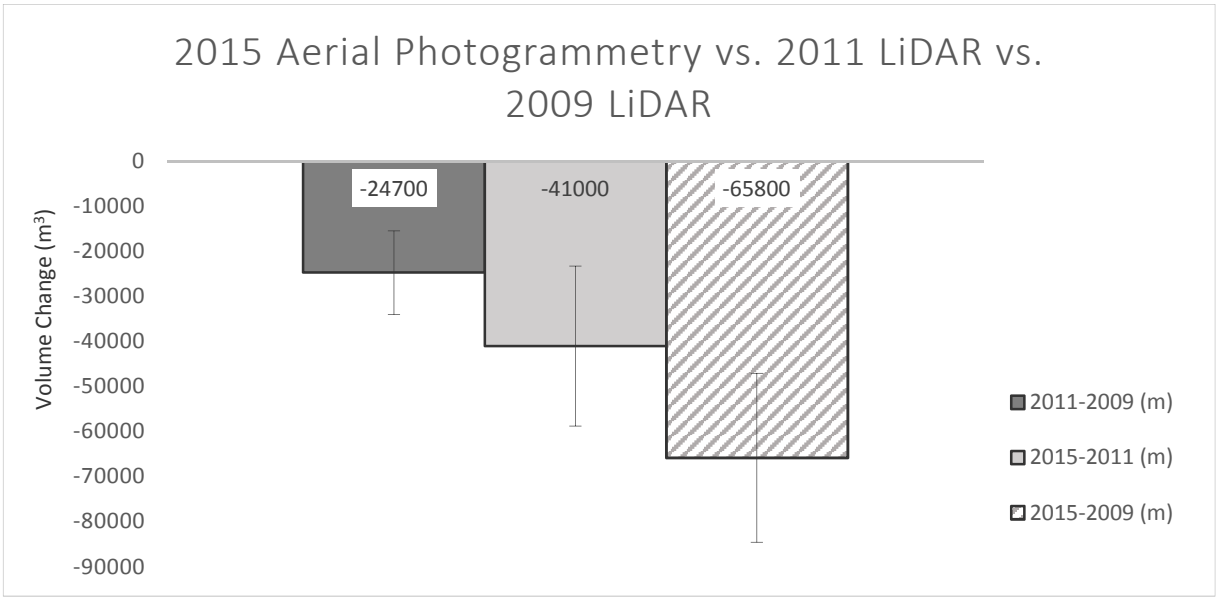

Figure 22: Barplot showing net volume change within the total extent of aerial photogrammetry captured in 2015. The 2011 and 2009 volume change is shown in dark gray, the 2015 and 2011 volume change is shown in light gray, and the 2015 and 2009 volume change is shown with the diagonal pattern. 80% confidence intervals are represented with error bars.

Analyses broken down into the three Subreaches (Upstream, Bridge, and Downstream) (Figure 12) showed statistically significant differences between their individual responses at the 80% confidence level (Figure 23). Both the Upstream and Bridge Subreaches showed net degradation between 2009 and 2011 (-3500 ± 1900 m^3 and -8400 ± 2600 m^3, respectively). The Bridge Subreach continued to be net degradational between 2011 and 2015 (-6100 ± 3500 m^3) (Figure 24). The Downstream Subreach showed a net aggradational trend between 2009 and 2011 (6200 ± 2700 m^3) (Figure 23). The Downstream Subreach, associated with 6200 m^3 of aggradation, overlaps with 18.6 % of the area subjected to gravel extraction in 2010 (Appendix Table 5).

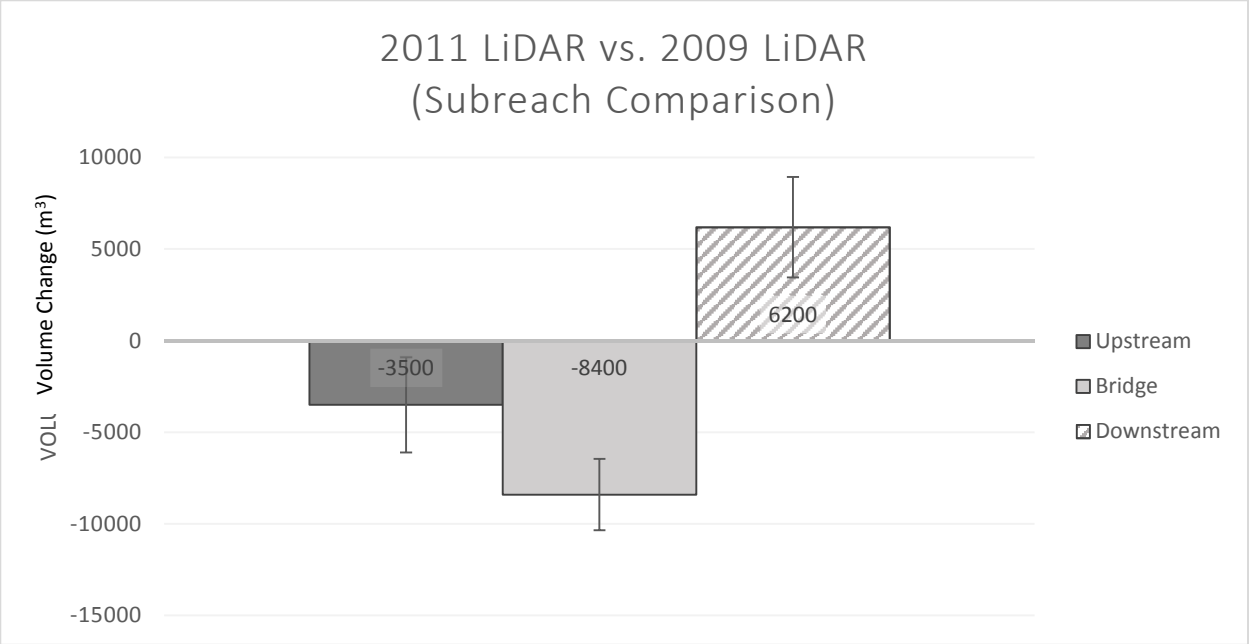

Figure 23: Barplots showing net change within all three Subreaches. Upstream Subreach is shown in dark gray, the East Bridge Subreach is shown in light gray, and the Downstream Subreach is show in a diagnonal pattern. 80% confidence intervals are represented with error bars.

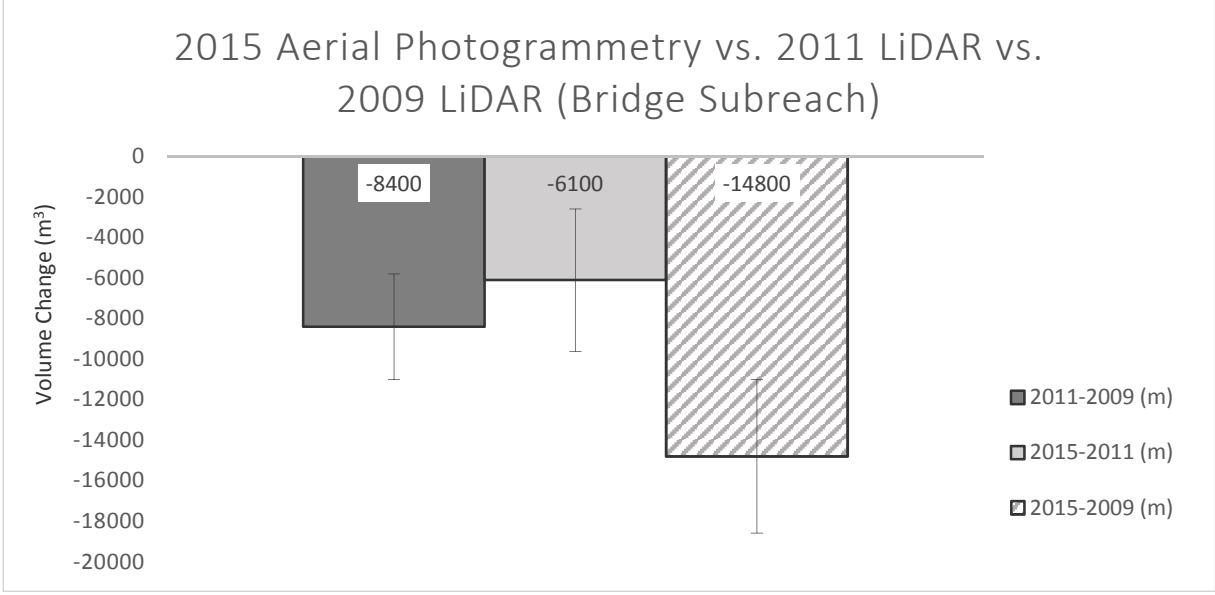

Figure 24: Barplot showing net volume change within the Bridge Subreach using aerial photogrammetry captured in 2015 and LiDAR captured in 2009 and 2011. The 2011 and 2009 volume change is shown in dark gray, the 2015 and 2011 volume change is shown in light gray, and the 2015 and 2009 volume change is shown with the diagonal pattern. 80% confidence intervals are represented with error bars.

Comparison of the four Influential Impact Zones (Figure 13), designed to outline the areas of primary anthropogenic impacts, shows statistically significant degradation at the 80% confidence interval, within the upstream revetment, confinement and gravel extraction zones, and aggradation within the downstream revetment zone (Figure 25). All degradational zones also correlated to a statistically significant increase in ruggedness from 2009 and 2011, corroborating net degradation. The downstream revetment zone showed a smaller magnitude of response, but still statistically significant, of aggradation.

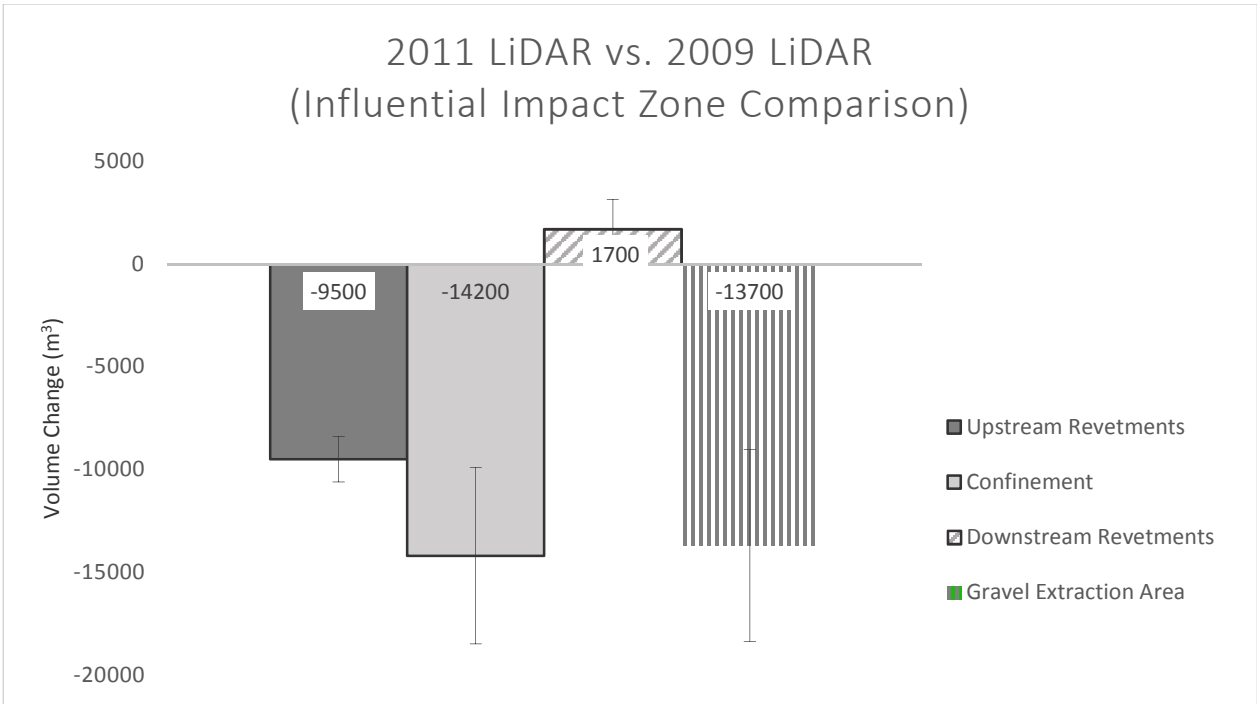

Figure 25: Barplot showing net volume change within each of the four Influential Impact Zones. The dark gray represents the Upstream Revetments, the light gray represents the confinement zone, the diagnonal stripes represent the downstream revetments and the vertical stripes represent the 2010 gravel extraction area. 80% confidence intervals are represented with error bars.

4.2 Morphologic Change Detection

Planform metrics used for morphologic change detection rely upon aerial photographs acquired over a range of temporal and spatial scales. To justify comparisons between years within

the Toklat System, as well as between the Toklat System and its reference reaches, data from the Park Headquarters weather station were used (Table 3).

Table 3: Weather station data associated with aerial photographs used for morphologic change detection analyses. Precipitation records were used as a proxy for discharge to minimize discrepancies between comparisons over time. The Park Headquarters weather station is indicated by "HQ."

Site	Date	Prior 48 Hour Precip. (cm)	Max Temperature (F)	Weather Station
Toklat	7/25/1953	0	80	HQ
Toklat	7/14/1964	0	74	HQ
Toklat	8/4/1988	0.33	55	HQ
Toklat	6/5/1996	0.03	60	HQ
Toklat	8/8/2004	0	79	HQ
Toklat	10/25/2009	0	34	Toklat River
Toklat	7/7/2011	0	67	Toklat River
Teklanika	8/28/1951	0.89	68	HQ
Teklanika	7/14/1964	0	74	HQ
Teklanika	8/4/1988	0.33	55	HQ
Teklanika	6/5/1996	0.03	60	HQ
Teklanika	8/8/2004	0	79	HQ
East Fork	7/25/1953	0	80	HQ
East Fork	7/14/1964	0	74	HQ
East Fork	8/4/1988	0.33	55	HQ
East Fork	6/5/1996	0.03	60	HQ
East Fork	8/8/2004	0	79	HQ

4.2.1 Braiding Index

Analyses of morphologic metric braiding index between the study site and its reference reaches produced statistically signficant results in both trends over time and in the comparison between sites along the Toklat River. A general decrease in braiding index for the period of record, and particularly post-1988, is evident on the Toklat River (Figure 26). This time period corresponds to the initiation of an annual gravel extraction (1985), the installation of the 1986 causeway and bridges, and the construction of the Visitor Rest Area (1988-1989). Incorporating the 2009 and 2011 Toklat data, unavailable for the reference reaches, shows a clear downward trend in BI from 1953 to 2011 (Figure 27). In contrast, the reference reaches displayed slight

upward trends in BI throughout their subreaches for the period of photographic record (1951-2004 on the TEK and 1953-2004 on the EF) (Figure 28).

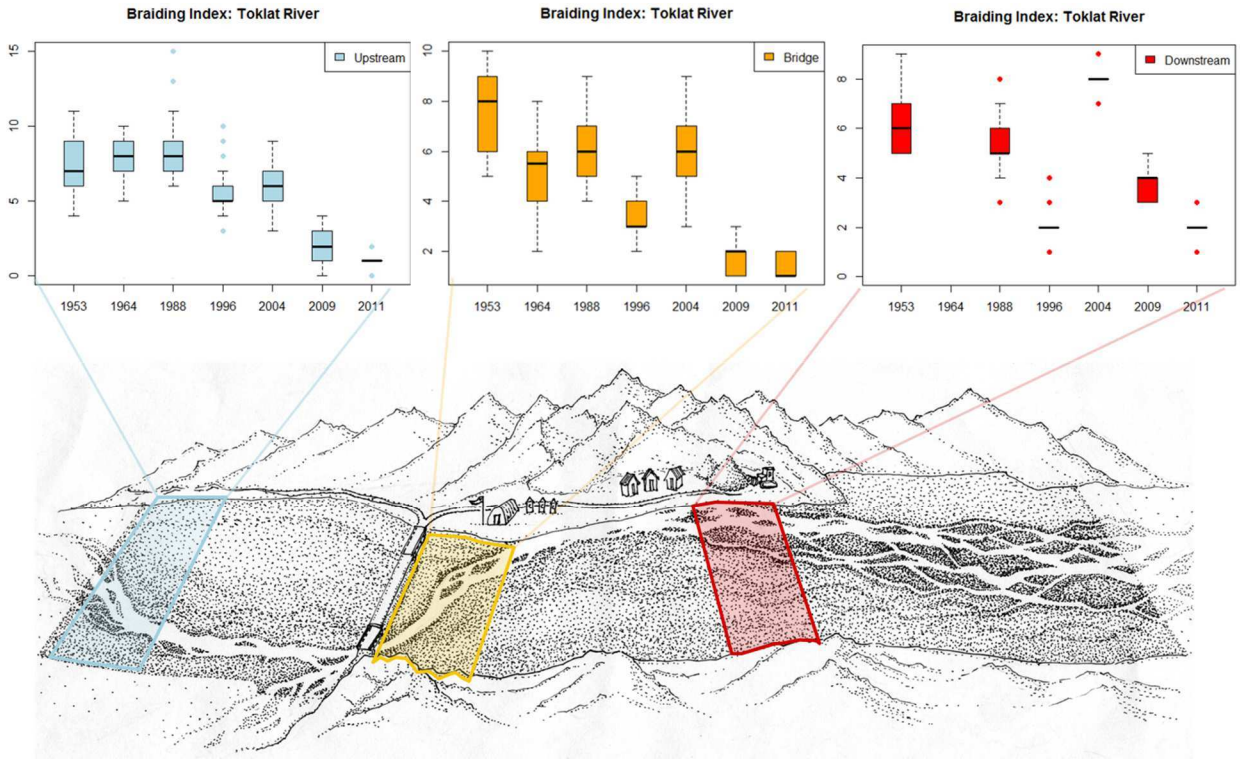

Figure 26: Boxplots showing braiding index measured within Subreaches of the Toklat River from 1953 to 2011. The Subreaches are shown spatially in relation to the study reach and represent Upstream (blue), Bridge (yellow), and Downstream (red), similar to figure 13. Y-axes are not on the same scale.

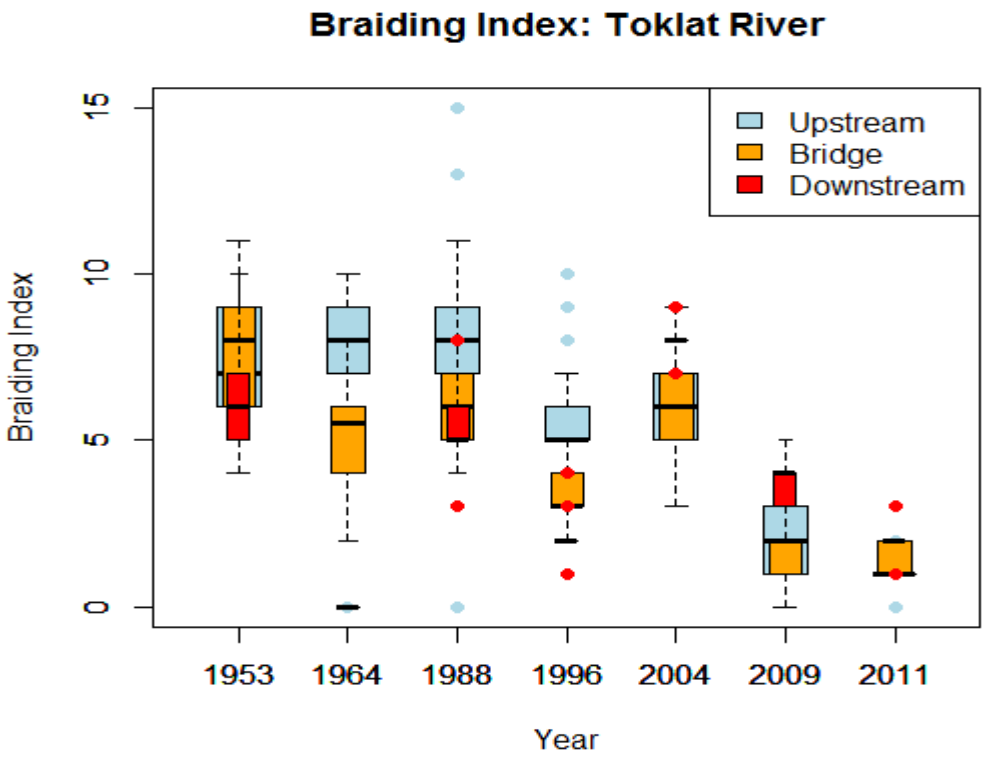

Figure 27: Boxplots showing braiding index measured within Subreaches of the Toklat River from 1953 to 2011. The Subreaches are Upstream (blue), Bridge (yellow), and Downstream (red).

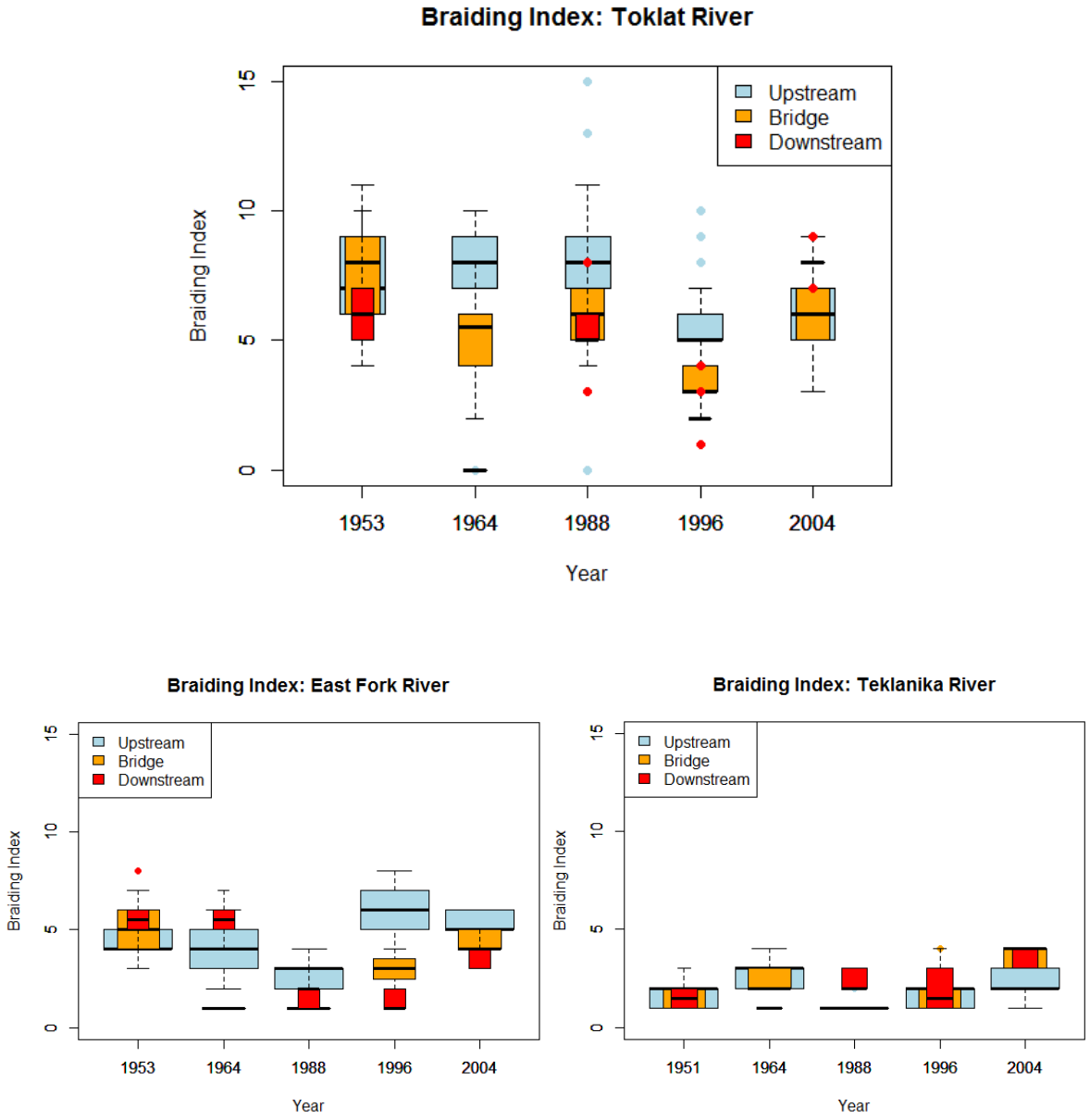

Figure 28: Boxplots showing braiding index measured within Subreaches of the Toklat, Teklananika and East Fork Rivers from 1953 to 2004. Analyses of the Teklanika incorporated aerial photographs from 1951 instead of 1953. The Subreaches are Upstream (blue), Bridge (yellow), and Downstream (red).

4.2.2 Braiding Beltwidths

Analyses of braiding beltwidths show a significant decreasing trend on the Toklat River within the Upstream Subreach (Figure 29 and Table 2), while the Bridge and Downstream

Subreaches stay relatively consistent throughout the period of record (1953-2011) (Figure 29). A substantial reduction in beltwidth occurs between 1988 and 1996 on the Upstream Subreach of the Toklat River, resulting in a loss of ~ 400 m. Slight decreases are seen between 1953 and 1988 on the Bridge Subreach and between 2004 and 2011 on the Downstream Subreach. These trends are distinctly different than those measured in the adjacent reference reaches (Figure 30). The reference reaches exhibit a near-stable trend over time with only slight fluctuations in beltwidth (Figure 31). The largest change between successive aerial photographs is seen on the East Fork between the years 1953 and 1964, where a distinct decrease in upstream beltwidth is evident. Lower magnitude fluctuations are seen on the Upstream Subreach of the Teklanika.

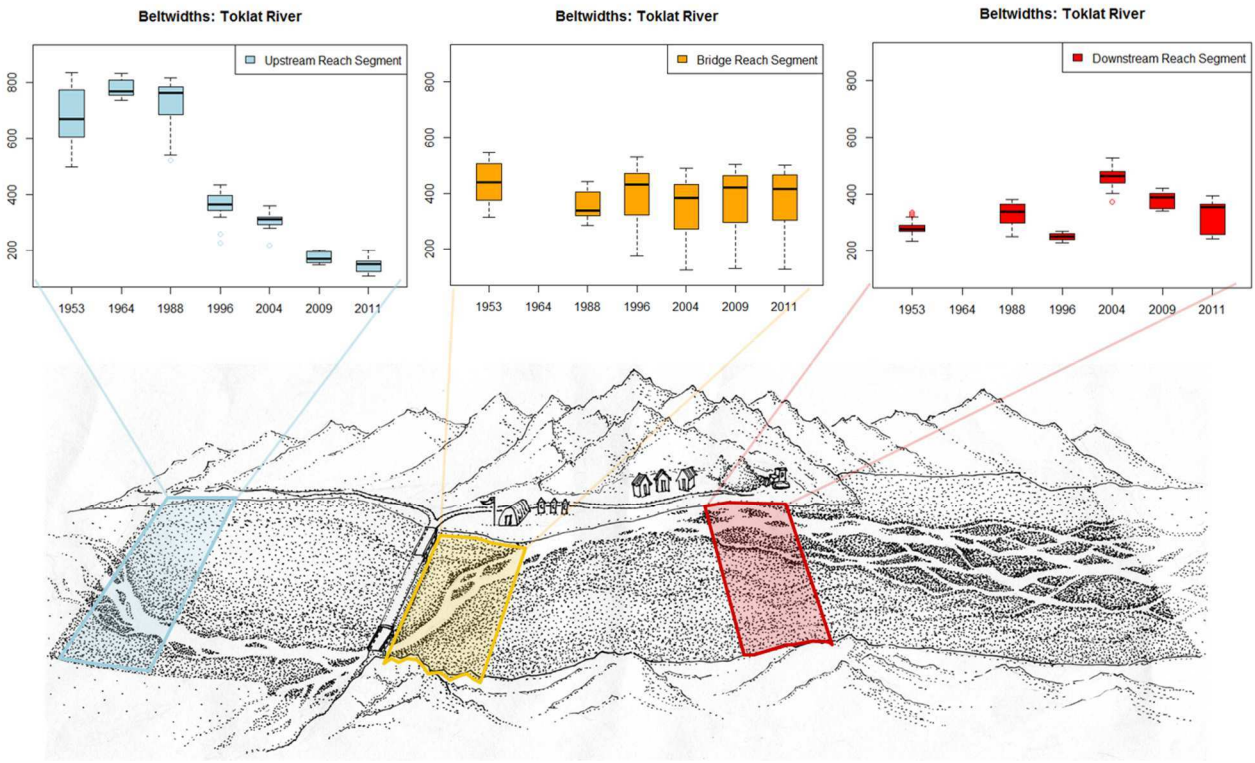

Figure 29: Boxplots showing braiding beltwidth measured within Subreaches of the Toklat River from 1953 to 2011. The Subreaches are shown spatially in relation to the study reach and represent Upstream (blue), Bridge (yellow), and Downstream (red).

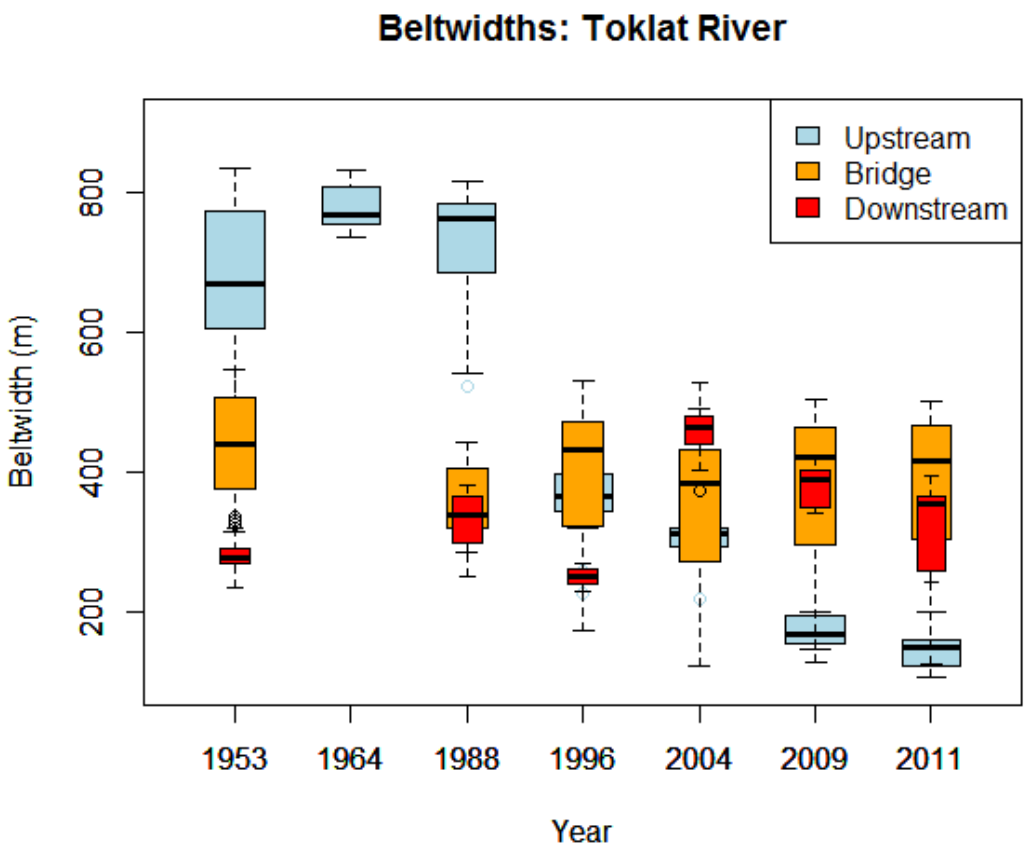

Figure 30: Boxplots showing braiding beltwidth measured within the Subreaches of the Toklat River from 1953 to 2011. The Subreaches are Upstream (blue), Bridge (yellow), and Downstream (red). Note continued decrease in the Upstream Subreach beltwidth in 2009 and 2011. Data from 1964 of the Downstream and Birdge Subreaches were unavailable.

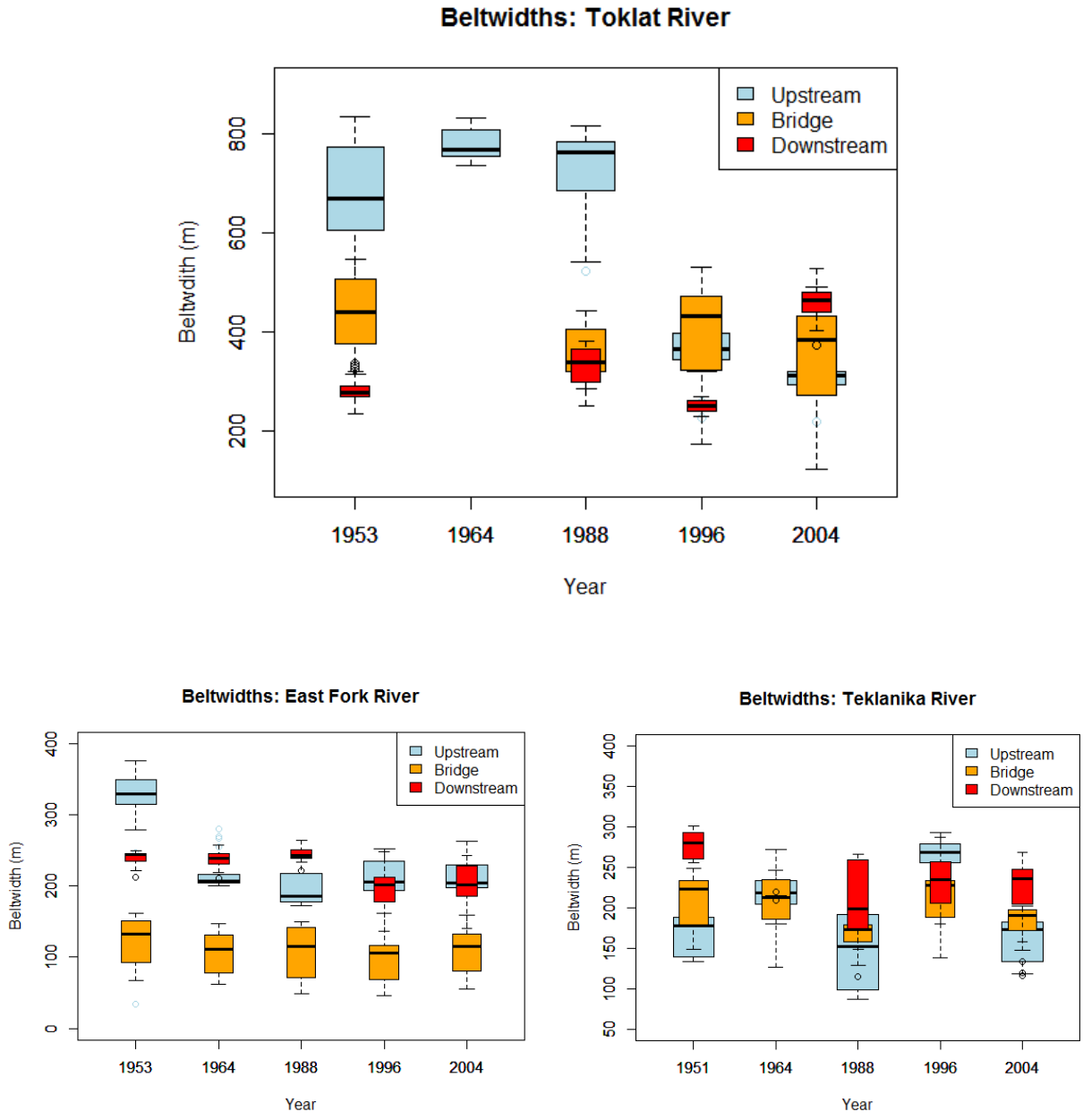

Figure 31: Boxplots showing braiding beltwidth measured withinthe Subreaches of the Toklat, East Fork and Teklanika Rivers from 1953 to 2004. Analyses of the Teklanika incorporated aerial photographs from 1951 instead of 1953. The Subreaches are Upstream (blue), Bridge (yellow), and Downstream (red). Note a distinct decrease in beltwidth evident in the Upstream Subreach of the Toklat River, a trend not evident in either reference reach.

4.2.3 Ruggedness

Ruggedness, measured as the variance of elevation data, shows statistically significant trends from 2009 to 2011 within all Subreaches on the Toklat River (Figure 32a and Table 2).

Ruggedness increased the most substantially at the Bridge Subreach from 2009 to 2011 ($p < 0.001$). The Upstream Subreach also experienced an increase in ruggedness from 2009 to 2011 ($p < 0.001$). Conversely, the Downstream Subreach shows decreased ruggedness ($p < 0.001$).

Ruggedness, with its correlation to volume change over the 2009-2011 period, is the only morphologic metric that correlates with sediment aggradation and degradation. The other two morphologic metrics did not show strong correlation to either aggradaton or degradation. No change in braiding index was seen in the Bridge Subreach, although that area showed the highest level of net degradation in volumetric analyses. BI and beltwidth show slight decreases within the Upstream Subreach, but an unexpected slight decrease in BI and beltwidth was also seen in the Downstream Subreach, an area experiencing net aggradation (Figure 32b and c). These data do not show any systematic correlation between braiding index and beltwidth.

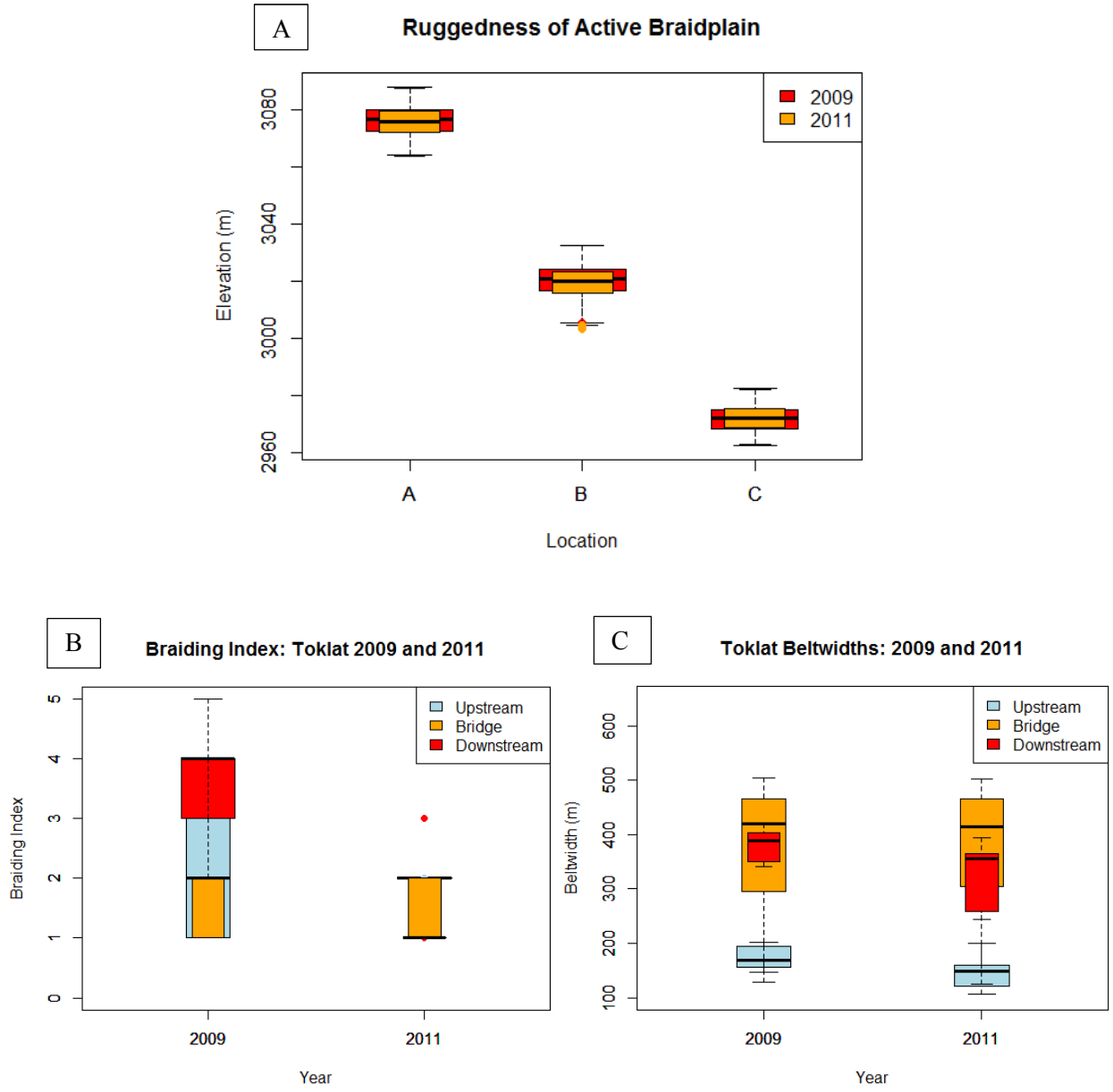

Figure 32: Boxplots showing morphologic metrics measured in 2009 and 2011 to correlate to volumetric change detection results. Image A shows ruggedness (variance of elevation values) measured within the Subreaches (A = Upstream, B = Bridge and C = Downstream)between 2009 (red) and 2011 (yellow). Image B and C show braiding index and beltwdith measured within each Subreach in 2009 and 2011: Upstream (blue), Bridge (yellow), and Downstream (red).

4.2.4 Slope

Braidplain slopes measured from Google Earth using a WGS84 EGM96 geoid indicate differences between the Toklat and its reference reaches, as well as differences within the Toklat

River study reach (Table 4). The braidplain slopes within the Toklat reach varied between Subreaches, indicating two breaks in slope within the study reach: (1) a decrease in slope downstream of at the East Bridge and (2) a return to reach average slope adjacent to Road Camp. The Subreach braidplain slope values and the slope breaks they indicate are corroborated by those CardnoENTRIX (2013) measured using the 2011 LiDAR data (Appendix A). Reach-averaged channel slopes measured from the thalwegs of survey data collected in May of 2015 along the Toklat River were high in comparison to braidplain slopes measured using Google Earth (Table 4). This discrepancy was expected due to the averaging effect of braidplain slope measurements, where floodplain, water surface and channel beds are all incorporated, in contrast to slope measurements connecting channel thalwegs.

Braidplain slopes measured from Google Earth were similar within the Upstream and Downstream Subreaches for the East Fork and Teklanika Rivers (Table 4). The greatest contrast between the reference reaches was within their respective Bridge Subreaches. Braidplain slopes within the Bridge Subreach for the EF were the highest of all its three Subreaches (0.018), but for the TEK this Subreach was the lowest of all three Subreaches (0.005).

Table 4: Braidplain slopes measured from Google Earth WGS84 EGM96 Geoid within the Subreaches of the Toklat and its reference reaches and channel slopes measured using cross-section surveys acquired upstream and downstream of bridges of the Toklat and its reference reaches. Note adjustment in braidplain slopes along Toklat over 7-month period.

Braidplain Slopes from WGS84 EGM96 Geoid				Channel Slopes from Section Surveys	
Subreaches				Reach-averaged	
River	Upstream	Bridge	Downstream	River	Channel Slope
Toklat	**0.018**	**0.013**	**0.015**	Toklat	**0.049**
East Fork	**0.013**	**0.018**	**0.012**	East Fork	**0.038**
Teklanika	**0.010**	**0.005**	**0.012**	Teklanika	**0.034**

4.2.5 Width-to-Depth Ratios

Trends in channel W:d measured in 2015 on the Toklat River indicate spatially distinct differences (Figure 33). The W:d locations show ascending increases in the W:d, a trend not measured in the reference reaches (Figure 33). Additionally, cross-sections from Location F, approximately 3 km downstream from the study reach, showed substantially higher W:d than those of the study reach. W:d values from the references reaches did not show an increasing trend (Figure 34). Cross-section data, from which the W:d data were extracted, are available in Appendix A.

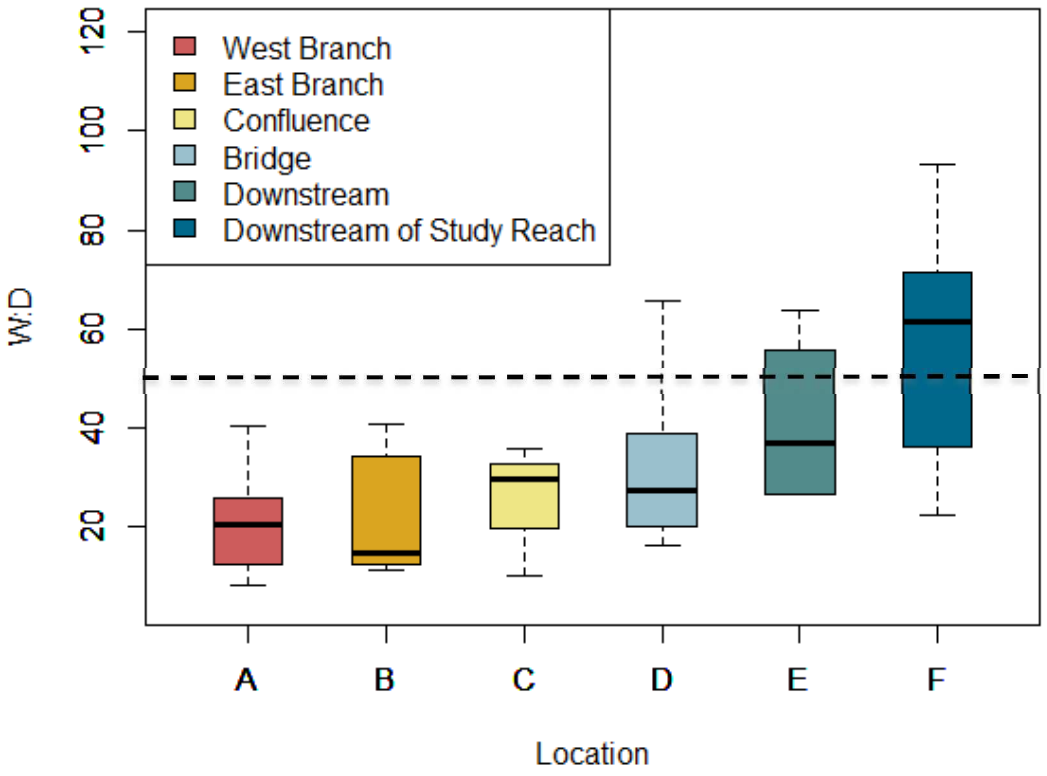

Figure 33: Boxplot showing W:d along the Toklat River. The Toklat W:d data were separated into West Branch (A), East Branch (B), confluence (C), adjacent to and downstream from the East Bridge (D), slightly downstream from the Road Camp (E), and downstream from the study reach (F) (Figure 33). Note increase in W:d from upstream (Locations A and B) to downstream of the study reach (Location E) and substantial increase 3 km downstream of study reach (Location F). Dotted line gives the literature-suggested theoretical average W:d for a braided river (Bridge, 1993; Dust, 2009; Eaton et al. 2010).

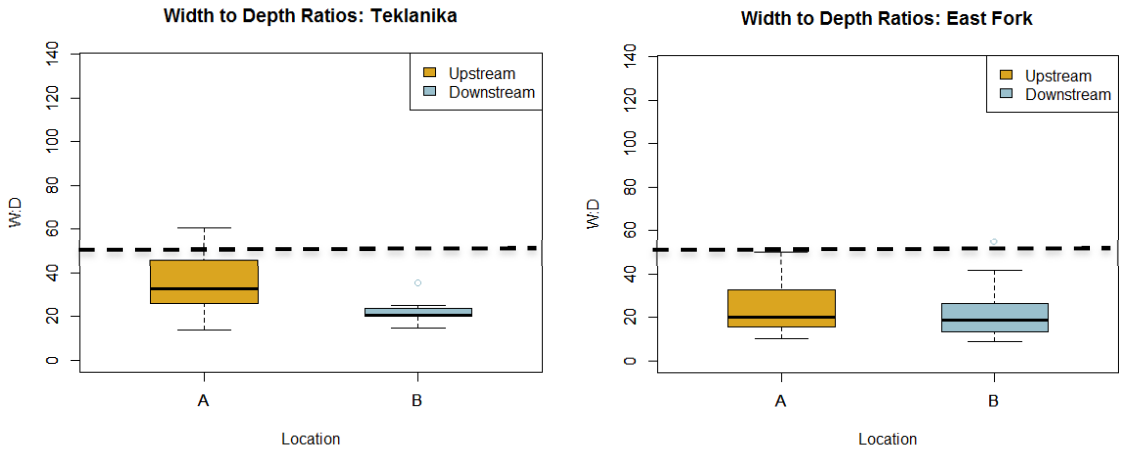

Figure 34: Boxplot showing W:d along the Teklanika and East Fork Rivers. Location A is upstream of each respective bridge, and location B is downstream. Dotted line gives the literature-suggested theoretical average W:d for a braided river (Bridge, 1993; Dust, 2009; Eaton et al. 2010).

4.2.6 Grain Size

Grain size analyses indicate spatial differences in the 50th percentile clast (D_{50}) and 84th percentile clast (D_{84}) within the Toklat and between the Toklat and its reference reaches (Figure 35). A consistent trend across the Toklat and its reference reaches is the general decrease in grain size downstream from the bridge or point of confinement. This trend is most evident on the Toklat River (Figure 35).

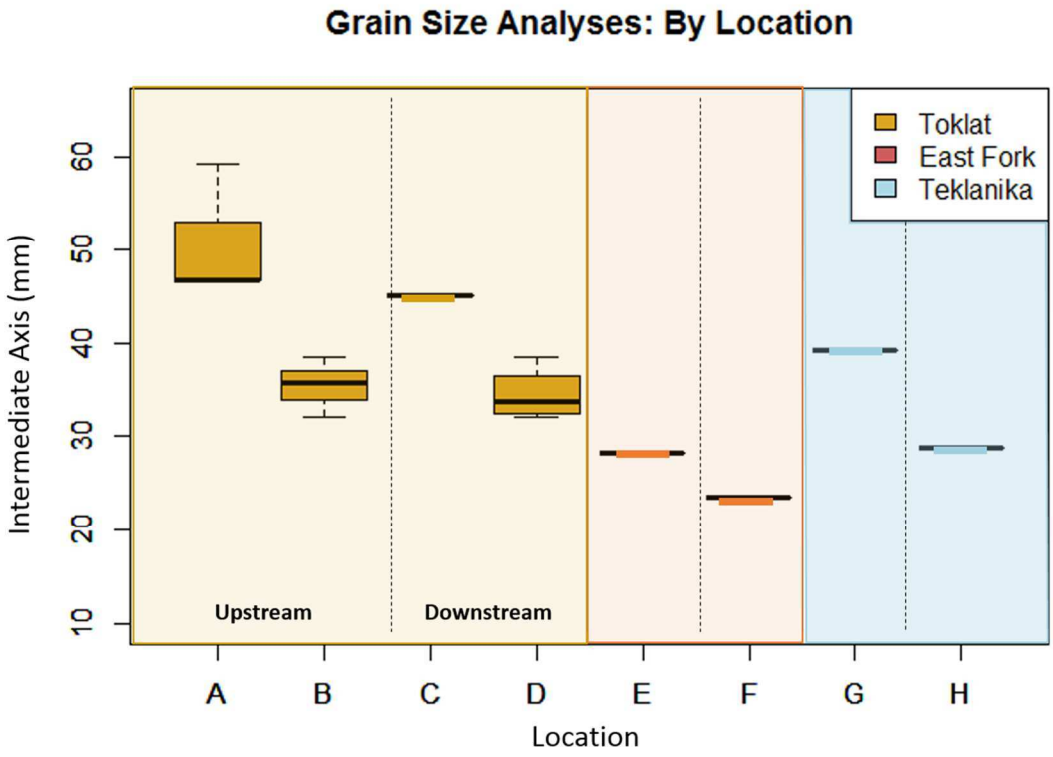

Figure 35: Boxplots showing spatial distribution of grain size on the Toklat River (yellow) and reference reaches (East Fork: red; Teklanika: blue). Specific locations on the Toklat are Upstream West Branch (A), Upstream East Branch (B), the confluence of the two branches at the East Bridge (C), and downstream of Road Camp (D). Specific locations of the reference reaches are upstream of the bridge on the East Fork (E) and downstream (F); and upstream of the bridge on the Teklanika (G) and downstream (H). Note vertical dashed line representing bridge or point of confinement along each river.

4.2.7 Repeat Oblique Photos

Oblique repeat photos of the Toklat River over a period of six decades show noticeable encroachment of vegetation, corresponding to the abandonment of floodplains upstream of the causeway and West Bridge (Figure 36). Downstream of the bridge, repeat photos show a decrease in beltwidth, increased ruggedness and flow concentration within the braidplain (Figure 37). Furthermore, the repeat photos document increased incision of the main channel upstream of the East Bridge (Figure 38). These qualitative assessments correlate to the quantitative results (e.g., Table 2), indicating volume loss in the Upstream Subreach and an increase in ruggedness in recent years.

Figure 36: Images taken in 1954 (left) and 2015 (right) looking northeast and downstream on the Toklat River. West Bridge is at image center indicated with brackets. Note loss of floodplain and encroachment of vegetation in previously active floodplain. Flow direction is away from the camera, indicated by arrow.

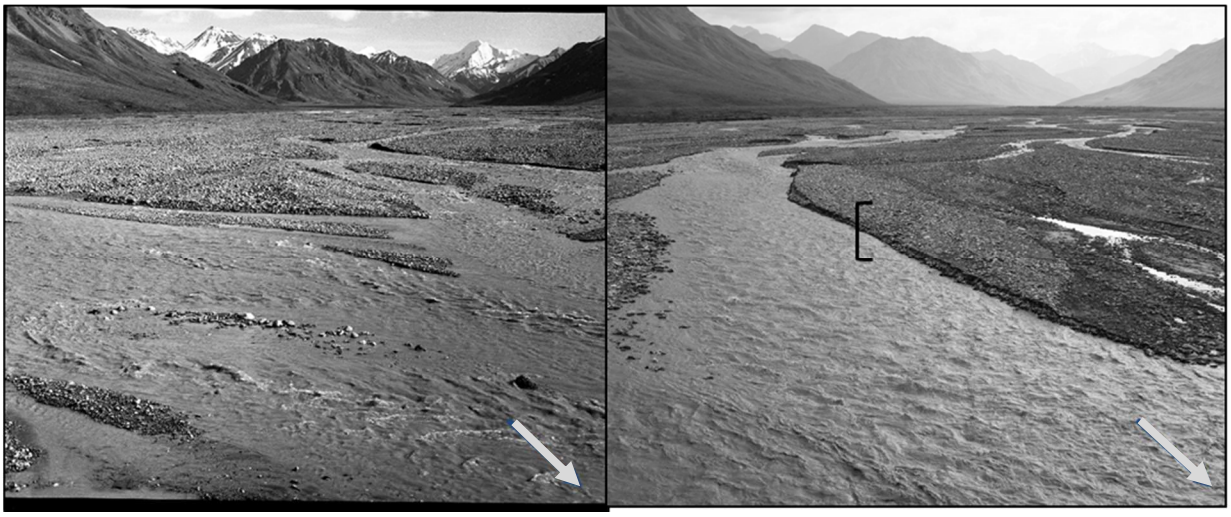

Figure 37: Images taken in 1965 (left) and 2015 (right) showing the Toklat River, looking south and upstream of the East Bridge. Note increased relief along river left bank of main channel (brackets) and concentration of flow into one main channel in 2015 image. Flow direction is towards the camera, indicated by arrow.

Figure 38: Images taken in 1965 (left) and 2015 (right) showing the Toklat River, looking southeast across the West Branch and upvalley into the East Branch. Note vegetation encroachment into the previously active floodplain (foreground) and apparent incision of main channel of the West Branch in the middle distance (brackets). Flow direction of the West Branch is indicated with an arrow.

Repeat photos also highlight differences between the Toklat River and its reference reaches. At the East Fork River, photos from 1967 to 2015 show minimal change apart from a recent debris flow downstream of the bridge (Figure 39). The Teklanika River also showed minimal net change to planform, ruggedness and beltwidth occupation, with minor fluctuations around a line of equilibrium (Figure 40). In contrast, images of the Toklat River show clear, one-directional morphologic change in the form of braidplain and floodplain abandonment (Figure 38).

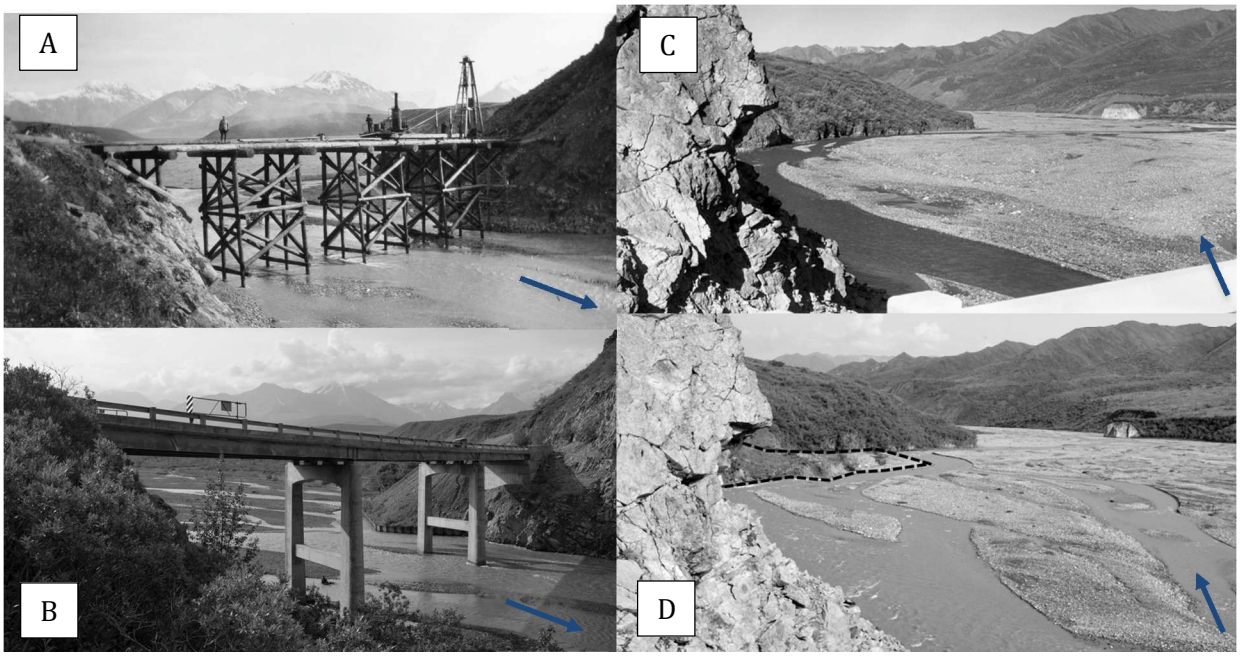

Figure 39: Repeat photographs of the East Fork River. Image A (1935) was reoccupied in 2015 (Image B), showing minimal planform change through the natural bedrock confinement. View is to the southwest looking across and slightly upstream of the bridge. Image C (1963) shows main channel flowing downstream of the bridge against bedrock, and Image D (2015), shows a recent landslide fan (outlined in black dashed line) forcing flow away from bedrock towards center of braidplain, and increased BI. Flow direction is indicated by arrow.

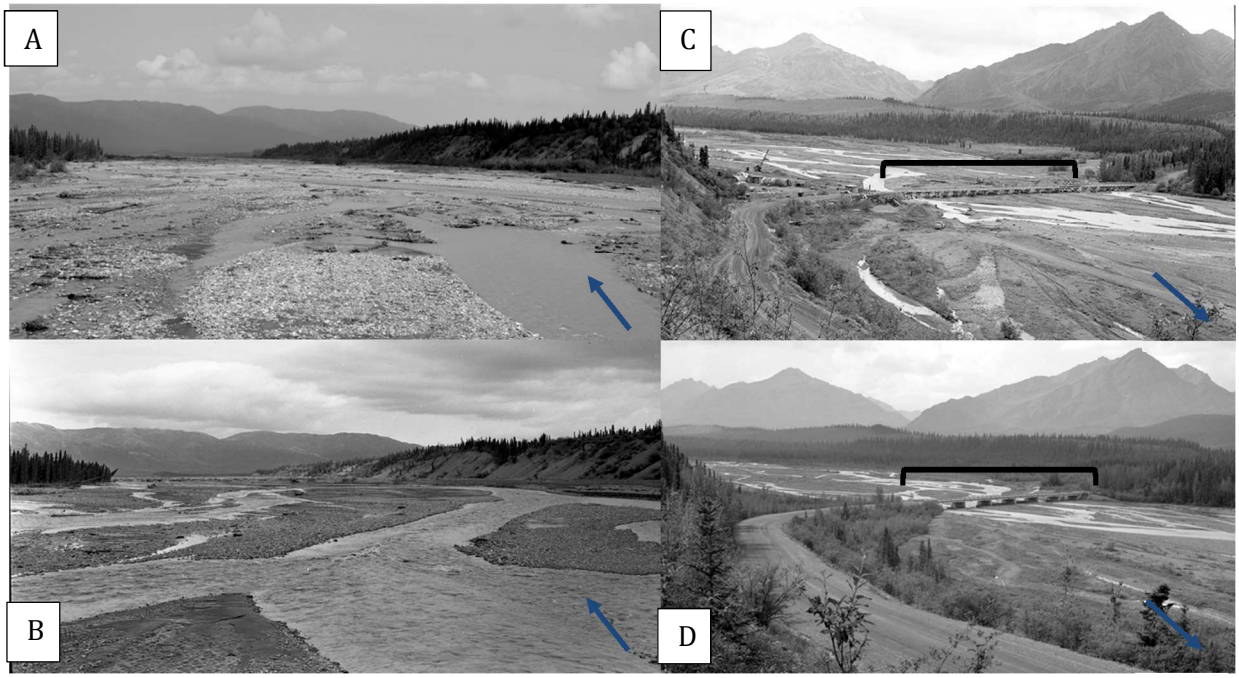

Figure 40: Repeat photographs of the Teklanika River. Image A (1960s) was reoccupied in 2015 (Image B), showing minimal planform change and comparable braidplain occupation. View is to the north downstream of the bridge. Image C (1955) shows similar planform to that of Image D (2015). Teklanika Bridge is shown with a bracket in C and D. Flow direction is indicated by arrow.

5. DISCUSSION

Analysis of braided river morphology to assess the effects of human disturbance requires an holistic approach that identifies response variables and the driving boundary conditions. Metrics of volume change including braiding index, beltwidth and ruggedness used in this research are response variables affected by a dynamic ratio of boundary conditions, water and sediment inputs. These metrics were developed in order to quantify the rate and spatial extent of river response to altered boundary conditions and external forcings across a range of braided river systems.

5.1 Toklat River Response to Human Disturbance

The response of the Toklat River to human disturbance due to confinement and gravel extraction was documented along the study reaches using volumetric and morphologic change detection. The migration of channel adjustments throughout the study reach is evident by the nature and timing of channel and planform response. It is useful to visualize these channel adjustments using Lane's balance, modified for braided rivers (Figure 41).

Recent work has incorporated W:d into Lane's Balance (Dust, 2014; Huang et al., 2014; Dust and Wohl, 2012) as a channel adjustment to changing boundary conditions. This addition to Lane's balance is appropriate for braided rivers because their channel geometry is especially sensitive to alteration, a consequence of unconsolidated sediment (Ashmore, 2013). Because of this sensitivity, W:d has been used as an indicator of the braiding threshold (Eaton et al., 2010; Bridge, 1993) and is used here as a potential channel response to altered inputs (Figure 41). In Figure 41, a decrease in W:d can be visualized as the scale bar sliding horizontally towards the viewer's right, a channel response to high sediment input (heavier sediment pan) relative to discharge (water bucket) that increases sediment transport (Dust and Wohl, 2014; 2012). In reality,

an adjustment to width likely gives rise to multiple partially compensating responses, such as alterations in grain sizes transported and slope, complicating this relationship. An increase in depth, associated with low W:d and increased shear stress, also relates to channel slope and substrate size. Increasing depth through sediment recruitment of material from the bed results in only the larger clasts remaining, or channel armoring (the movement of the sediment pan to the viewer's left, increasing grain size). This decrease in W:d or increase in depth can also be balanced by a decrease in slope (the movement of the water bucket towards the center of the scale). The flatter slope results in decreased shear stress and stream power, thus reducing sediment transport capacity (Buffington and Montgomery, 1997; Schumm, 1993; Ashworth and Ferguson, 1986). Multiple, simultaneous responses of a channel to alteration allows it to maintain a state of dynamic equilibrium, where every adjustment is met with multiple responses that compensate for the initial stimulus over time.

When a system is disturbed this equalizing response, or return to a state of dynamic equilibrium, may not occur. Unequal inputs of water and sediment can produce channel geometries that enhance this imbalance. The instances of braided planform simplification following a net degradational imbalance of inputs are widespread (Ashmore and Rennie, 2013; Horn et al., 2012; Fotherby, 2009; Rempel and Church, 2009; Rinaldi et al., 2005; Church et al., 2001; Meador and Layher, 1998; Kondolf, 1997; Montgomery and Buffington, 1997; Graf, 1981). This degradation has been documented to correspond to decreased W:d and likely increased transport rates (Dust and Wohl, 2012; Kondolf et al., 2002; Germanoski and Schumm, 1993).

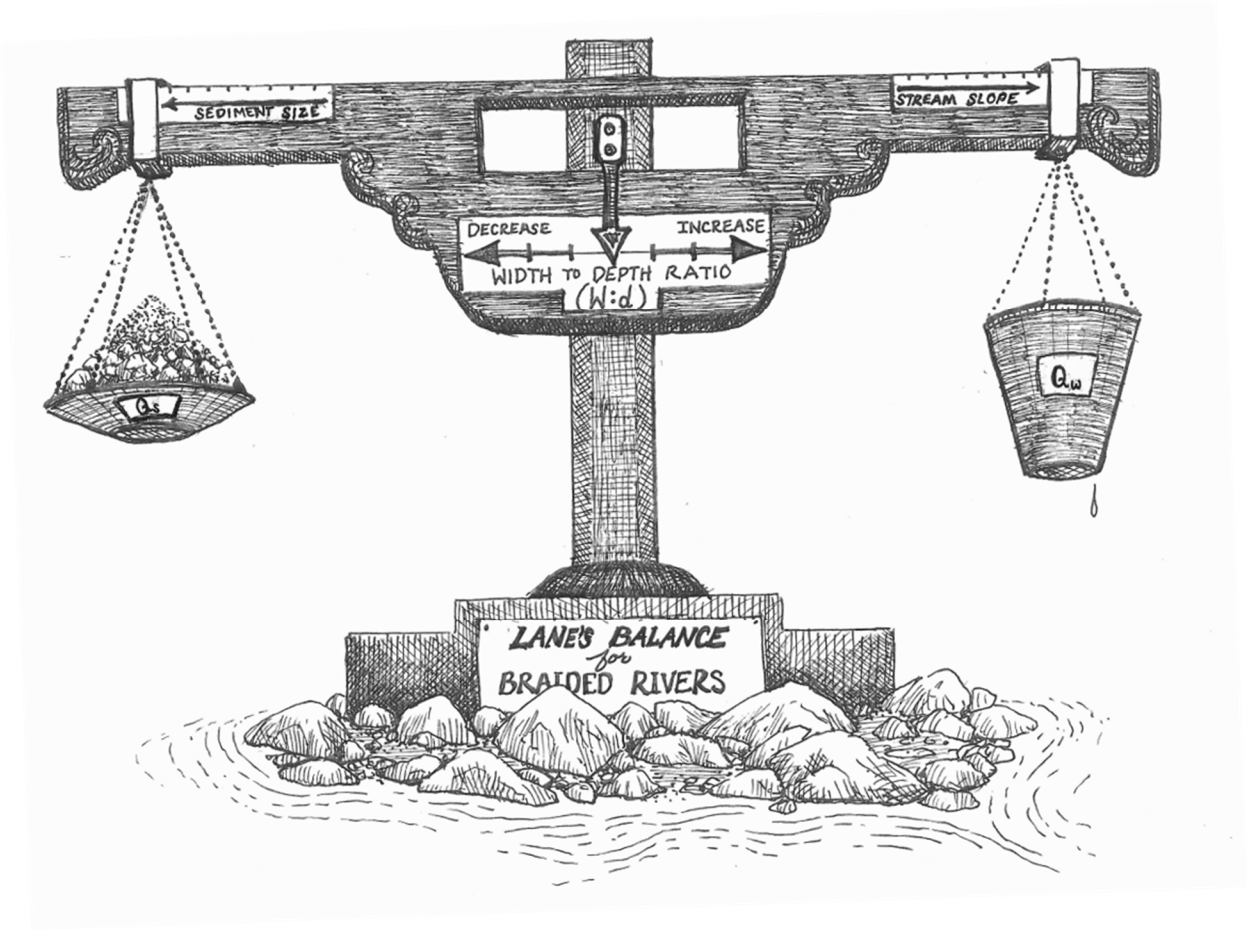

Figure 41: Illustration showing Lane's balance modified for braided rivers. Water bucket and sediment pan represent regime boundary conditions that can be slid along the scale beam to adjust for changing slope and sediment size. Modified from Dust and Wohl's (2014) expanded Lane's relation.

5.1.1 Upstream Subreach

The following sections interpret the results of this research over time and space, using the Toklat River Subreaches, in the context of Lane's balance. In 1953, the Upstream Subreach was occupied by the West Branch of the Toklat River that split within this region to flow equally between the East and West Bridges. The braidplain at this time occupied the majority of the valley width, resulting in high BI and beltwidths. At this point the causeway blocked only 45% of the valley width downstream. In 1954, the bridge and causeway were rebuilt following a flood, with the causeway increasing its relative width to occupy 62% of the valley width. High BI and beltwidths continued to characterize the Upstream Subreach in 1964. The annual gravel extraction

initiated in 1985 with unknown volumes allotted. In 1986, the current bridges and causeway were built, with 60% of the valley blocked by the causeway spanning between the East and West Bridges. In 1988, the Visitor Rest Area was built downstream of the West Bridge on what was part of the active braidplain as recently as 1953 (Figure 6a). This construction placed fill material within the previously active braidplain and erosion mitigation structures directly downstream from the West Bridge, impeding flow paths (CardnoENTRIX, 2012). Between 1988 and 2011, braiding beltwidth decreased (from 675 m to 275 m) and BI decreased (from 8 to 1).

The decrease in beltwidth and BI is consistent with field data collected in 2015 within this Subreach, low W:d (~21), and relatively large D_{84} (47 mm). Narrowed beltwidths are associated with a decrease in channel W:d by minimizing the ability of a river to laterally expand (Ashmore and Sauks, 2006; Ashmore et al., 2011; Bertoldi et al., 2009; Egozi and Ashmore, 2009; Surian and Cisotto, 2007; Surian, 1999). Decreased W:d likely results in higher grain size in response to bed recruitment. The Upstream Subreach also had the highest braidplain slopes (0.018) measured from Google Earth and corroborated by 2011 LiDAR data (CardnoENTRIX, 2013).

The high D_{84} within the Upstream Subreach suggests channel armoring has occurred in response to increased stream power and shear stress. The low beltwidth, BI, and W:d, and high slope are interpreted as the result of imbalanced inputs creating excess shear stress and stream power. Channel and planform geometry known to increase sediment transport (Dust and Wohl, 2012; Kondolf et al., 2002; Germanoski and Schumm, 1993) characterizes the Upstream Subreach, an area experiencing net degradation (-3500 ± 1900 m^3 between 2009 and 2011). Morphologic metrics combined with the historical background of human disturbance indicates the Toklat River through this Subreach is not adjusted to alteration in the forms of increased confinement by the

causeway and Visitor Rest Area, as well as potential upstream migration of sediment depletion by the gravel extraction.

5.1.2 Bridge Subreach

Braiding index within the Bridge Subreach on the Toklat River decreased from 1953 to 1996, a period of time that incorporates: (1) two iterations of bridge and causeway construction in 1954 and 1986, with the causeway blocking 62% and 60% of valley width, respectively; (2) initiation of annual extraction of unknown volumes in 1985; and (3) the construction of the Visitor Rest Area on previously active braidplain from 1988-89. Beltwidth decreased slightly between 1953 to 1988 and then remained stable, despite high flows captured in 2004. High flows in 2004 resulted in higher BI, and mark the last year that flow occupied the West Bridge. Lower BI followed in 2009 and 2011, while beltwidth remained stable. This Subreach showed the largest volume of sediment removed between 2009 and 2011 (-8400 ± 2600 m^3).

Degradation within this reach between 2009 and 2011 primarily occurred within the area that was occupied by the main channel in 2009 and abandoned in 2011. This focused degradation within the Bridge Subreach may be due to flow coalescence adjacent to the East Bridge, indicated by the concentration of degradation within the previously active channels, rather than evenly across the braidplain. The East and West Branches have converged beneath the East Bridge since 2005 (CardnoENTRIX 2012). Flow coalescence has been shown to create conditions of high stream power due to the relative increase in discharge (Ashmore and Parker, 1983; Mosely, 1976).

Field data are consistent with planform and volumetric change indicating degradation. The low W:d (~27) and large D_{84} (45 mm) measured at the confluence suggest greater erosive power associated with convergence of flow. To compensate for a local increase to stream power, Lane's balance predicts a decrease to slope, visualized in Figure 41 as the movement of the water bucket

towards the center of the scale. Braidplain slopes measured downstream of the East Bridge from Google Earth and 2011 LiDAR data, respectively (0.013-0.011) (CardnoENTRIX, 2013), were noticeably lower than those measured within the Upstream Subreach (0.018) and averaged across the study reach.

The lower slope and large grain size imply channel response to an initial stimulus of excess energy, likely generated by the combination of flow coalescence and confinement. As evidenced by the continued net degradation, these channel geometry adjustments are not capable of compensating entirely for excess energy, but can simultaneously adjust over time and space to work towards dynamic equilibrium. The reduction in braidplain slope and increase in W:d, although unable to fully compensate for imbalances to energy within this Subreach, may influence the channel response farther downstream.

5.1.3 Downstream Subreach

Downstream from the East Bridge and adjacent to the Toklat Road Camp, an interesting transition occurs, indicated by morphologic metrics and volume change. The Downstream Subreach was the only Subreach characterized by increasing beltwidths up until 2009. During the high flow year of 2004, braiding index and braiding beltwidth increased downstream substantially more than in the other two Subreaches, a trend that Ashworth et al. (2007) associate with channel avulsion and depositional environments. Consistent with this interpretation, volumetric change detection showed net aggradation (6200 ± 2700 m^3) occurring within this Subreach (Table 2). Ruggedness decreased within this zone, a probable consequence of channel bed deposition. The Downstream Subreach also showed a marked increase in average W:d (~36) and a decrease in average grain size (32 mm). The slope of the braidplain through the Downstream Subreach was equal to the reach averaged slope of 0.015-0.013 m/m as measured from Google Earth and 2011

LiDAR data, respectively. These characteristics suggest that a substantial decrease in local stream power and shear stress occurred between the Bridge and Downstream Subreaches, likely caused by the flattening of braidplain slopes downstream of the East Bridge.

5.1.4 Comparison to Reference Reaches

The morphologic metric beltwidth shows varying trends over time that highlight differences between the Toklat and its reference reaches. The Teklanika shows minor fluctuations through time with no clear trends exhibited within any Subreach. Conversely, the Toklat shows a clear trend of decreasing beltwidth within the Upstream Subreach. Distinct differences within trends exhibited in the Upstream Subreach between the Toklat and Teklanika suggest there is a driver at play on the Toklat that is not present on the Teklanika.

Beltwidth trends within the Upstream and Bridge Subreaches indicate similarities between the East Fork and Toklat. The beltwidth decreases 43% (from ~350m to ~200m) on the East Fork between 1953 and 1964 and decrease 50% on the Toklat between 1988 and 1996 (from ~800 to ~400m). However, the decrease in upstream beltwidth on the East Fork levels off in 1964, where that of the Toklat continues to decrease throughout the period of record. The continued decrease in beltwidth on the Toklat River is attributed to the unnatural source of confinement and exacerbation of this driver by the initiation of gravel extraction practices.

The Upstream and Downstream Subreaches of both the Tokalt and East Fork exhibit the largest changes in beltwidth, commonly in opposite directions, with minimal change exhibited in the area of the East Bridge. For example, an increase in downstream beltwidth occurred alongside a decrease to upstream beltwidth around 1988. The minimal change in beltwidth measured within the Bridge Subreaches on the Toklat and East Fork Rivers and causeway, despite the net

degradation known to be occurring within this Subreach on the Toklat River, suggests a decreased ability to respond to changing boundary conditions adjacent to confinement.

5.2 Review of Methodologies

My methodology was designed to acknowledge that braided river systems have inherent qualities that limit accurate quantification of flow and sediment transport processes. These qualities include varied and high rates of sediment mobility, intricate channel bed and floodplain topography, vast wetted channel area, and rapidly changing planform (Ashmore and Rennie, 2013; Curran and McTeague, 2011; Brasington et al., 2003; Hicks et al., 2002; Emmett et al., 1996; Nicholas et al., 1995). To quantify sediment transport in braided rivers, at least ten years of sediment collection data are recommended to produce reliable results (Curran and McTeague, 2011; Ashmore, 1991; Wolman, 1954), a time frame that was infeasible within this research project. Thus, the research design shifted focus of investigation from sediment transport to sediment storage based on the understanding that changes in net storage of sediment on the braidplain, and the morphologic features created by that stored sediment, is of greater geomorphic and management interest than the quantity of sediment passing through the reach. Investigating the visible expressions of stored sediment through planform change over long periods of time and over a greater spatial range was incorporated through morphologic metrics of change.

The intricacies of braided river floodplain and channel structures and the variability of their inherent processes of morphologic formation and destruction require high-resolution data to capture associated trends (Chandler et al., 2016; Williams et al., 2014; Lane et al., 2010; Wheaton et al., 2010; Hicks et al., 2008; Rumsby et al., 2008; Brasington et al., 2003, 2000; Westaway et al., 2003; Stojic et al., 1998). High-resolution data, however, are often cost-prohibitive to acquire at sufficiently short intervals to capture these short-term trends. My research incorporated high-

resolution data sets available previously (airborne LiDAR) and those using newer, more cost-efficient techniques (aerial photogrammetry) in an effort to overcome these logistical difficulties. Both approaches produced statistically significant findings of volumetric change in sediment storage across the braidplain, with analysis and adjustments for spatially variable error using available software. The comparable results between these two approaches suggest that trends of volume change derived from aerial photogrammetry are comparable to those derived from LiDAR, but they have less certainty in the precision of volume estimates.

For purposes of monitoring future change to the Toklat River as a result of human activities, volumetric techniques were paired with morphologic metrics to assess the reliability and applicability of the morphologic metrics. The results of morphologic metrics could be improved by capturing images at similar flows. Braiding index from different years require aerial photographs that capture consistent flow or incorporate some way of normalizing the results based on discharge differences (Ashmore and Sauks, 2006; Hughes et al., 2006; Brasington et al., 2003; Fuller et al., 2003). At present, braiding index results in this analysis are likely skewed due to disparities in discharge between dates in different years of available aerial photographs. Even without consistent flow conditions in the aerial photographs, trends in the morphologic metrics could be identified that broadly correspond to the degradational signals indicated by volume change detection. Correlation between volumetric and morphologic change detection is most evident in the braiding beltwidth and ruggedness metrics, recognizing that the latter metric requires the greater precision of LiDAR-derived point data. This correlation indicates that the spatial and temporal scales of morphologic signatures are large (reach-scale and over decades) and can be detected even with more cost-efficient lower-resolution methods.

Channel characterizing data collected over a single season exhibited interesting results, but will require longer-term surveying in order to assess any temporal trends. W:d values show spatially distinct variations through the Toklat field site but need to be surveyed over time in order to clarify whether this is a persistent or a temporary trend. Grain size analyses could also be conducted throughout the reach every year in order to assess if this trend persists over time. Similarly, continued slope measurements can be used to track the boundaries of these spatially distinct areas and understand their evolution over time. Despite a lack of repeat measurements, W:d, slope, and grain size help characterize the study reach on the Toklat and interpret the underlying processes that manifest as changes to planform or sediment storage. The channel characteristics measured within areas of known change are consistent with those predicted by braided river literature, suggesting the Toklat River may serve as an example for a more generalized framework for braided river response to alteration.

5.3 Revisiting Hypotheses and Research Objectives

5.3.1 Revisiting Hypothesis 1

> Human activity has led to degradation of the braidplain adjacent to the road-crossing and within the gravel extraction zone.

The volumetric change detection results show a statistically significant trend of degradation adjacent to and upstream of the East Bridge on the Toklat River. The spatially distinct volumetric analyses show this area lost the largest volume of sediment between the years 2009 and 2011. For example, the 2010 gravel extraction zone (see Figure 25) has a volume loss of -13,700 ± 4600 m^3, indicating a shortfall in the replenishment of sediment after the 2010 extraction of 17,100 m^3. This suggests a recovery time greater than at least a year for channels excavated in 2010. The causeway, acting as a confining agent, also appears to have resulted in channel degradation on the order of

gravel allotment volumes (-14,200 ± 4300 m^3). Net degradation characterizes both the braidplain adjacent to the bridge and causeway and within the gravel extraction zone. As such, hypothesis 1 is supported by the data.

5.3.2 Revisiting Hypothesis 2

> This degradation correlates to metrics of braided river morphologic change, indicated by the literature to be an increase to ruggedness and a decrease to braiding index and braiding beltwidth.

The braiding index analysis on the Toklat River shows a general decrease in BI from 1953 to 2011, with only one exception to this trend in 2004 associated with high flows levels. BI decreased most substantially upstream and just downstream of the East Bridge, in the areas of greatest degradation. A decrease in BI was also measured adjacent to Road Camp, where aggradation was quantified between 2009 and 2011, indicating that BI may not always be strictly tied to depositional trends. Braiding beltwidth decreased most substantially upstream on the Toklat, with a slight decrease at and just downstream of the East Bridge. Similarly to BI, a slight decrease in beltwidth measured adjacent to the Road Camp, an area characterized by net aggradation, suggests this metric may not correlate directly to volume change or it may be expressed over longer timescales. Ruggedness showed statistically significant differences between 2009 and 2011 in all Subreaches and within the area of gravel extraction, where an increase in ruggedness correlated with net degradation, and a decrease in ruggedness correlated with net aggradation. This implies an increase in ruggedness correlates to net degradation and can be a useful morphologic metric for future monitoring of this system and others. Overall, Hypothesis 2 is partially supported by the data, with consistent correlation to volume change exhibited by ruggedness, but less consistent trends revealed by BI and beltwidth.

5.3.3 Revisiting Hypothesis 3

> The causeway is contributing to the majority of degradation, indicated by comparisons of temporal variation between planform change of this system and two reference reaches.

The Toklat River exhibited clear trends in beltwidth both upstream and downstream of the East Bridge, with very minimal change to this metric adjacent to East Bridge. The reference reach exemplifying natural confinement, the East Fork, displayed similar trends. Both rivers showed decreases to beltwidth upstream of the bridge simultaneous to slight increases downstream, with no measurable change adjacent to the bridge. These similarities are contrasted with the Teklanika, where no clear trends are visible upstream of, at, or downstream from the bridge. The lack of change present in the zone of confinement, matched by a clear decrease to beltwidth upstream of the bridge, indicates the Toklat River morphology is driven by similar forcings to that of the East Fork. However, the decrease to beltwidth on the East Fork does not persist, while on the Toklat, beltwidth continues reducing. The persistence of a declining beltwidth on the Toklat River indicates that influences to morphologic process are more complex or of a higher magnitude than those on the East Fork River.

The temporal variations of planform change between the Toklat River and its reference reaches indicate confinement, in the form of a causeway, influences morphologic change on the Toklat, but other impacts are contributing to the magnitude of this planform change. The abandonment of flow beneath the West Bridge likely contributed to low beltwidths measured upstream of the causeway on the Toklat River. A probable catalyst for this abandonment was the construction of the Visitor Rest Area on ~75 m of previously active braidplain. This infrastructure increased confinement directly by decreasing the available braidplain downstream of the West Bridge and indirectly by influencing flow abandonment beneath the West Bridge. Infrastructure,

flow abandonment, and the causeway all contributed to the magnitude of reduced beltwidth upstream of the road-crossing.

Volumetric comparisons within the Toklat River study reach indicate degradation adjacent to the East Bridge is comparable to volumes allotted for gravel extraction, and that volumes removed via gravel extraction may not have a rapid replenishment rate. Volumetric change detection within the area encompassing the 2010 gravel extraction sites resulted in a lower bound of degradation at the 80% confidence level of -18,300 m^3. This was comparable to the lower bound of degradation associated with confinement (18,500 m^3). Based on results of this research, areas adjacent to and upstream of the East Bridge experienced comparable degradation to those of the gravel extraction. Furthermore, volumes removed via gravel extraction may not be replenished as rapidly as Park resource management requires. Replenishment rates are likely dependent on the proximity of gravel extraction locations to confinement and the flow characteristics it generates. Volumetric change and the percentage of gravel extraction locations within each of the Subreaches indicate confinement on the Toklat River dictates the spatially distinct response of this braided river to gravel extraction. The area directly downstream of the East Bridge is net degradational and contains 12% of the total 2010 gravel extraction locations, while the area adjacent to Road Camp, incorporating 19% of gravel extractions from 2010, is net aggradational.

Although degradational volumes are comparable and net aggradation has occurred in areas that have experienced gravel extraction, attention must be paid to the variable mechanisms of gravel transfer. Confinement entrains gravel and transports it downstream without it leaving the system, while gravel extraction removes it entirely. This discrepancy may affect the timeframe of influence associated with each human disturbance. The removal of gravel entirely from the system may contribute to legacy effects that are beyond the timeframe of this research.

The interconnected relationship of confinement, by the causeway and infrastructure, and gravel extraction inhibits determining which is the most influential. Furthermore, I suggest that emphasis on only one of these impacts, as Hypothesis 3 states, is unproductive. I propose that the combined effect of confinement, by the causeway and infrastructure, and gravel extraction, is essentially doubling the volume loss along this reach of the Toklat River, indicating that Hypothesis 3 is partially supported.

Perhaps of more interest to the Park and braided river management in general than identifying the anthropogenic disturbance of greatest influence is a discussion of the magnitude of these influences. The magnitude of volume, planform and channel change within the study reach has been well-documented and has substantial implications for the adjacent Park infrastructure and resource management of the Toklat River. However, the longitudinal effects of these combined impacts downstream of the study reach are estimated to be minimal. Downstream of the study reach, W:d ratios and volume change indicate a return to dynamic equilibrium. W:d values measured 4 km downstream of the study reach (~60) were double those averaged within the study reach (~30) (Figure 33) and more representative of values typical of naturally braiding rivers (Eaton et al., 2010; Dust, 2009; Fredsoe, 1978). The high W:d values measured 4 km downstream of the study reach are likely indicative of balanced sediment and water inputs. Furthermore, at the farthest downstream extent of the LiDAR coverage, a proportional amount of aggradation and degradation, or sediment continuity, is visually signified by active braidplain volumetric change detection results (Figure 20). The results of volume change detection and W:d suggest all measureable effects of human disturbance are generally constrained to the field site, implying the Toklat River downstream of the human impacts has likely reached a state of dynamic equilibrium.

This is may not be a stationary state, however, and further removal of gravel from the system via gravel extraction may cause downstream effects over a longer time scale than a few decades.

5.4 Braided River Response to Confinement and Gravel Extraction

A conceptual model that integrates braided river processes using Lane's balance, the qualitative channel response described by Schumm (1977), and results from volumetric and morphologic change detection analyses on the Toklat River, is presented as a potential tool to predict the direction of coarse-grained braided river response to confinement and gravel extraction (Figure 42). Although the results of this research are based on a case study, the consistency of these results with braided river literature and Lane's balance implies a generalized and more broadly applicable framework for braided river response. This conceptual model explores that framework, drawing upon channel and planform responses from this research and other studies. Channel and planform adjustments presented in this model are all potential responses that one could expect to see in a similar system with similar disturbance levels.

The catalyst of channel and planform change in this model is confinement from infrastructure, which then dictates the spatially distinct response of the river to subsequent gravel extraction. The spatially distinct response delineations "Knickpoint Migration Zone," "Incision Zone" and "Adjustment Zone," (Figure 42) reference the measured characteristics of the Upstream, Bridge and Downstream Subreaches, respectively. The delineations of this model describe the spatial distribution of a single stage of braided river response after an indeterminate time following confinement initiation. Discussion incorporates the predicted response if gravel extraction occurs within each of these zones, based on the results of this research that indicate a spatially distinct river response to gravel extraction based on proximity to confinement and flow confluence. The zone delineations defined are bound on either end with a braided river in dynamic

equilibrium (Figure 42), where every adjustment is met with multiple responses that compensate for the initial stimulus over time to return to a state of sediment continuity. The downstream dynamic equilibrium is based on the results of this research indicating sediment continuity downstream of the Toklat River study reach. The upstream dynamic equilibrium is not a permanent state, but representative of the temporal extent of upstream knickpoint migration that over time will likely continue to extend upstream (Graf, 2006; Surian and Rinaldi, 2003; Williams and Wolman, 1984).

Confinement decreases the available braidplain width, resulting in a decrease in the W:d of the confined channels (Hicks et al., 2008; Rinaldi et al., 2005; Surian and Rinaldi, 2003). Confinement also increases unit stream power as lateral mobility decreases, forcing convergence of flow. Another response to increase localized stream power is sediment recruitment from the channel bed, rather than from the confined banks. This will likely lead to an increase in grain size, as the channel armors its bed to inhibit further erosion. The recruitment of material from the channel bed will likely lead to a local baselevel drop, forcing a slope adjustment. A local baselevel drop can also be accomplished through gravel extraction. Over time, the channel will attempt to minimize slope. This will occur in the form of knickpoint migration, the upstream dispersal of incision to minimize slope breaks at the channel bed (Schumm, 1993). The literature indicates that this response can occur across a range of timescales, dependent on boundary conditions and grain characteristics (Surian and Rinaldi, 2003; Schumm, 1993). This suggests that predictions of braidplain slope depend on the period of time since initiation of incision and the rate of knickpoint advancement upstream. Thus, slope change is indicated as an increase and decrease due to the dependence on time since initiation of confinement.

Speculations on the influence of gravel extraction as the sole human disturbance are not incorporated into this model due to the limitations of this case study. However, the literature supports that gravel extraction can lead to similar channel and planform change as discussed below (Hicks et al., 2008; Piégay et al., 2006; Kondolf et al., 2002; Meador and Layher, 1998; Collins and Dunne, 1989). This model is constrained to situations exemplified on the Toklat, but may be applicable to systems affected by confinement, or a combination of confinement followed by gravel extraction.

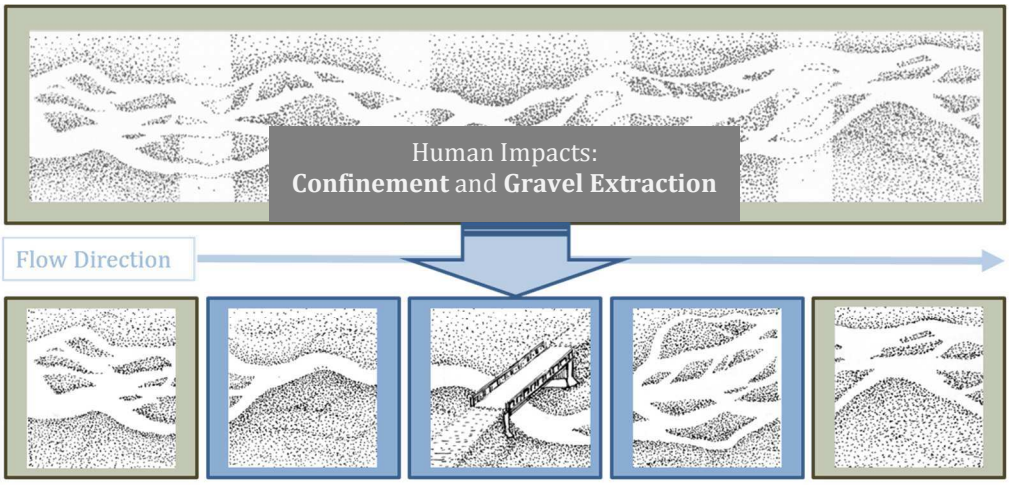

	Dynamic Equilibrium	*Knickpoint Migration Zone*	*Incision Zone*	*Adjustment Zone*	*Dynamic Equilibrium*
Width to Depth Ratio	~	--	--	+	~
Grain Size (D84)	~	+	+	--	~
Braidplain Slope	~	±	±	±	~
Braiding Index	~	--	--	+	~
Average Beltwidth	~	--	~	+	~
Ruggedness	~	+	+	--	~
Net Volume Change	~	--	--	+	~
Stream Power	~	+	+	--	~

Figure 42: Conceptual model showing predicted and spatially distinct responses of a braided river to confinement. The direction of channel or planform alteration is indicated with "+" to symbolize an increase from a state of dynamic equilibrium, "--" to symbolize a decrease., or "~" implies no change. Change to braidplain slope is purposely symbolized with "±," indicating variable change over time.

5.4.1 Knickpoint Migration Zone

Within the Knickpoint Migration Zone, results from this research and predictions from Lane's balance indicate that with respect to the original pre-confinement channel, the W:d could decrease, grain size could increase and slope could decrease if the channel successfully adjusts its bed to accommodate excess unit stream power. Alternatively, slope may increase directly at the knickpoint between the former bed surface and the bed surface that has experienced baselevel drop. Channel slope at the intersection of the knickpoint and the previous channel bed will presumably be high, reflecting the original channel slope. Channel gradient downstream of the knickpoint will likely be flatter than the original channel slope due to baselevel drop. Planform could be expressed as a decrease in braiding index and beltwidth in response to baselevel adjustment and decreasing W:d. If gravel extraction were to occur within this zone following confinement, it would likely exacerbate all of the channel and planform adjustments mentioned previously, and enhance channel degradation.

5.4.2 Incision Zone

The results of this research suggest that confinement and confluence of flow associated with confinement have increased local stream power on the Toklat River in this zone. In similarly confined systems, the channel could respond to this increase in stream power by recruiting sediment from the bed and increasing depth. Channel width would be unable to increase due to physical confinement inhibiting lateral expansion, likely decreasing W:d and braiding index. Grain size could increase as the bed armors. Flow characterized by increased stream power, a consequence of flow confluence, promotes continuous incision and local baselevel drop. Flow characterized by increased stream power can also be associated with increased ruggedness. Continued degradation of the channel bed at the point of confluence could lead to incision that can

migrate upstream in the form of a knickpoint. This can be visualized in Figure 42 as a temporary overlap between the Knickpoint Migration Zone and the Incision Zone, followed by the slow separation of these two zones over time. This could result in a steep channel slope at the knickpoint itself and decreased channel slope directly downstream. If gravel extraction were to occur within this zone, it would likely enhance all channel and planform responses, and contribute to local baselevel drop and knickpoint formation. Over time, the combined sources of local baselevel drop, flow confluence and gravel extraction could result in the undermining of the confining infrastructure.

5.4.3 Adjustment Zone

Downstream of the Incision Zone is the Adjustment Zone, where channel geometry, planform and process have the lateral ability to adjust to altered flow conditions. The results of this research suggest that increased stream power, caused by confluence and confinement, is spatially limited. Sediment brought into transport within this high energy zone will not continue to be transported unless the high stream power and shear stress, associated with confinement and confluence, persist. Furthermore, the flattening of channel slope, mentioned in the downstream section of the incision zone, results in a decrease in both shear stress and stream power. Channel response to the decrease in channel slope, and thus stream power and shear stress, occurs downstream of the confinement. Within the Adjustment Zone, net degradation transitions to net aggradation due to the loss of transport capacity. Aggradation is associated with a decrease in D_{84}, as progressively finer particles can no longer be transported by flow and are deposited. Channel slope will likely approach a reach-average value to maintain sediment flux. The results of this research suggest the W:d increases downstream of the confinement, a channel geometry change associated with decreased sediment transport capacity (Dust and Wohl, 2012). This would indicate

that increases to W:d within the Adjustment Zone correlate to decreased sediment transport capacity, and thus aggradation, if W:d values are comparable to those measured at the Downstream Subreach. If gravel extraction were to occur within this zone, the characteristics of the Incision Zone would likely replace those of the Adjustment Zone, increasing the spatial extent of net degradation and the downstream distance towards a state of dynamic equilibrium.

5.5 Application and Management

This research has significant implications for the Toklat River and its management. I have documented and quantified the effects of confinement by the causeway, adjacent infrastructure, and gravel extraction within a two-year time scale and through volumetric change detection, and within a six-decade timescale using morphologic change detection. Repercussions of these practices are well documented by research conducted on systems experiencing these impacts to a higher degree (Ashmore and Rennie, 2013; Horn et al., 2012; Fotherby, 2009; Rempel and Church, 2009; Huang and Nanson, 2007; Basher, 2006; Rinaldi et al., 2005; Church et al., 2001; Meador and Layher, 1998; Kondolf, 1997; Montgomery and Buffington, 1997; Graf, 1981).

The results of this research indicate that the combined effects of gravel extraction and confinement are resulting in removal of at least double the volumes allotted for gravel extraction. It is furthermore suggested that exclusive focus on one human disturbance limits the understanding of how all of these impacts enhance one another. The Toklat River has adjusted not to each disturbance specifically but instead has responded to their cumulative effect. This being the case, it is still valuable to discuss actions that address each issue and to attempt to anticipate the river response.

The enhanced degradation occurring adjacent to the road crossing may lead to undermining of infrastructure. Substantial damage to infrastructure has occurred regularly throughout time on

an approximate decadal flood timescale (Figure 43). This flood magnitude can be expected to occur regularly and result in future damage to infrastructure. To minimize the effect of these floods and prevent large scale undermining of infrastructure associated with the road crossing, reduction in the sources of confinement along this reach of the Toklat River is recommended. Management practices that decrease confinement may also decrease stream power and thus reduce the magnitude of degradation. This is corroborated by the literature (Piégay et al., 2006; Kondolf et al., 2002; Kondolf, 1997). Reduction in confinement could take the specific forms of: (1) removal or reduction of the causeway; and/or (2) removal or relocation of infrastructure encroaching on previously active floodplain.

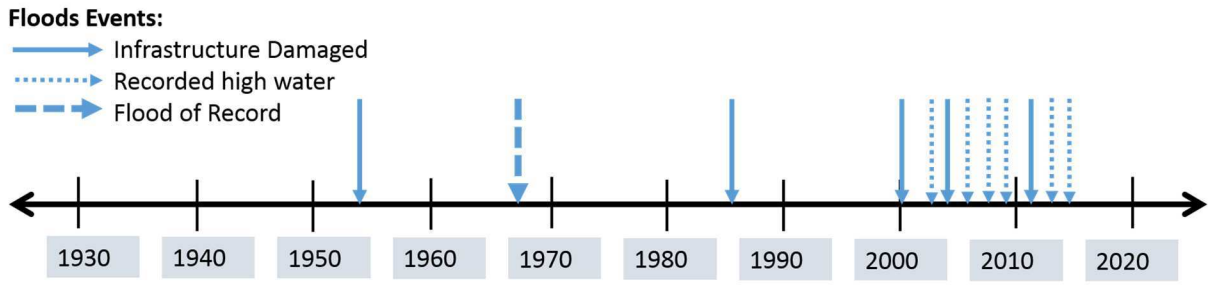

Figure 43: Timeline showing flood and high water events along the Toklat River.

The practice of gravel extraction on the Toklat River is contributing to net degradational trends within the braidplain and the magnitude of these trends appear to be enhanced by increased proximity to confinement. Time limitations of this study facilitated volumetric change analysis of the total spatial coverage of only one year of gravel extraction. Based on these results, the replenishment rate of the 2010 extraction is slow, but if aggradation continued at the rates indicated, full replenishment could take place over five years. This indicates that if the gravel extraction was the only human disturbance to this reach of the Toklat, the volumes allotted for removal would be sustainable. However, because the volumes removed via gravel extraction

consist of half or less of the total volumes degraded from this reach, this combined volume is likely unsustainable. To minimize degradation associated with gravel extraction, recommendations could include: (1) termination of the practice of gravel extraction; (2) reduction in the volumes removed via gravel extraction; (3) data-driven selection of locations for gravel extraction; and indirectly associated with gravel extraction, and/or (4) reduction in confinement associated with the causeway and Visitor Rest Area.

Data-driven selection of locations for gravel extraction incorporates proximity to confinement and known areas of degradation, and increasing the available active braidplain laterally. When selecting locations to remove gravel, consideration of sediment imbalances may avoid enhancing degradation. Removal of sediment in an area that is actively eroding streambed sediment, and lacking equal replenishment, will enhance the rate and magnitude of degradation. Gravel extraction activities should occur at or downstream of areas of net aggradation (i.e., adjacent to and laterally across the braidplain from Road Camp) and avoid areas characterized by net degradation (i.e., between the East Bridge and the Visitor Rest Area). Furthermore, using the next decade of extractions to excavate into the minimally active floodplain on the eastern side of the study reach could potentially increase the active beltwidth of the river. Increasing the beltwidth in this area by data-driven extraction plans could potentially mitigate incisional trends by extending lateral mobility and connectivity, as well as rejuvenate altered riparian zones (Graf, 2006; Piégay et al., 2006; Gran and Paola, 2001; Kondolf et al., 2001; Meador and Layher, 1998).

6. CONCLUSIONS

The Toklat River in Denali National Park and Preserve is experiencing net degradation of the braidplain adjacent to a source of river confinement and within areas experiencing gravel extraction. The mutual influence of human disturbance along the Toklat River is indicated by spatially and temporally varied volumetric change detection and morphologic change detection results. Comparisons of 2009 and 2011 LiDAR-derived DEMs showed a statistically significant volumetric loss of -30,300 ± 27,600 m^3 over 4 km of active braidplain within the study reach Volume loss between 2009 and 2011 adjacent to the road crossing of the Toklat River (-14,200 ± 4300 m^3) is comparable to that of the area encompassing the 2010 gravel extraction (-13,700 ± 4600 m^3). Morphologic metrics used in this research indicate alteration to planform and degradation of the floodplain on multiple timescales. Decadal periods of probable degradation are signified by a decrease in braiding index from eight to one and a loss in beltwidth of ~400 m upstream of the road crossing, initiating in 1988 and continuing until the present. Shorter periods of degradation documented with volume change are corroborated by an increase to ruggedness within the active braidplain. Low W:d within the study reach in comparison to those measured farther downstream suggest altered inputs are driving changes to channel geometries within the study area. Long-term comparisons between the Toklat River and reference reaches highlight continuous decreases to beltwidth evident on the Toklat that are not apparent on the Teklanika or East Fork Rivers.

This research suggests that metrics of morphologic change may reflect large scale volumetric change, identifies locations of degradation with implications for Park infrastructure and natural resource extraction, and provides a conceptual framework for pursuing monitoring efforts on the Toklat River that may be applicable elsewhere. The Toklat River provides a unique

opportunity to quantify disturbance specific to confinement and gravel extraction, in an area of environmental and social importance.

7. REFERENCES

Allan, J. D., 2016. Landscapes and riverscapes: The influence of land use on stream ecosystems. Annu. Rev. Ecol. Syst. 35, 257-284.

Arding, J. S., Enfield, E. F., Olstad, P. V., Elfman, G. S., 1998. Stream biodiversity: The ghost of land use past. Ecology 95, 14843-14847.

Ashmore, P., 2013. Morphology and dynamics of braided rivers. Treatise Geomorphol. 9, 289–312.

Ashmore, P., Rennie, C.D., 2013. Gravel-bed rivers: From particles to patterns. Earth Surf. Process. Landforms 38(2), 217-220.

Ashmore, P., Bertoldi, W., Tobias Gardner, J., 2011. Active width of gravel-bed braided rivers. Earth Surf. Process. Landforms 36(11), 1510-1521.

Ashmore, P., Sauks, E., 2006. Prediction of discharge from water surface width in a braided river with implications for at-a-station hydraulic geometry. Water Resources Research 42(3), 1–11.

Ashmore, P., 1991. Channel morphology and bed load pulses in braided, gravel-bed streams. Source Geogr. Ann. Ser. A, Phys. Geogr. 73, 37–52.

Ashmore, P., 1991. How do gravel-bed rivers braid? Can. J. Earth Sci. 28, 326–341.

Ashmore, P., Parker, G., 1983. Confluence scour in coarse braided streams. Water Resources research 19-2, 392-402.

Ashworth, P. J., Best, J. L., Jones, M. A., 2007. The relationship between channel avulsion, flow

occupancy and aggradation in braided rivers: insights from an experimental model. Sedimentology 54-3, 497-513.

Ashworth, P.J., Ferguson, R.I., 1986. Interrelationships of Channel Processes, Changes and Sediments in a Proglacial Braided River. Phys. Geogr. 68, 361–371.

Basher, L.R., 2006. Monitoring of riverbed stability and morphology by regional councils in New Zealand: application to gravel extraction management. Landcare Research, Nelson.

Bertoldi, W., Zanoni, L., Tubino, M., 2009. Planform dynamics of braided streams. Earth Surf. Process. Landforms 34, 547–557.

Boix-fayos, C., Barbera, G. G., Lopez-bermudez, F., Castillo, V. M., 2007. Effects of check dams, reforestation and land-use changes on river channel morphology: Case study of the Rogativa catchment (Murcia, Spain). Geomorphology 91, 103-123.

Bradford, M.J., Korman, J., Higgins, P.S., 2005. Using confidence intervals to estimate the response of salmon populations (Oncorhynchus spp.) to experimental habitat alterations. Can. J. Fish. Aquat. Sci. 62, 2716–2726.

Brasington, J., Langham, J., Rumsby, B., 2003. Methodological sensitivity of morphometric estimates of coarse fluvial sediment transport. Geomorphology 53(3), 299–316.

Brasington, J., Rumsby, B.T., McVey, R. a, 2000. Monitoring and modelling morphological change in a braided gravel-bed river using high resolution GPS-based survey. Earth Surf. Process. Landforms 25, 973–990.

Brice, J. C.,1960. Index for description of channel braiding. Geological Society of America Bulletin 71, 1833.

Brice, J. C., 1964. Channel patterns and terraces of the Loup River in Nebraska. US Govt. Print. Off. 422-D.

Bridge, J. S., 1993. The interaction between channel geometry, water flow, sediment transport and deposition in braided rivers. Geological Society of America, Special Publications, 75, 13-71.

Bryant, J. 2011. Snapshots from the Past: A Roadside History of Denali National Park and Preserve. US Department of the Interior, National Park Service, 2011.

Buffington, J.M., Montgomery, D.R., 1997. A systematic analysis of eight decades of incipient motion studies, with special reference to gravel-bedded rivers. Water Resources Research 33(8), 1993–2029.

CardnoENTRIX, 2013. Toklat River Assessment. NPS Final Rep.

CardnoENTRIX, 2012. Toklat River Monitoring for 2012. NPS Final Rep.

Chandler, J., Ashmore, P., Paola, C., Gooch, M., Varkaris, F., 2016. Monitoring River-Channel Change Using Terrestrial Oblique Digital Imagery and Automated Digital Photogrammetry. Ann. Assoc. Am. Geogr. 92, 631–644.

Church, M., Ham, D., Weatherly, H., 2001. Gravel Management in Lower Fraser River. Report prepared for the City of Chilliwack.

Collins, B.D., Dunne, T., 1989. Gravel transport, gravel harvesting, and channel-bed degradation in rivers draining the southern Olympic Mountains, Washington, U.S.A. Environ. Geol. Water Sci. 13(3), 213-224.

Coulthard, T. J., Macklin, M. G., 2001. How sensitive are river systems to climate and land-sue

changes? Journal of Quaternary Science 16(4), 347-351.

Croke, J., Todd, P., Thompson, C., Watson, F., Denham, R., Khanal, G., 2013. Geomorphology The use of multi temporal LiDAR to assess basin-scale erosion and deposition following the catastrophic January 2011 Lockyer flood, SE Queensland, Australia. Geomorphology 184, 111–126.

Crossman, J., Futter, M.N., Whitehead, P.G., 2013. The Significance of Shifts in Precipitation Patterns: Modelling the Impacts of Climate Change and Glacier Retreat on Extreme Flood Events in Denali National Park, Alaska. PLoS One 8, 1–18.

Curran, J., McTeague, M., 2011. Geomorphology and Bank Erosion of the Matanuska River, Southcentral Alaska. USGS Sci. Investig. Rep. 5214.

Denali National Park and Preserve Geologic Resources Inventory Report, 2010. Nat. Resour. Rep.

Dust, D., Wohl, E., 2014. "Response to commentary by Huang et al. regarding "Conceptual model for complex river responses using an expanded Lane's relation." Geomorphology, 209, 143-146.

Dust, D., Wohl, E., 2012. Geomorphology Conceptual model for complex river responses using an expanded Lane's relation. Geomorphology 139-140, 109–121.

Dust, D., 2009. On the Nature and Mechanics of Floodplain Response and Stability in the Semi-arid Environment of Southern California. Colorado State Univ.

Eaton, B.C., Millar, R.G., Davidson, S., 2010. Channel patterns: Braided, anabranching, and single-thread. Geomorphology 120(3), 353-364.

Egozi, R., Ashmore, P., 2009. Experimental analysis of braided channel pattern response to

increased discharge. J. Geophys. Res. Earth Surf. 114, 1–15.

Emmett, W.W., Burrows, R.L., Chacho, E.F., 1996. Coarse-particle Transport in a Gravel-bed River. Int. J. Sediment Res. 11(2), 8-21.

ESRI, 2016. ArcGIS Desktop: Release 10.3. Redlands, CA: Environmental Systems Research Institute.

Fotherby, L.M., 2009. Valley confinement as a factor of braided river pattern for the Platte River. Geomorphology 103(4), 562-576.

Fredsoe, J., 1978. Meandering and braiding of rivers. Fluid Mech. 84, 609–624.

Fuller, I.C., Large, A.R.G., Charlton, M.E., Heritage, G.L., Milan, D.J., 2003. Reach-scale sediment transfers: An evaluation of two morphological budgeting approaches. Earth Surf. Process. Landforms 28(8), 889-903.

Germanoski, D., Schumm, S. a., 1993. Changes in Braided River Morphology Resulting from Aggradation and Degradation. J. Geol. 101, 451–466.

Graf, W.L., 2006. Downstream hydrologic and geomorphic effects of large dams on American rivers. Geomorphology 79, 336–360.

Graf, W.L., 1981. Channel instability in a braided, sand bed river. Water Resour. Res. 17(4), 1087-1094.

Gran, K., Paola, C., 2001. Riparian vegetation controls on braided stream dynamics. Water Resour. Res. 37, 3275–3283.

Hicks, D.M., Duncan, M.J., Lane, S.N., Tal, M., 2008. Contemporary morphological change in

braided gravel-bed rivers: new developments from field and laboratory studies, with particular reference to the influence of riparian vegetation. Developments in Earth Surface Processes 11, 557-584.

Hicks, D.M., Duncan, M.J., Walsh, J.M., Westaway, R.M., Lane, S.N., 2002. New views of the morphodynamics of large braided rivers from high-resolution topographic surveys and time-lapse video. IAHS Publication 373-380.

Hong, L. B., Davies, T. R., 1979. A study of stream briading. Geological Society of American Bulletin. 90, 1839-1859.

Horn, J.D., Joeckel, R.M., Fielding, C.R., 2012. Progressive abandonment and planform changes of the central Platte River in Nebraska, central USA, over historical timeframes. Geomorphology 139, 372-383.

Howard, A.D., Keetch, M.E., Vincent, C.L., 1970. Topological and Geometrical Properties of Braided Streams.

Huang, H.Q., Nanson, G.C., 2007. Why some alluvial rivers develop an anabranching pattern. Water Resour. Res. 43(7).

Huang, H.Q., Qing, H., Liu, X., Nanson, G.C., 2014. Geomorphology Commentary on a "Conceptual model for complex river responses using an expanded Lane diagram by David Dust and Ellen Wohl." Geomorphology 209, 140–142.

Hughes, M.L., McDowell, P.F., Marcus, W.A., 2006. Accuracy assessment of georectified aerial photographs: Implications for measuring lateral channel movement in a GIS. Geomorphology 74, 1–16.

Jang, J.S.R., 1993. ANFIS: Adaptive-Network-Based Fuzzy Inference System. IEEE Trans. Syst. Man and Cybernetics 23(3), 665–685.

Javernick, L., Brasington, J., Caruso, B., 2014. Modeling the topography of shallow braided rivers using Structure-from-Motion photogrammetry. Geomorphology 213, 166–182.

Jacob-Rousseau, N. 2015. Water diversions, environmental impacts and social conflicts: the contribution of quantitative archives to the history of hydraulics. Water History 7, 101-129.

Karle, K., 1990. Replenishment Potential for Gravel Removal Sites for the Toklat River, Denali National Park and Preserve. Natl. Park Serv.

Kondolf, G.M., 1997. Hungry water: Effects of dams and gravel mining on river channels. Environ. Manage. 21, 533–551.

Kondolf, G.M., Piégay, H., Landon, N., 2002. Channel response to increased and decreased bedload supply from land use change: Contrasts between two catchments. Geomorphology 45(1), 35-51.

Kondolf, G.M., Smeltzer, M.W., Railsback, S.F., 2001. Design and Performance of a Channel Reconstruction Project in a Coastal California Gravel-Bed Stream. Environ. Manage. 28, 761–776.

Lane, S.N., Widdison, P.E., Thomas, R.E., Ashworth, P.J., Best, J.L., Lunt, I. a., Sambrook Smith, G.H., Simpson, C.J., 2010. Quantification of braided river channel change using archival digital image analysis. Earth Surf. Process. Landforms 35, 971–985.

Leopold, L., Wolman, G., 1957. River Channel Patterns: Braided, Meandering and Straight.

Maizels, J., 1979. Proglacial Aggradation and Changes in Braided Channel Patterns during a Period of Glacier Advance: An Alpine Example. Phys. Geogr. 61, 87–101.

Mapstone, B.D., 1995. Scalable Decision Rules for Environmental Impact Studies: Effect Size , Type I , and Type II Errors. Ecol. Appl. 5, 401–410.

Meador, M.R., Layher, A.O., 1998. Instream Sand and Gravel Mining: Environmental Issues and Regulatory Process in the United States. Fisheries. 23(11), 6-13.

Montgomery, D.R., Buffington, J.M., 1997. Channel-reach morphology in mountain drainage basins. Bull. Geol. Soc. Am. 109(5), 596-611.

Mosley, P., 1982. Analysis of the Effect of Changing Discharge on Channel Morphology and Instream Used in a Braided River, Ohau River, New Zealand. Water Resources Research 18(4), 800–812.

Mosley, P., 1976. Streamflow generation in a forested watershed, New Zealand. Water Resources Research 15(4), 795-806.

Nicholas, A.P., 2000. Modelling bedload yield in braided gravel bed rivers. Geomorphology 36(1), 89–106.

Nicholas, A.P., Ashworth, P.J., Kirkby, M.J., Macklin, M.G., Murray, T., 1995. Sediment slugs: large-scale fluctuations in fluvial sediment transport rates and storage volumes. Prog. Phys. Geogr. 19(4), 500-519.

NPS, 1992. Planning end Resources Office. Natl. Park Serv. Environ. Assess. 182.

Peizhen, Z., Molnar, P., Downs, W.R., 2001. Increased sedimentation rates and grain sizes 2 ± 4

Myr ago due to the influence of climate change on erosion rates. Nature 410, 891–897.

Piégay, H., Grant, G., Nakamura, F., Trustrum, N., 2006. Braided river management: from assessment of river behavior to improved sustainable development. Braided Rivers: Process, Deposits, Ecology and Management, Sambrook Smith GH, Best, JL, Bristow, CS, & Petts, GE (Eds), 257-276.

Podolak, C. J., 2013. Predicting the planform configuration of the braided Toklat River, Alaska, with a suite of rule-based models1. JAWRA 49-2, 390-401.

Rempel, L.L., Church, M., 2009. Physical and ecological response to disturbance by gravel mining in a large alluvial river. Can. J. Fish. Aquat. Sci. 66)1), 52-71.

Rinaldi, M., Wyzga, B., Surian, N., 2005. Sediment mining in alluvial channels: Physical effects and management perspectives. River Res. Appl. 21(7), 805-828.

Rumsby, B.T., Brasington, J., Langham, J.A., McLelland, S.J., Middleton, R., Rollinson, G., 2008. Monitoring and modelling particle and reach-scale morphological change in gravel-bed rivers: Applications and challenges. Geomorphology 93(1), 40-54.

Sapozhnikov, V., Foufoula-Georgiou, E., 1996. Self-affinity in braided rivers. Water Resources Research 32(5), 1429–1439.

Schumm, S.A., 1993. River Response to Baselevel Change: Implications for Sequence Stratigraphy. J. Geol. 101, 279–294.

Schumm, S. A., 1977. The fluvial system. Vol. 338. New York: Wiley.

Scown, M.W., Thoms, M.C., Jager, N.R. De, 2016. An index of floodplain surface complexity.

Hydrology and Earth System Sciences 20(1), 431–441.

Sousanes, P.J., Hill, K.R., 2015. Annual Climate Summary 2013 Central Alaska Network. Nat. Resour. Data Ser. CAKN.

Sousanes, P.J., Hill, K.R., 2013. Central Alaska Network Natural Resource Data Series NPS/CAKN/NRDS—2013/423.

Stojic, M., Chandler, J., Ashmore, P., Luce, J., 1998. The Assessment of Sediment Transport Rates by Automated Digital Photogrammetry. Photogramm. Eng. Remote Sensing 64, 387–395.

Surian, N., Cisotto, A., 2007. Channel adjustments, bedload transport and sediment sources in a gravel-bed river, Brenta River, Italy. Earth Surf. Process. Landforms 32(11), 1641-1656.

Surian, N., Rinaldi, M., 2003. Morphological response to river engineering and management in alluvial channels in Italy. Geomorphology 50(4), 307–326.

Surian, N., 1999. Channel changes due to river regulation: The case of the Piave River, Italy. Earth Surf. Process. Landforms 24(12), 1135–1151.

Takagi, T., Oguchi, T., Matsumoto, J., Grossman, M.J., Sarker, M.H., Matin, M.A., 2007. Channel braiding and stability of the Brahmaputra River, Bangladesh, since 1967: GIS and remote sensing analyses. Geomorphology 85, 294–305.

Vandenberghe, J., 2003. Climate forcing of fluvial system development: an evolution of ideas. Quaternary Science Reviews 22(20), 2053-2060.

Walling, D.E., 2006. Human impact on land – ocean sediment transfer by the world's rivers. Geomorphology 79, 192–216.

Walling, D.E., Landon, N., He, Q., Lie, F., 2004.Contemporary changes in sediment yield in an alpine mountain basin due to afforestation (the upper Drome in France). Catena 55, 183-212.

Westaway, R.M., Lane, S.N., Hicks, D.M., 2003. Remote survey of large-scale braided, gravel-bed rivers using digital photogrammetry and image analysis. Int. J. Remote Sens. 24(4), 795-815.

Westoby, M.J., Brasington, J., Glasser, N.F., Hambrey, M.J., Reynolds, J.M., 2012. "Structure-from-Motion" photogrammetry: A low-cost, effective tool for geoscience applications. Geomorphology 179, 300-314.

Wheaton, J.M., Brasington, J., Darby, S.E., Kasprak, A., Sear, D., Vericat, D., 2013a. Morphodynamic signatures of braiding mechanisms as expressed through change in sediment storage in a gravel-bed river. J. Geophys. Res. Earth Surf. 118(2), 759-779.

Wheaton, J.M., Brasington, J., Darby, S.E., Kasprak, A., Sear, D., Vericat, D., 2013b. Morphodynamic signatures of braiding mechanisms as expressed through change in sediment storage in a gravel-bed river. J. Geophys. Res. Earth Surf. 118, 759–779.

Wheaton, J.M., Brasington, J., Darby, S.E., Sear, D.A., 2010. Accounting for uncertainty in DEMs from repeat topographic surveys: Improved sediment budgets. Earth Surf. Process. Landforms 35(2), 136-156

Williams, G.P., Wolman, M.G., 1984. Downstream effects of dams on alluvial rivers. U.S. Geol. Surv., Prof. Pap.

Williams, R.D., Brasington, J., Vericat, D., Hicks, D.M., 2014. Hyperscale terrain modelling of braided rivers: Fusing mobile terrestrial laser scanning and optical bathymetric mapping. Earth Surf. Process. Landforms. 39 (2), 167-183.

Wohl, E., 2006. Human impacts to mountain streams. Geomorphology 79, 217–248.

Wolman, G., 1954. A Method of Sampling Coarse River-Bed Material. Am. Geophys. Union Trans. 35, 951–956.

8. APPENDIX

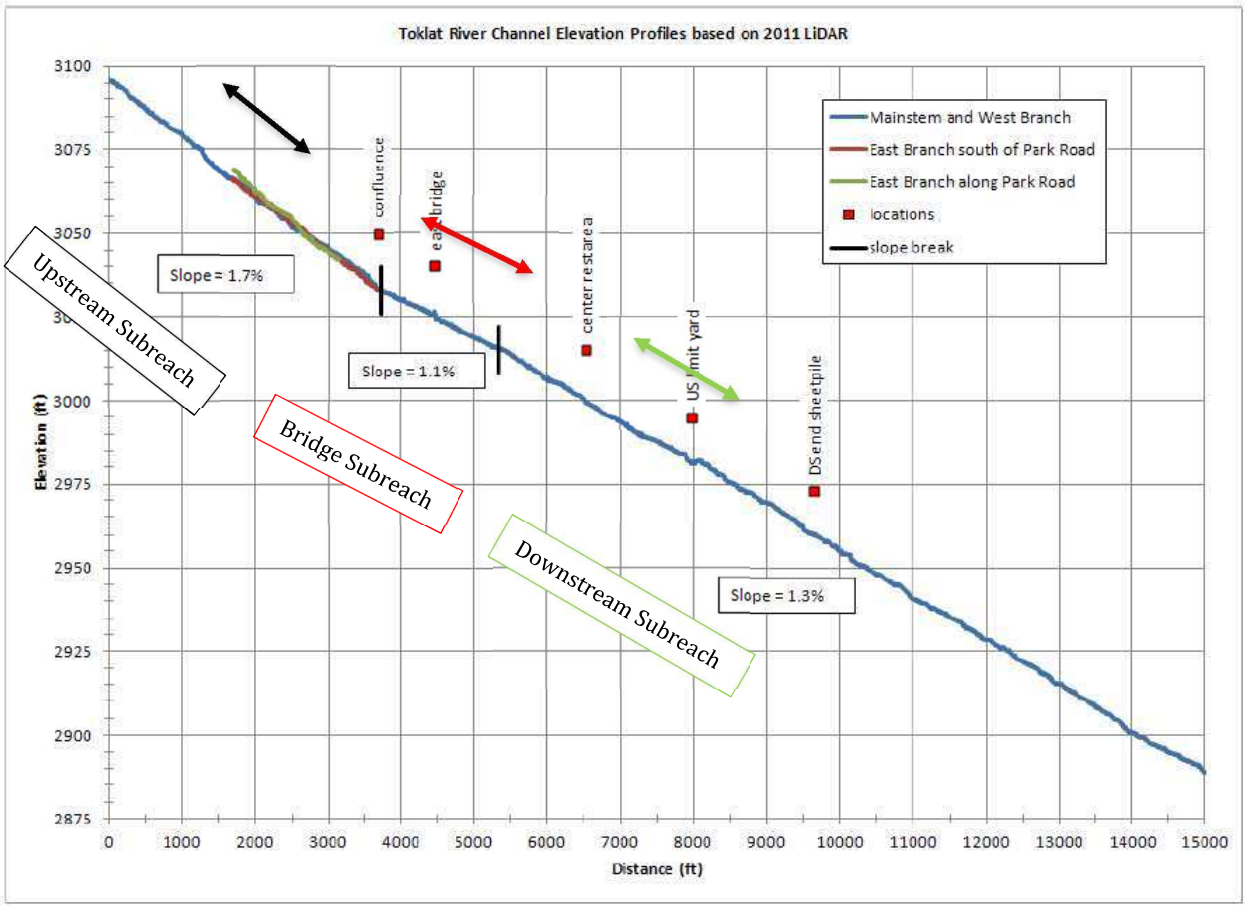

Figure 44: Longitudinal profile derived from 2011 LiDAR by CardnoENTRIX (2013). Slopes here corroborate braidplain slopes measured from Google Earth WGS84 EGM96 geoid in October of 2015 within the Subreaches of the Toklat River. The highest slopes are indicated in the Upstream Subreach (black arrow), the lowest slopes are downstream of the causeway in the downstream portion of the Bridge Subreach (red arrow), and reach-averaged slopes are attained in the Downstream Subreach (green arrow).

Table 5: Table shows the percentage of area that experienced gravel extraction incorporated within volumetric analyses within the Subreaches and the aerial photogrammetry extent. Values were measured using the percentage of excavated channel length falling within the boundaries of the indicated areas. LiDAR incorporated all areas that experienced gravel extraction since 2008 and the Upstream Subreach incorporated none due to its location beyond the wilderness exclusion boundary.

	Percentage of Total Extraction Sites within Area Indicated (%)				
Extraction Year	Upstream Subreach	Bridge Subreach	Downstream Subreach	Aerial Photogrammetry	LiDAR
2008	0	0	24.3	0	100
2010	0	12.1	18.6	33.9	100
2012	0	0	24.8	31.5	100
2014	0	0	0	0	100
Total Extractions	0	2.4	18.1	18.5	100
Total Since 2010	0	3	16.5	23.5	100
Total Since 2012	0	0	15.8	20.1	100

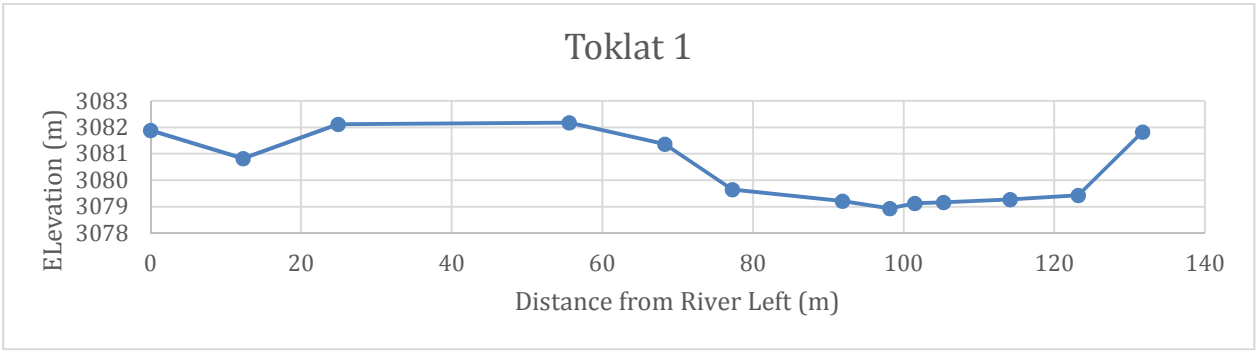

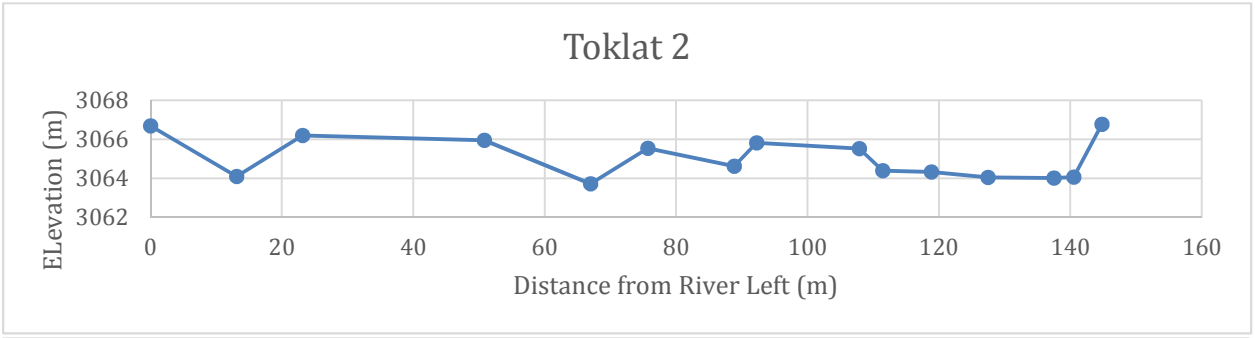

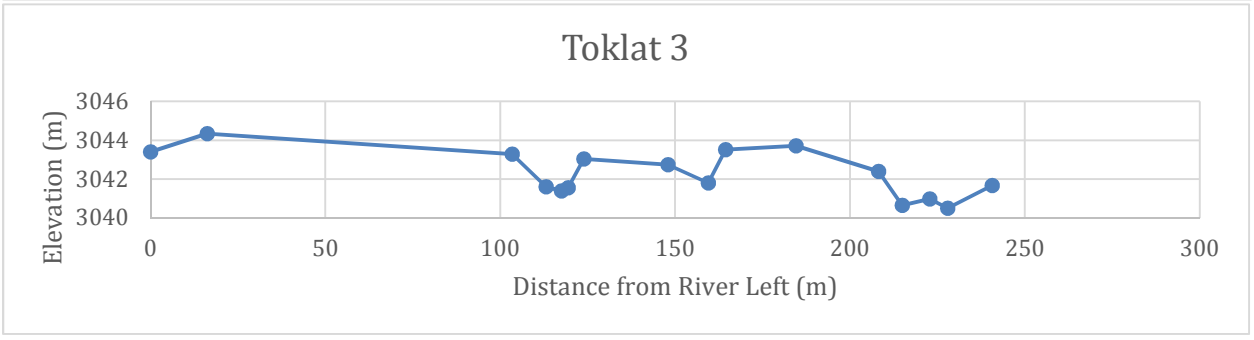

Figure 45: Three cross-sections measured in May of 2015 within the West Branch of the Toklat upstream of the East Bridge.

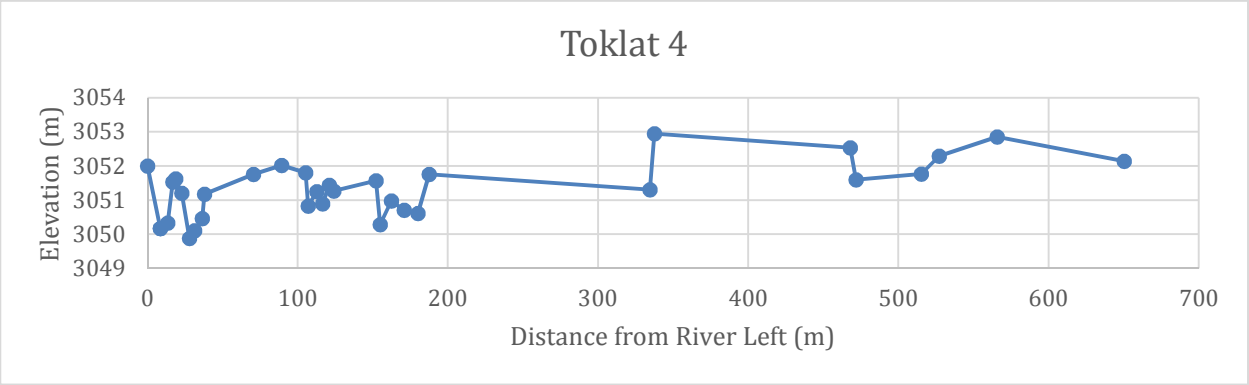

Figure 46: Cross-section measured in May of 2015 of the East Branch of the Toklat upstream of the East Bridge.

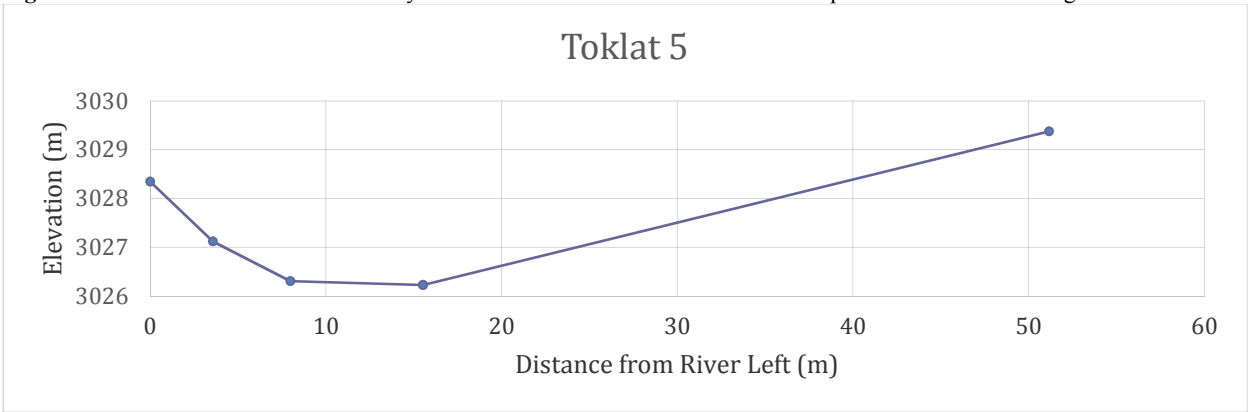

Figure 47: Cross-section measured in May of 2015 of the confluence between the East and West Branches of the Toklat River upstream of the East Bridge.

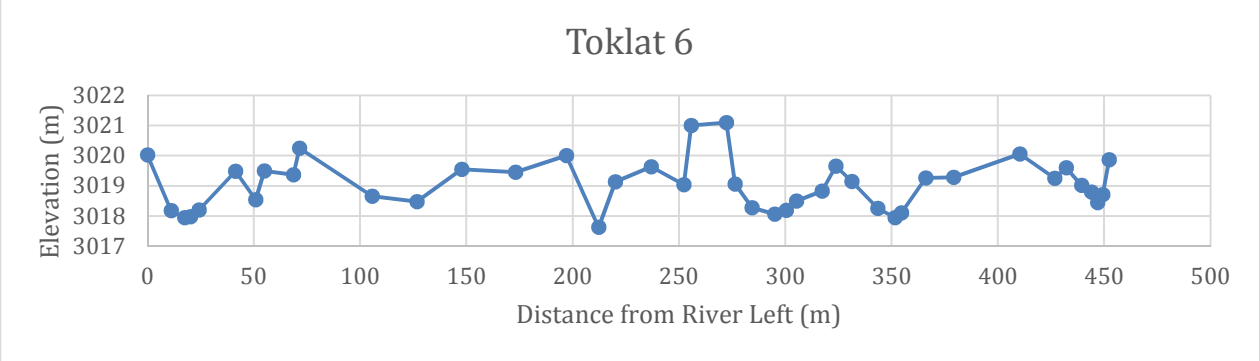

Figure 48: Cross-section measured in May of 2015 downstream of the East Bridge on the Toklat River.

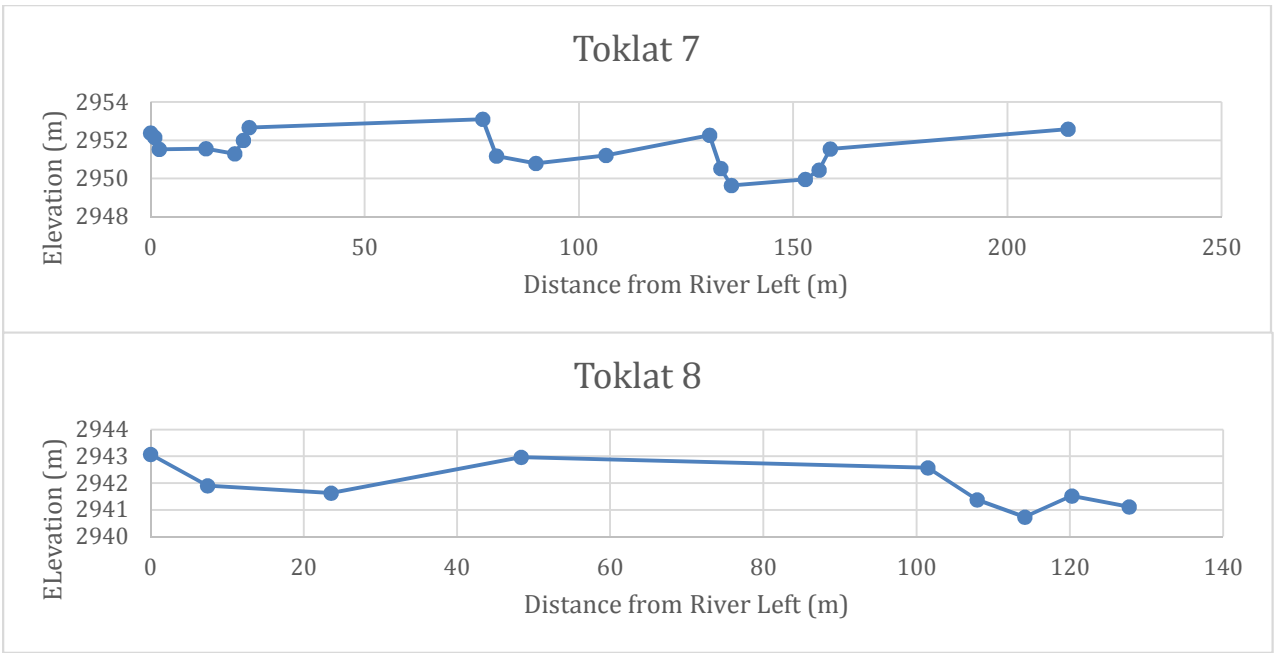

Figure 49: Two cross-sections measured in May of 2015 downstream of Road Camp on the Toklat River.

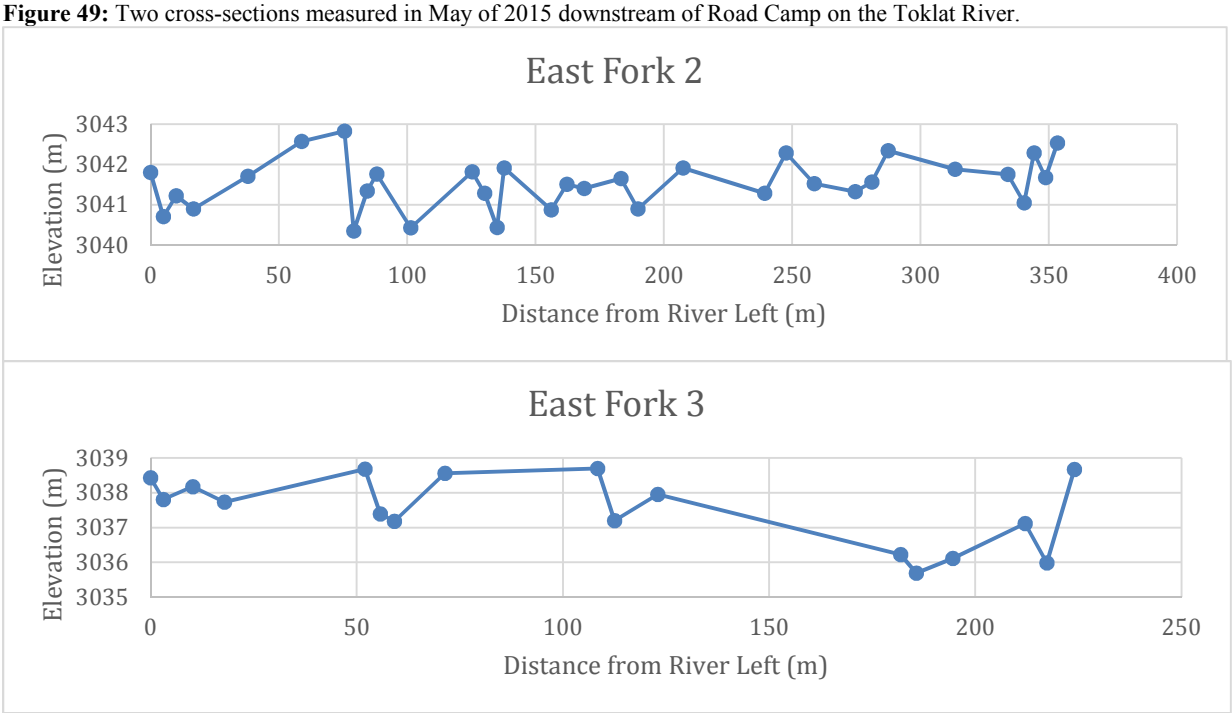

Figure 50: Two cross-sections measured in May of 2015 upstream of the Bridge on the East Fork River.

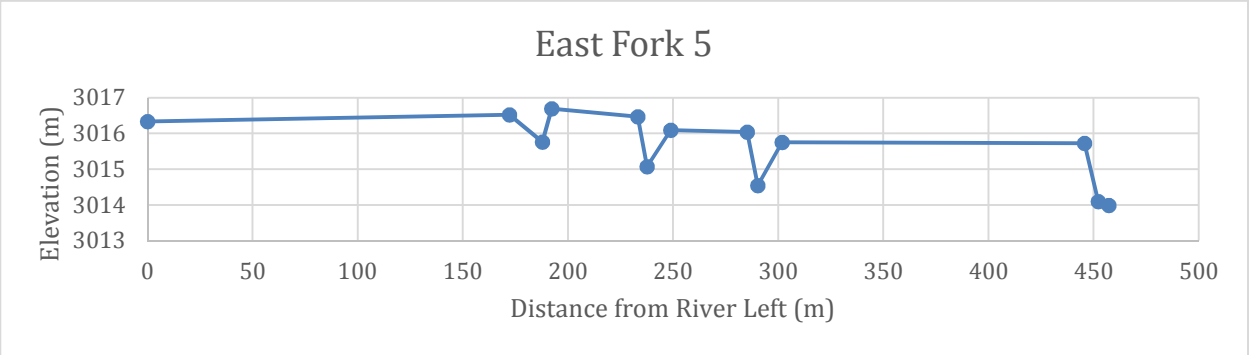

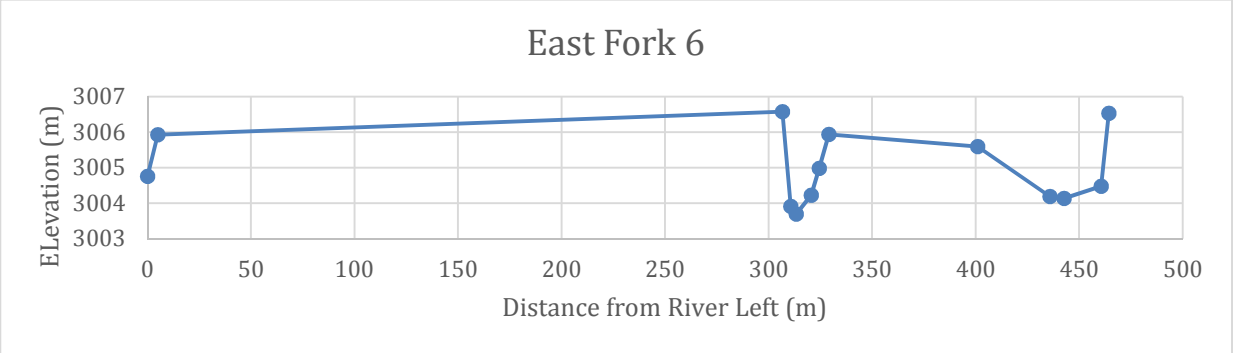

Figure 51: two cross-sections measured in May of 2015 downstream of the Bridge on the East Fork River.

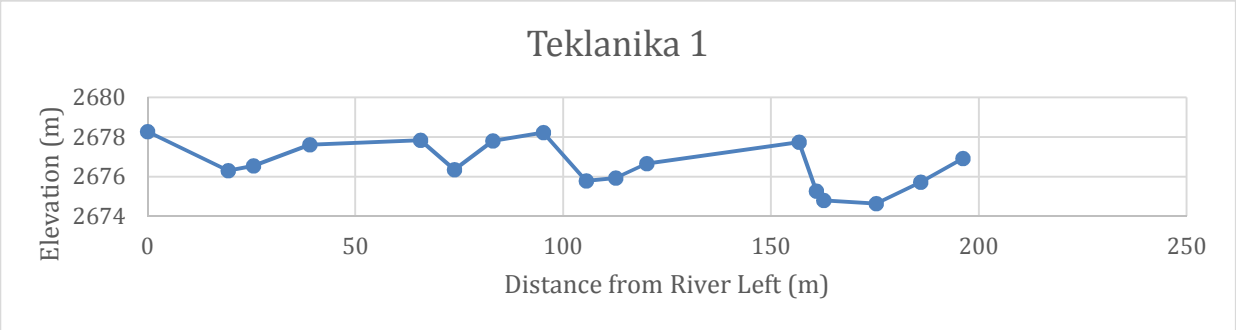

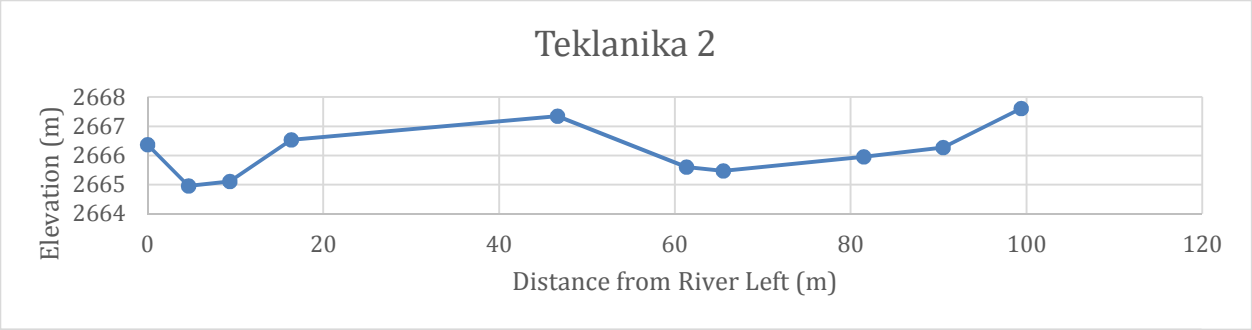

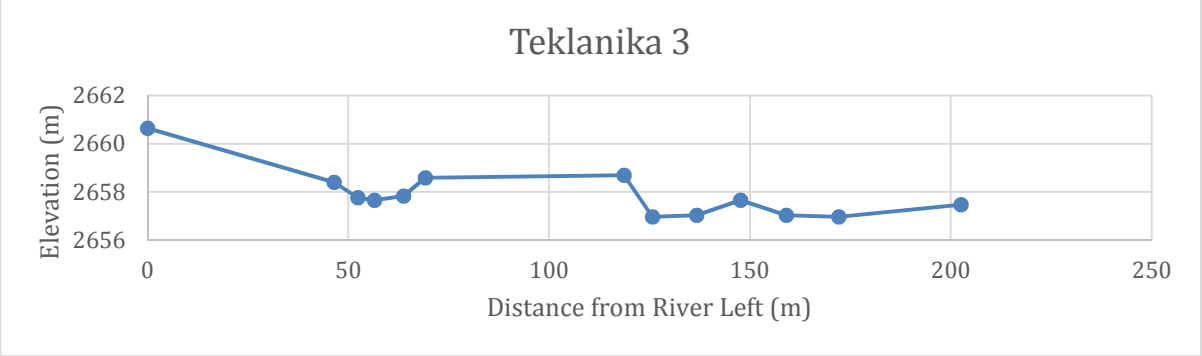

Figure 52: Two cross-sections measured in May of 2015 upstream of the Bridge on the Teklanika River.

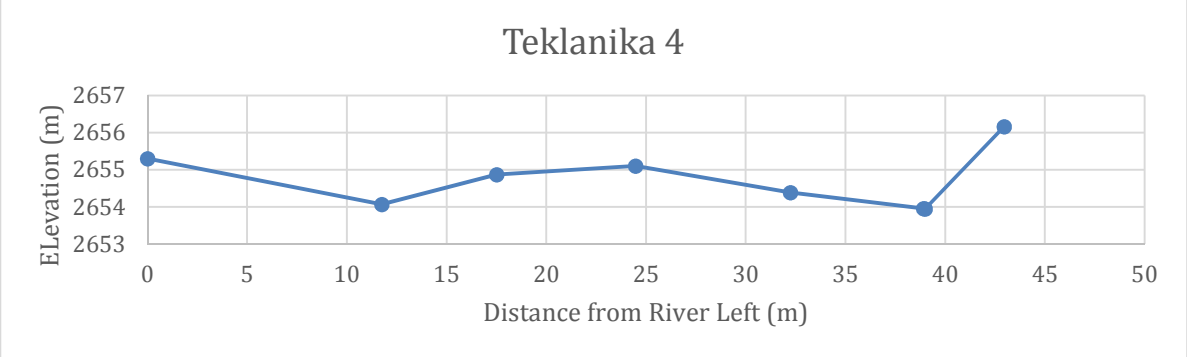

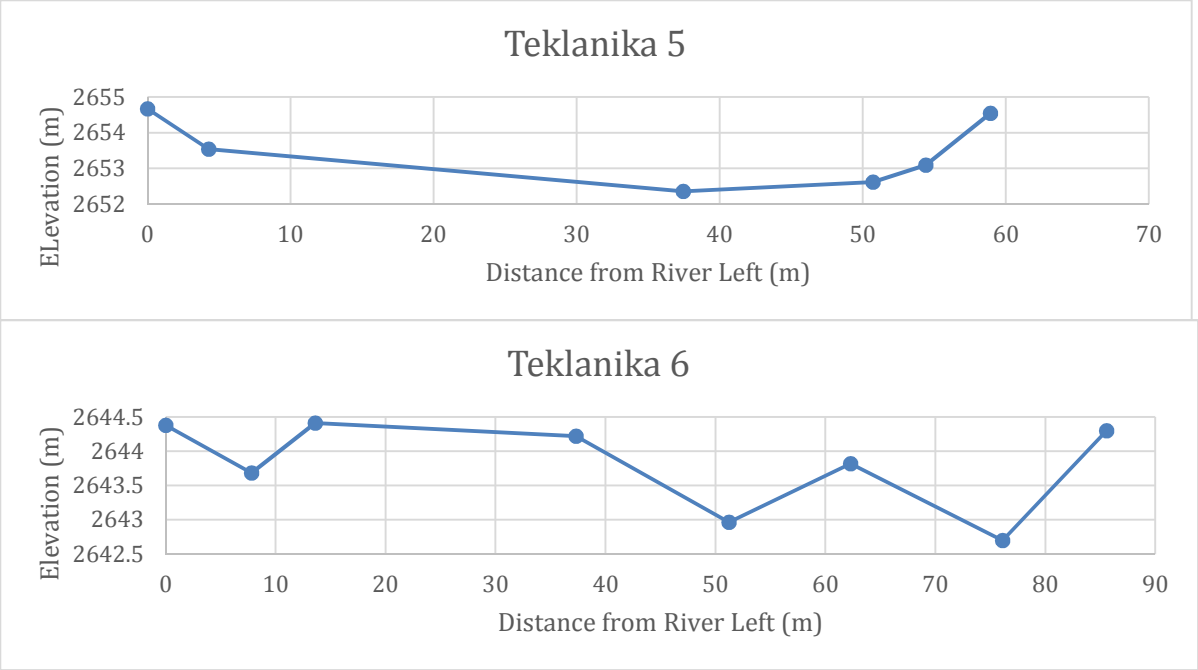

Figure 53: Two cross-sections measured in May of 2015 downstream of the Bridge on the Teklanika River.